UNIVERSIDADE DE LISBOA
FACULDADE DE CIÊNCIAS
DEPARTAMENTO DE ENGENHARIA GEOGRÁFICA, GEOFÍSICA E ENERGIA


# Simulative Analysis of Tire Influence on Energy Consumption and Driving Dynamics of an Electric Driven Vehicle

Marcelo Valentim Calado do Rosário

**Mestrado em Engenharia da Energia e Ambiente**

Dissertação orientada por:
Professor Miguel Brito
Doutor Martin Gießler

2024

"Life would be tragic if it weren't funny."

- **Stephen Hawking**

# Acknowledgments

The completion of this dissertation was only possible with the help of other persons:

- Thank you to the Karlsruher Institut für Technologie, especially, to Doctor Martin Gießler for welcoming me, challenging me with an interest and recent topic where I was allowed to apply my knowledge, and the one that I learned from Doctor Martin Gießler, and for all the patience, attention, and availability. Thank you.

- Thank you to Professor Miguel Brito for accept to be my supervisor.

- Thank you to Professor Guilherme Gaspar, from the beginning of this challenge, until its completion. Was with the help of the Professor Guilherme Gaspar that I could find Doctor Martin Gießler in Germany where, in cooperation with, I wanted to develop my dissertation. Thank you for follow-up before, during and after I was in Germany. Also, thank you for all the patience, attention, and availability. Thank you.

- Thank you to the most important people in this all world: my Father, Rui Rosário, my Mother, Carla Antunes, and my Sister, Camila Rosário. All this was only possible because of your patience, knowledge, and for always believe in me. Thank you for always be there for me and for help me, even when I didn't want to. Thank you for taking care of me and for the effort so I could have everything. A thank you is not enough for what you made, what you are making, and for what you will do. I will always be in your debt. But I want you to know in my way, I love you all. Thank you. And thank you Bolt.

# Sumário

Os veículos elétricos a bateria têm vindo, cada vez mais, a integrar o sector da mobilidade. Não só por serem eficientes na conversão de energia elétrica em energia mecânica, mas por apresentarem poucas ou nenhumas emissões de gases poluentes. No entanto, este tipo de veículos ainda não consegue disponibilizar as autonomias desejáveis, o que não acontece com os veículos de motor de combustão interna. Um dos principais fatores que leva a este baixo tempo de funcionamento é a reduzida capacidade das suas baterias. No entanto, existem outros parâmetros que podem aumentar ou reduzir o consumo elétrico do veículo, e consequentemente afetar a sua autonomia: a aerodinâmica do veículo, o sistema de transmissão, as perdas de Joule, entre outras. Desta forma, é de elevada importância a compreensão e minimização do impacto destes parâmetros no funcionamento do veículo.

Com este intuito, o Karlsruher Institut für Technologie (KIT) desenvolveu um sistema de testes experimentais para um veículo ligeiro de passageiros a bateria (Mercedes Benz Classe A) associado a modelos de desempenho utilizando o software IPG CarMaker. Os modelos são utilizados, na sua maioria, para a análise do consumo energético e consequente modificação do sistema de tração, como a instalação de um sistema regenerativo.

Nesta dissertação o modelo de simulação do veículo foi desenvolvido em termos da configuração dos pneus e chassis de forma a investigar a sua influência no consumo de energia elétrica e na dinâmica de condução (aceleração, travagem, estabilidade do veículo, entre outras). Os três principais fatores que permitem avaliar a qualidade do chassis são a dinâmica de condução, o conforto de condução e a segurança durante a condução. Assim, para além de avaliação do impacto destes fatores no consumo elétrico, enfase também deve ser dado ao comportamento do veículo em função destes. Tendo em conta estes fatores, as simulações foram divididas em três casos de estudo: dinâmica de condução de segurança, direção dinâmica e condução económica.

Para avaliar a segurança durante a condução, considerou-se analisar a influência de dois sistemas de segurança ativa, com o condutor (70 kg): sistema anti bloqueio de travões (ABS) e sistema autónomo de travagem de emergência (AEB). O primeiro permite que as rodas não bloqueiem durante uma travagem, proporcionando uma distância de travagem menor e contornar obstáculos. O AEB monitoriza a estrada e, caso detete um obstáculo onde é necessário travar, mas o condutor não o faça, trava autonomamente.

Para testar a influência do AEB, o acionamento dos travões por parte do condutor é “eliminado” do modelo, sendo colocado um obstáculo a uma determinada distância do veículo-teste. Foram simulados três testes diferentes (Teste 1.1.1., Teste 1.1.2. and Teste 1.1.3.), onde o objetivo é que veículo-teste se aproxime do obstáculo e o sistema AEB acione os travões quando necessário.

Para avaliar o outro sistema, (Teste 1.2.1., Teste 1.2.2.), foi selecionado um modelo já definido no software IPG CarMaker, onde existem dois tipos de estradas retas com diferentes coeficientes de atrito. Na estrada com alto coeficiente de atrito, o veículo acelera até atingir uma velocidade elevada e, quando se encontra na superfície de menor coeficiente de atrito, são aplicados os travões até o veículo imobilizar.

Na análise da estabilidade do veículo foram selecionados três tipos de testes com o condutor, onde o sistema de Controlo de Estabilidade (ESP) foi avaliado em dois deles. O veículo é levado ao seu extremo ao nível da sua agilidade enquanto corpo rígido. Um dos testes simulados foi o Teste Circular (Teste 2.1.), de raio constante, de acordo com a norma ISO 4138: num percurso circular e de raio constante, o veículo acelera, lentamente, até sair da rota definida. A Mudança de Pista Dupla (Teste 2.2.1. and Teste 2.2.2.), de acordo com a norma ISO 3888-2: o veículo entra na pista de obstáculos com uma velocidade de, pelo menos, 80 km/h e tem de contornar obstáculos sem derrubar nenhum cone ou sair da pista. O outro teste (Teste 2.3.1. and Teste 2.3.2.) onde foi avaliado o ESP foi o *Moose Test-*

equivalente ao teste anterior, mas o veículo tem de entrar na pista, cujas dimensões da pista são menores, e com uma velocidade compreendida entre 60 km/h e 65 km/h e no qual tem de ser mantida constante ao longo do percurso.

Por fim, para a análise do consumo, o veículo foi definido com 4 utilizadores (70 kg/ utilizador) e, para o mesmo percurso, um outro teste apenas com o condutor. Foram definidos dois testes (Teste 3.1. and Teste 3.2.) onde o veículo foi levado ao extremo na sua performance: o veículo acelerava até atingir os 50 km/ h, mantinha a velocidade durante um intervalo de tempo, voltava a acelerar, desta vez até aos 80 km/ h, e o mesmo procedimento até aos 130 km/ h; no outro teste e, para as mesmas velocidades, quando o veículo atingia a velocidade desejada, o condutor travava até imobilizar o veículo. Depois, repetia o processo para as outras duas marcas de velocidade. Um outro teste (Teste 3.3.) foi o *Worldwide harmonized Light vehicles Test Cycles* (WLTC) para veículos elétricos. Permite simular um comportamento típico deste tipo de automóveis e analisar o seu respetivo consumo. Os restantes testes foram baseados em casos reais: *Real Driving Emissions* (RDE) (Teste 3.4.) onde foi modelada uma viagem típica na cidade de Karlsruhe e, posteriormente, o seu perfil de velocidade foi aplicado numa linha reta (Teste 3.5). Os outros dois casos, representam uma viagem típica de um estudante de Lisboa, na sua ida para a Universidade de Lisboa (Teste 3.6), e no seu regresso a casa (Teste 3.7). É importante realçar que para as simulações onde a pressão do pneu foi 2.2 bar, e a classificação de velocidade dos pneus foi Q (Q 2.2 bar), o veículo não concluiu o percurso RDE, nem o percurso reto com a perfil de velocidade anterior. Isto justifica-se pela baixa capacidade da bateria instalada no veículo (25.17 kWh). Para tal, dimensionou-se uma bateria (42 kWh) para o veículo de teste, tendo em conta um veículo ligeiro de passageiro (*Fiat 500e Cabrio*) com dimensões e estrutura equivalentes.

Dentro do sector dos pneus e das suas diferentes características que poderiam influenciar o consumo do veículo, foram selecionados como relevantes e possíveis de serem avaliados no software os seguintes fatores: pressão dos pneus, 2.2 bar e 2.9 bar, o coeficiente de resistência de rolamento caraterístico dos pneus, e cuja diferença é obtida escolhendo pneus com diferentes classificações de velocidade, Q e H. Por último, foram definidas cargas extras que influenciariam a força vertical que é aplicada nas rodas. Estas cargas foram consideradas tendo em conta a ocupação do veículo apenas com o condutor, noutro caso, ocupado com 4 utilizadores.

Nas simulações relativas à segurança do veículo, a presença do ABS permitiu com que a distância de travagem diminuísse 14 m, face à inexistência do sistema. Além disso, este sistema permite distribuir a força que é aplicada nas quatro rodas, quando os travões são acionados. Nos três testes que prosseguiram com a análise do AEB, não houve qualquer colisão e o veículo imobilizou. Foi possível observar que, quanto maior fosse a velocidade relativa do veículo, em relação ao obstáculo, mais rápido o tempo de resposta do sistema AEB à travagem. Para uma velocidade relativa de 50 km/ h, e após a deteção do obstáculo, o tempo de resposta foi de, aproximadamente, 2 segundos enquanto para uma velocidade relativa de 80 km/ h, o sistema demorou menos de 1 segundo.

Relativamente à estabilidade do veículo, o ESP demonstrou que, além de corrigir a direção do veículo, reduz a sua velocidade. Isto permite ao condutor desviar-se de pequenos objetos que possam aparecer na via, com reduzida possibilidade de capotar e/ou despistar-se. No percurso circular testado, onde o raio de curvatura foi 42 metros, o veículo sofreu uma sobreviragem ao atingir 68 km/ h.

Na análise do consumo de energia, quando o carro estava equipado com pneus do tipo Q 2.2 bar, não foi possível terminar o percurso RDE, cujo consumo foi 0.27 kWh/ km e as perdas de energia através dos pneus foram 0.126 kWh/ km. Para a mesma classificação de velocidade, Q, mas com uma maior pressão, 2.9 bar, as perdas foram 0.099 kWh/ km e o consumo total foi 0.21 kWh /km. Apesar das pequenas diferenças, foi o suficiente para o veículo concluir o percurso com uma bateria de 25.17 kWh e autonomia de 104 km. Com a pressão 2.2 bar e com uma classificação H, ou seja, menor coeficiente de resistência de rolamento, o consumo total foi 0.22 kWh/ km, com perdas de 0.105 kWh/ km nos

pneus. Este parâmetro não é tão influenciador como a pressão dos pneus, no entanto, foi essencial na distância percorrida pelo veículo. Por fim, considerando apenas o condutor, as perdas através dos pneus foram 0.110 kWh/ km e o consumo foi 0.23 kWh/ km. A pressão e o coeficiente de resistência de rolamento dos pneus foram os fatores que mais contribuíram para o consumo total elétrico do veículo.

**Palavras-chave:** Carro Elétrico, Perdas de Energia, Pressão dos Pneus, Resistência de Rolamento, Bateria.

# Abstract

EVs have increasingly become part of the mobility sector. However, these vehicles cannot achieve the desirable autonomy due to reduced battery capacity. Other parameters that can increase or reduce the vehicle's electrical consumption are their aerodynamics, and transmission system, among others.

KIT has a battery-powered passenger vehicle (Mercedes Benz A-Class) that has already been developed through other works, along with simulation models programmed in the IPG CarMaker software.

In this dissertation, the vehicle simulation model was developed regarding the tire and chassis model to investigate its influence on electrical energy consumption and driving dynamics. The simulations were divided into three cases of study: dynamics of safety conducting, dynamic driving and economic driving.

To assess safety during conduction, it was considered to analyse the influence of two active safety systems: ABS and AEB. The first allows the wheels to not block during a braking, providing a smaller braking distance and bypassing obstacles. The AEB monitors the road and if it detects an obstacle where it is necessary to stop, but the driver doesn't do so, it stops autonomously.

The dynamic driving was tested with the ESP, whose purpose is to help the vehicle strengthen the loss of traction on the road. And with the analyse of the steering wheel angle behaviour.

In last case of study, and within the tire sector and its different characteristics that could influence vehicle consumption, the following factors were evaluated: tire pressure, 2.2 bar and 2.9 bar, the coefficient of resistance, whose difference is obtained by choosing tires with different velocity ratings, Q and H. Lastly, extra loads were defined that would influence the vertical force that is applied to the wheels. These loads were considered in view of the occupancy of the vehicle only with the driver, in another case, occupied with 4 users.

**Keywords:** Electric Vehicle, Energy Losses, Rolling Resistance, Tire Pressure, Battery.

# Nomenclature

| | |
|---|---|
| $\delta_{AM}$ | Ackermann effect |
| ACC | Adaptive Cruise Control |
| $F_a$ | Aerodynamic Drag |
| AC | Alternate Current |
| ABS | Anti-Lock Braking System |
| $F_Z$ | Applied Load |
| AEB | Automatic Emergency Braking |
| BEV | Battery Electric Vehicle |
| BMS | Battery Management System |
| BLDC | Brushless DC Motors |
| $\gamma$ | Camber Angle |
| $CO_2$ | Carbon Dioxide |
| CG | Centre of Gravity |
| $F_c$ | Climbing Resistance |
| CVT | Continuously Variable Transmission |
| CVTs | Continuously Variable Transmissions |
| CAN bus | Controller Area Network |
| DOD | Depth of Charge |
| $a$, $b$, $c$, $\alpha$, and $\beta$ | Dimensionless Parameter |
| DC | Direct Current |
| Dist. W/ ABS | Distance with ABS |
| Dist. W/O ABS | Distance without ABS |
| Dr. | Doctor |
| F | Driving Resistance |
| ECE | Economic Commission for Europe |
| EV | Electric Vehicle |
| EVs | Electric Vehicles |
| ESP | Electronic Stability Control |
| ETRTO | European Tyre & Rim Technical Organization |
| FTP | Federal Test Procedure |
| FL | Front Left |
| FR | Front Right |

| | |
|---|---|
| FT | Full Toroidal |
| GPS | Global Positioning System |
| GUI | Graphical User Interface |
| HT | Half Toroidal |
| HV | High Voltage |
| $F_{x,\,w}$ | Horizontal Wheel Force |
| HEV | Hybrid Electric Vehicle |
| $F_I$ | Inertial Resistance |
| IVT | Infinitely Variable Transmission |
| IVT-I | Infinitely Variable Transmission Type I |
| IVT-II | Infinitely Variable Transmission Type II |
| IVTs | Infinitely Variable Transmissions |
| P | Inflation Pressure |
| $v_i$ | Initial Vehicle Velocity |
| FAST | Institute of Vehicle System Technology |
| ICE | Internal Combustion Engines |
| ISO | International Organization for Standardization |
| J10-15 | Japanese 10-15 Driving Cycle |
| KIT | Karlsruhe Institute of Technology |
| $F_{y,\,w}$ | Lateral Force |
| $C_\alpha$ | Lateral Stiffness |
| Li-ion | Lithium-Ion |
| $LiFeMgPO_4$ | Lithium-Iron Magnesium Phosphate |
| $v_{max}$ | Maximum Vehicle Speed |
| MCU | Motor Control Unit |
| NEDC | New European Driving Cycle |
| PMSM | Permanent Magnet Synchronous Motors |
| PV | Photovoltaic |
| PHEV | Plug in Hybrid Electric Vehicle |
| c | Position of the Centre of the Tire Contact |
| $\vec{X}$ | Projection of a Vector onto the x-axis |
| $\vec{Y}$ | Projection of a Vector onto the y-axis |
| $\vec{Z}$ | Projection of a Vector onto the z-axis |

| | |
|---|---|
| *RADAR* | Radio Detection and Ranging |
| RDE | Real Driving Emissions |
| RL | Rear Left |
| RR | Rear Right |
| $F_{r,\,fr}$ | Resistance due to Rolling Friction and Residual Braking |
| $F_{r,\,\alpha}$ | Resistance due to Tire Slip Angle |
| $F_R$ | Result Force |
| $F_{r,\,tr}$ | Road Rolling Resistance |
| $F_r$ | Rolling Resistance |
| $k_r$ | Rolling Resistance Coefficient |
| $F_{RR}$ | Rolling Resistance Defined by CarMaker |
| 1G | Single-Speed Gear Drives |
| $\alpha$ | Slip Angle |
| $v$ | Speed |
| $\sigma$ | Standard Deviation |
| SOC | State of Charge |
| SOH | State of Health |
| SFTP | Supplemental Federal Test Procedure |
| SDG | Sustainable Development Goals |
| SRM | Switched Reluctance Motors |
| $v_{belt}$ | Tire Belt Speed |
| TIP | Tire Industry Project |
| $F_{r,\,t}$ | Tire Rolling Resistance |
| $\delta_{v,\alpha}$ | Tire Sideslip Angle |
| $\delta$ | Toe Angle |
| 2G | Two-Speed Gear Drives |
| TYDEX | Tyre Data Exchange Format |
| UDC | Urban Driving Cycle |
| VUT | Vehicle Under Test |
| VCU | Vehicle Control Unit |
| Vel. W/ ABS | Velocity with ABS |
| Vel. W/O ABS | Velocity without ABS |
| $F_{z,\,w}$ | Vertical Wheel Load |

| | |
|---|---|
| WLTC | Worldwide Harmonized Light Vehicles Test Cycles |
| WLTP | Worldwide Harmonized Light Vehicles Test Procedure |

# Index

# Figures Index

# Tables Index

# 1 Introduction

## 1.1 Framework

Electric vehicles, in addition to being more sustainable, are more efficient in converting the energy that feeds the engine into mechanical energy, with no appreciable emissions of polluting gases associated to their use if this electricity comes from renewable energy sources. In addition to the batteries, the central element of the EV is an electric motor. These motors must have certain characteristics, such as high starting torque, high power density and good efficiency [9]. To be economically viable, the EVs should perform as well as vehicles using internal combustion engines, namely when it comes to their performance during acceleration, operation in all environments, time for re-establishing the 'fuel' levels, and safety.

Electric vehicles have been largely adopted not only because of their reduced carbon footprint but also because of their autonomy (average range of 361 km [1]) and efficiency. It is possible to analyse, from the graph presented in Figure 1.1, the total sales of the EV (PHEV + BEV) have increased since 2012 and in 2022 broke a new record with 10.2 million sales. According to the Stated Policies Scenario (STEPS), in 2025, it would be possible to sell more than double the number of vehicles of 2022 [2,3].

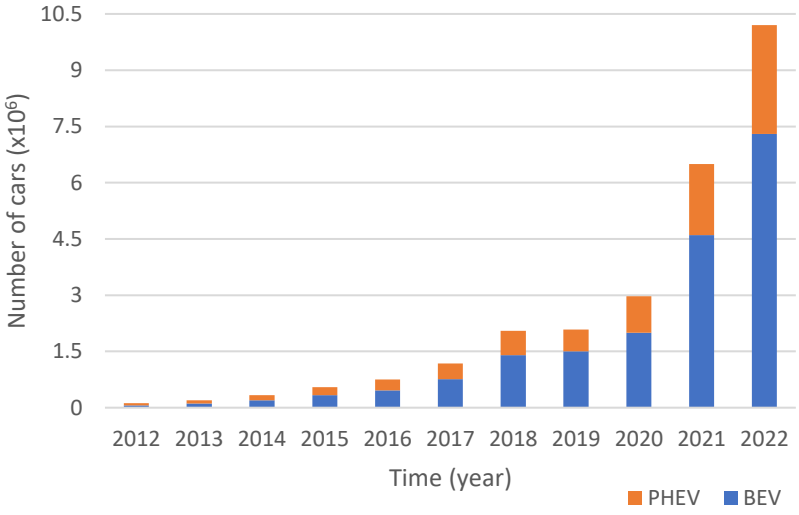


Figure 1.1- Number of battery electric vehicles (BEV) and plug-in hybrid electric vehicles (PHEV) sold in the world between 2012 and 2022 [3]

In 2015, all the United Nations Member State defined 17 Sustainable Development Goals and 169 targets to stimulate action until 2030 in important areas for humanity and the planet- The 2030 Agenda for Sustainable Development [4].

The global forum for the tire industry on sustainable issues, the Tire Industry Project (TIP), is working on the impacts of tires on human health and the environment and this sector can be more sustainable in the future. To achieve the SDGs, TIP developed a study "Sustainability Driven: Accelerating Impact with a Tire Sector SDG Roadmap." where the SDGs highlighted: good health and well-being, quality education, gender equality, clean water and sanitation, among others [5].

Due to tire production, TIP and other organizations started to worry about the environmental impacts. Decarbonizing operations and the sustainable use of natural resources are some of the paths that can reduce the operation's impact. During the tire rolling, one the evaluated targets in this work, some particles are also generated and can influence human health and have an environmental impact. It is necessary to develop standardized methodologies to identify tire tread materials, understand and identify the potential negative impacts and mitigate them.

## 1.2 Targets and Investigation Questions

One of the aims of this work is to evaluate the tire influence on energy consumption of an electric driven vehicle. In the tire field, several factors must be taken into account that influence the consumption per km of an EV: tire pressure and the rolling resistance of the tire itself. Being able to choose the most suitable tire for a given EV and driving conditions, e.g. by comparing tires based on the tire lable, will allow a reduction in tire's fine dust emission, tire noises, force transmission on wet roads, and in electricity consumption, which results in larger economies and comfort for the user as well as higher car autonomy. Also, the weight to which the vehicle is subject to [10]. So, the first research question is:

- **What tire (and chassis) related parameters have most influence in the energy consumption?**

The other target of this work is to evaluate the tire influence in the driving dynamics of an EV. Safety is one of the most important driving parameters that reflects the tire's performance. Users and technology have an important influence on the safety and environmental impacts and in the various modes of transport. So, another research question is:

- **What is the combination of tires, vehicle properties and road conditions that minimizes the electrical consumption of electric driven vehicles?**

In order to answer the above research question, this work comprises the following main steps:

- Perform simulations for the test cases:
    - Get started with CarMaker software;
    - Definition of test cases;
    - Parametrization of test cases;
    - Setup of test cases;
    - Data analysis of simulation results;

## 1.3 Document Organization

This work is divided into five main sections:

- In the first section is described the evolution of the electric cars, and how this dissertation is integrated in the Sustainable Development Goals.
- The second section describes the different vehicle components and different studies and tests that have been done in electrical vehicles worldwide, with a focus on the work carried out at Karlsruher Institut für Technologie (KIT).
- The third section describes the software including the developed and parametrized models and the methods applied in the case study.
- The fourth section is the results presentation and their analysis.
- In the last section, the conclusions of the dissertation and future recommendations for further works

# 2 Literature Review

## 2.1 Suspension

The suspension system is one of the most important systems directly connected with the wheels' behaviour. They determine the movement of the wheels during compression/extension and steering. After determining the specifications of the vehicle, the next step is to define the layout of this system. To do it, the suspension kinematics and the individual components (links and joints) must be optimized.

First, it is important to set the vehicle in a coordinate system. For a rigid vehicle, ISO defines ISO 8851.3/ DIN 70000 [6] a Newtonian vehicle coordinate system. The axis system must follow the right-handed rule, where the z vector, $\vec{Z}$, is equal to the external product between the x vector, $\vec{X}$, and the y vector, $\vec{Y}$ [7]. The centre point of the system is located on the road surface in the same plane as the front axle. From the driver's point of view, the direction of the positive semi-axis of the x is from the centre (0,0,0) to the vehicle's front. The direction of the positive semi-axis of the y is from the centre (0,0,0) to the left and the positive semi-axis of the z is upwards. The wheel motion is also characterized by a coordinate system where the vehicle is in its neutral position: the centre point is located at the centre of the tire's contact, and it moves parallel to the wheel's rolling axis during lateral dynamics. Figure 2.1 shows in more detail the vehicle and wheel coordinate system.

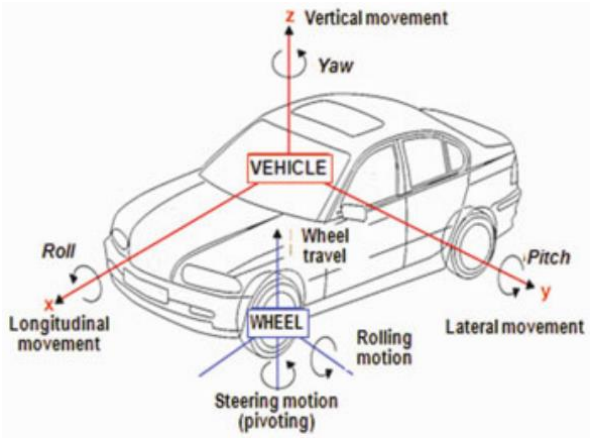


Figure 2.1- Newtonian vehicle coordinate system according to ISO 8851.3/ DIN 70000 for a car [6]

As said before, there are various suspension parameters that are crucial to understand the kinematics of this system, like the vehicle, the roll and pitch centre, and the wheel travel. Some of these characteristics are described and explained in the next paragraphs.

Regarding the vehicle, the wheelbase, the wheelbase change, and the vehicle centre of gravity are the most relevant to the work that was carried out. The wheelbase, L, is the distance between the centre of the front wheels and the centre of the rear wheels, in the xy plane (horizontal plane). The wheelbase change is the change in the position of the point of contact between the road and the wheelbase. In this work, it is possible to represent the car through its centre of gravity, CG- an imaginary point where the total weight of the body is concentrated.

Wheel travel parameters allow us to predict and analyse the position of the wheel during its movement at a certain time and a certain position in the car. The position of the centre of the tire contact, *c*, is variable and as known as spring travel. It is measured from the neutral position, 0 mm, and it's positive during compression and negative during extension. This suspension's behaviour induces a response from the vehicle's self-steering- toe change. This toe angle, δ, is the angle between the wheel

to the longitudinal axis of the vehicle. It can be measured in millimetres or degrees and if the top of the wheels is closer than the bottom, this is called toe-in. When the opposite occurs, it is called toe-out. The angle between the vertical plan that goes through the centre of the wheel and the vertical plan that is perpendicular to the road surface, camber angle, γ, is also affected by suspension kinematics (Figure 2.2). Is measured in degrees, and it is positive when the top of the wheel is more external than the bottom. When the opposite occurs, it is negative [6].

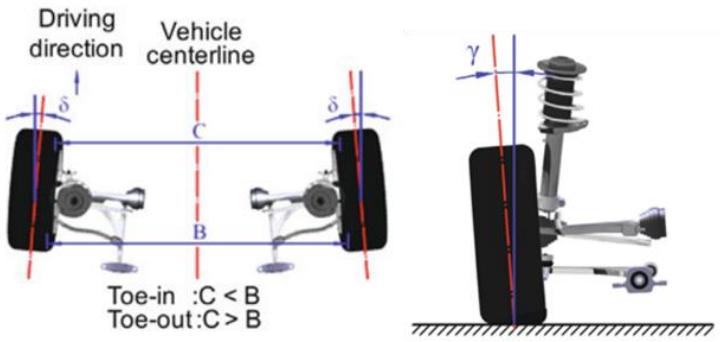


(a) (b)

Figure 2.2- Representation of the toe angle (a) and the camber angle (b) [6]

The tire slip angle, α, also known as the sideslip angle, is another parameter where the tires have energy losses. The angle between the speed vector of the wheels and the speed vector of the vehicle's body changes mostly during steering kinematics together with the Ackermann effect, $\delta_{AM}$- the difference in small turn radius between the front tires (Figure 2.3) [6].

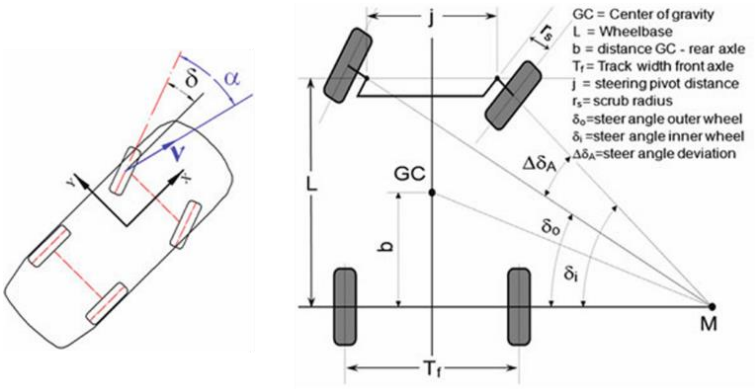


(a) (b)

Figure 2.3- Representation of the sideslip angle (a) and the Ackermann effect (b) [6]

## 2.2 Driving Dynamics

The factors that determine driving dynamics, ride comfort and driving safety are represented in Figure 2.4. A good vehicle performance is only achieved if the primary components and characteristics are all optimized.


Figure 2.4- Three chassis requirements (driving dynamics, driving comfort, driving safety) divided into categories [6]

The analysis of the car's movement can be done in the three-domain dynamics or space plan [6]:

- Longitudinal: the objects of interest are the resistance forces (air drag, rolling resistance, and others) and the energy needed to overcome these barriers. In this domain, the properties that are also relevant are, for instance, the braking and traction of the wheels on different surfaces (e.g. dry and wet surfaces).
- Lateral: the ability of the vehicle to remain stable when moving, especially when curving at high speeds, $v$.
- Vertical: this is the less important dynamic; it is related to the optimization of the springs and dampers.

The driving resistances can be divides in two categories: when the car is in movement without acceleration- steady-state resistances. And with variable speed- dynamic resistance. In a movement where the speed is constant only the steady-state resistances are present. But, in a travel where the vehicle is accelerating, both forces occur.

The driving resistance, $F$, is the resulting force, $F_R$, that is necessary to be applied to the driven wheels (front, back or both) to allow its movement- rolling movement. As show in Eq. 2.1, this movement depends on the aerodynamic drag, $F_a$, the rolling resistance of the four wheels, $F_r$, the climbing resistance, $F_c$, and the inertial resistance, $F_I$. The most relevant force to the current framework is the rolling resistance because it is directly connected to the tires itself. So the other forces will not be described in detail.

$$F_R = F_a + F_c + F_I + 4 \cdot F_r \ [N] \qquad \text{Eq. 2.1}$$

In brief, the aerodynamic drag, $F_a$, is the resistance caused by the air, in this case. Results from the airflow through the vehicle and cause small turbulences in the environment. The climbing resistance, $F_c$, it's caused by the inclination of the road, together with the vehicle's total weight and with the gravitational acceleration. The inertial resistance, $F_I$, represents de force that the car must overcome to alter its state of motion.

In what concerns the rolling resistance, a steady-state resistance, can be divided in several components: tire, $F_{r,t}$, and road, $F_{r,tr}$, rolling resistances, resistance due to tire slip angle, $F_{r,\alpha}$, and resistance due to rolling friction and residual braking, $F_{r,fr}$ [6].

- Tire rolling resistance depends on the rubber compound used in the tire (tire resistance), the capacity of the tire's deformation (flexing resistance), the contact between the tire and the road (frictional resistance), and the aerodynamic losses (air resistance).
- Road rolling resistance is caused by the force that the tire needs to apply to keep/starts its rotational movement in irregular road surfaces- shock absorption-, deformed road surfaces, and possibly water layer.
- The suspension geometry forces the tires to roll with a sideslip angle. In addition to this, a tire with lateral stiffness, $C_\alpha$, creates a lateral force, $F_{y,w}$.
- Resistance due to rolling friction and residual braking is caused by the vertical wheel load, $F_{z,w}$, and a horizontal wheel force, $F_{x,w}$.

In most cases, it is possible to assume that the tire rolling resistance, $F_{r,t}$, is equal to the total rolling resistance $F_r$. With this linear relation it is defined as a dimensionless parameter- coefficient of rolling resistance, $k_r$- and depends on the total rolling resistance and on the vertical wheel force, $F_{z,w}$, as represent in Eq. 2.2. In the most calculations, this coefficient is assumed constant with the vertical wheel load [6].

$$k_r = \frac{F_r}{F_{z,w}} \quad \text{Eq. 2.2}$$

For small sideslip angles the lateral force, $F_{y,w}$, can be defined as [6]:

$$F_{y,w} = C_\alpha \cdot \frac{\alpha}{2}\ [N] \quad \text{Eq. 2.3}$$

However, a certain part of this force is acting in the opposite direction to the wheel's direction movement. So, there will be a toe angle formed by the opposite forces that are acting in the wheels. This toe angle, $\delta_{v,\alpha}$, corresponds to the tire sideslip angle. So, the resistance due to tire slip angle, $F_{r,\alpha}$ can be calculated as follows [6]:

$$F_{r,\alpha} = \left(\frac{\alpha}{2}\right)^2 \cdot C_\alpha = \left(\frac{\delta_{v,\alpha}}{2}\right)^2 \cdot C_\alpha\ [N] \quad \text{Eq. 2.4}$$

As in the total rolling resistance, it is possible to define a coefficient of sideslip rolling resistance, $k_{r,\alpha}$ [6]:

$$k_{r,\alpha} = \frac{F_{r,\alpha}}{F_{z,w}} \quad \text{Eq. 2.5}$$

All these forces cause power losses at the wheels and, therefore, the efficiency will be not 100 %. So, all the other components of the car need to compensate these losses. If the tires are not adapted to the car or to the road, these losses will be higher, and all the costs related with the car and with the user will be higher than expected.

Also, the temperature influences the tire's behaviour; however, its effect was not taken into account in this work. The main focus was the energy lost in different types of tires and with different parameters, and with the rotational movement of the wheel and the contact between the road and the tire would increase the temperature of the tire, which would increase the thickness of the tire and, therefore,

greater contact with the road. The area of the tire in contact with the asphalt is larger, so the energy losses are expected to be bigger than what is determined for all case studies.

## 2.3 Tires and Wheels

The tires are the car's components that connect the vehicle to the road. The force that is transferred by the cars influences the safety of the passengers and the comfort of the vehicle. The motor vehicle industry and law define which shape, construction and materials must be used with a certain car category. All these parameters result in better safety during the travel, comfort, and driving conditions.

According with the European Tyre & Tim Technical Organization (ETRTO), a tire labelled with 185/55 R15 81H, the H stands for the maximum speed rating. Different letters mean different maximum speeds [6].

## 2.4 Electrical Vehicle

### 2.4.1 Configuration

All the vehicles that use electricity to power the motor to generate the rotation movement of the wheels are electric based. However, each one of them has distinct characteristics that make them different from each other. There are three types: battery electric vehicles (Figure 2.5), plug-in hybrid electric vehicles, and hybrid electric vehicles (HEV). Battery electric vehicles are fully electric vehicles, where the battery packs can be recharged by both plugging-in the vehicle to a charge station and the regenerative braking. The energy stored in the battery supplies power to the inverter. The inverter is a device that controls the amount of power supplied to the electric drive motor(s) based on the position of the accelerator pedal. This supplied electrical energy is used to generate an electromotive force, which rotates the shaft of the electric motor(s). This axle is coupled to the vehicle's wheels and causes forward or backward movement, depending on the direction in which the axle is rotating.

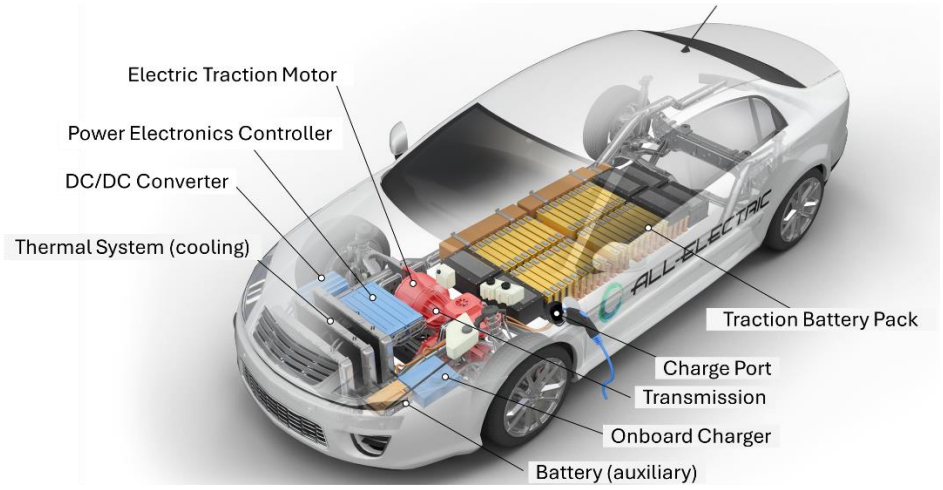


Figure 2.5- Example of the main components of an all-electric vehicle [8]

### 2.4.2 Electrical Engine

Electric motors convert electrical energy into mechanical energy. Two main types of electric motors are used in electric vehicles:

- Direct current motor (DC motors) which is used in the Nissan Leaf (Figure 2.6 (a)) [9]
- Alternate current motor (AC motor) which is used in the Tesla Model S (Figure 2.6 (b)) [9]

(a) (b)

Figure 2.6- Example of a car with a DC motor, Nissan Leaf, (a) and of a car with an AC motor, Tesla Model S (b) [10,11]

According to its functionalities and parameters, DC motors can be divided into other categories: brushed DC motors, and brushless DC motors (BLDC) [12,13]. Equivalent to these motors, AC motors can be divided into [12]:

- Asynchronous motors - have an electromagnetic induction that delivers the necessary power to the stator and rotor. They can produce a high torque; however, the control systems are complex and expensive. The efficiency varies between 90% and 93% [14].
- Permanent magnet synchronous motors (PMSM) - has a permanent magnet rotor (brushless DC motor) and stator produce a sinusoidal flux (induction motor). These motors are efficient (75% to 92%.), however, they are expensive and require complex systems [15].
- Another motor that works with alternate current is the switched reluctance motors (SRM). They use the magnetic resistance to generate torque, and the efficiency can reach 99% [14].

### 2.4.3 Battery

An electric vehicle's battery defines the vehicle's range, acceleration capacity and recharging time. The batteries can be divided into primary batteries and secondary batteries. An EV is equipped with several modules from the same rechargeable battery type, and they can be organized in series or in parallel. Li-ion batteries have a high energy density and specific energy associated with long cycle life.

Different factors affect the battery performance. It is important to highlight that the parameters can only be discussed separately and the interactions with each other can influence the battery's behaviour in a more severe way than the forecasted:[16–18]

- The total amount of electric energy generated by chemical reactions in the battery is designed as capacity and can be measured in kWh.
- The C-rate describes the rate which the battery can discharge relatively to its maximum capacity. 1C means that the battery will be empty after 1h of work. For instance, a fully charged battery of 100 ampere- hour (Ah) capacity discharges at 100 A.
- The state of health (SOH) indicates the percentage of the actual capacity compared with the capacity of a new battery. This indicator allows to analyse the deodorization of the battery.
- The state of charge (SOC), as measured in percentage (%), indicates how much from the maximum capacity is still available in the battery. Some self-discharges may occur due to losses in lengthy discharges. This happens mostly after high current drains and due to the discharge temperature. The opposite of SOC is the depth of discharge (DOD) and translates the percentage that was discharged from the maximum capacity.

- The voltage level of a battery as different values, according to what is under analysis. The value varies according to the state of charge of the battery- open-circuit voltage. This is measured when there is no load applied in the battery- the measured is independent from the current. It is important to know when the battery is completely discharge or charge. So, it is necessary to design a minimum or a maximum working voltage, respectively- cut-off voltage.
- Battery efficiency also depends on its internal resistance. The value can be different during charging and discharging. E.g.: for lithium-ion batteries, the efficiency varies between 70% and 90% [19].
- The chemistry of the battery defines the nominal energy per mass unit- specific energy density [Wh/kg]- and the maximum power per mass unit- specific power density [W/kg]. If a constructor designs a vehicle to reach a certain range, it is with the first parameter that define the weight required to reach the respective electric range and, with the second one, a certain performance target.
- Both volumetric energy density [Wh/L] and volumetric power density [W/L] depends on the battery's chemistry. They are calculated per mass unit, and they define the battery size required to achieve a certain electric and performance range, respectively.
- The temperature of the discharge process affects the capacity and voltage characteristics.

### 2.4.4 Regenerative Braking

The BEVs can be recharged without being connected to the grid or another external energy source. The connection between the drive wheels and electric motor allows to recover energy when the driver is not accelerating the car (acceleration pedal released) and when it is braking- regenerative braking.
The most common regeneration braking is mechanical, electrical and hydraulic. At the braking moment, the momentum generated accelerates the flywheel and so, slows down the vehicle- mechanical regeneration. Also, at this moment, the electric motor acts as a generator and converts the kinetic energy of the vehicle's movement into electric energy which it is stored in the battery. Not only does the conversion from electric energy to mechanical energy present losses but also the regenerative braking. During the process of kinetic energy conversion, there are losses due to roll and air resistance, mechanical brakes, transmission, and battery regarding internal resistance. High losses occur during vehicle braking because it needs energy to the friction brakes and the regenerative braking. Combining these two systems and the integration of the electronic braking control systems, the immobilization of the vehicle is safe.

The regenerative system helps to slow the vehicle, which allows to reduce the work applied by the brake pads and rotors. Also, it allows to increase the driving range. However, kinetic energy it is too low at reduced speeds, so the electric energy generate can be not enough to charge the battery, in order to increase the driving range [20].

## 2.5 Electric Vehicle Performance and Testing

### 2.5.1 Overview

Due to global warming, and the zero-carbon targets, governments have been creating regulations to foster the market of BEV, where challenges related to battery prices and performance, tires, vehicle design, and so on are still under resolution. Some changes may be made in the vehicles that allow for reducing their energy consumption [6]:

- Reduce the use of auxiliary systems like air conditioning;
- Start and stop system allows to turn off the vehicle when it is stopped;

- Reduce the rolling resistance by increasing the tire pressure to reduce the contact between tire-road;
- Use improved vehicle aerodynamics, so the air resistance can be lowered;
- Drive at constant and reduced speed;
- Reduce vehicle weight, so the vehicle's inertia could be lowered;
- Optimized working temperature to keep the performance of the battery;
- Change the powertrain topology.

In this field, some of the work that has been developed is to allow electric vehicles to have comparable autonomies and speeds as ICE vehicles of the same kind.

### 2.5.2 Influence of Vehicle Parameters

A small passenger vehicle was modelled and simulated in MATLAB [21], with characteristics similar to those of an internal combustion engine (ICE) vehicle. For example, the power required by an ICE for acceleration was calculated for an electric vehicle, where the same exercise was also performed for the energy demand, costs and range. The characteristics of the vehicle, and of the tires (175/65R14) used in this study can be found in Table 2.1. The energy recouped is limited by the maximum power of the motor, and by the maximum charging power of the battery. In this case, the percentage of energy recouped through braking was 50%. Four different driving cycles were selected: Federal Test Procedure (FTP) urban, FTP highway, New European Driving Cycle (NEDC), and US06.

Table 2.1- Information of the vehicle, and the tires used in the study [21]

| Vehicle Mass<br>kg | Battery Mass<br>kg | Tire Radius<br>m | Tire Rolling Resistance Coefficient |
|---|---|---|---|
| 1000 | 300 | 0.3 | 0.007 |

Some of the parameters evaluated were vehicle mass, rolling resistance coefficient, regenerative braking efficiency, and the drivetrain. All of these, except the drivetrain, were changed by ± 50% of its initial value. Four different types of systems were implemented in the drivetrain: using the default values, with 4 kW accessory draw, over ECE-15 multiplied by 2.5, and combined with the worse effects of all parameters from Figure 2.7. The energy consumption of the vehicle was between 140 Wh/km, for the default values drivetrain, and 230 Wh/km, for the combined with the worse effects.

In the Figure 2.7, the parameter that highlights is the vehicle mass. The vehicle mass shows a higher difference in the energy consumption: 0.023 kWh for ± 50% of its initial value, about 15%. The rolling resistance coefficient only presents a difference of 10% for ± 50% of its initial value.

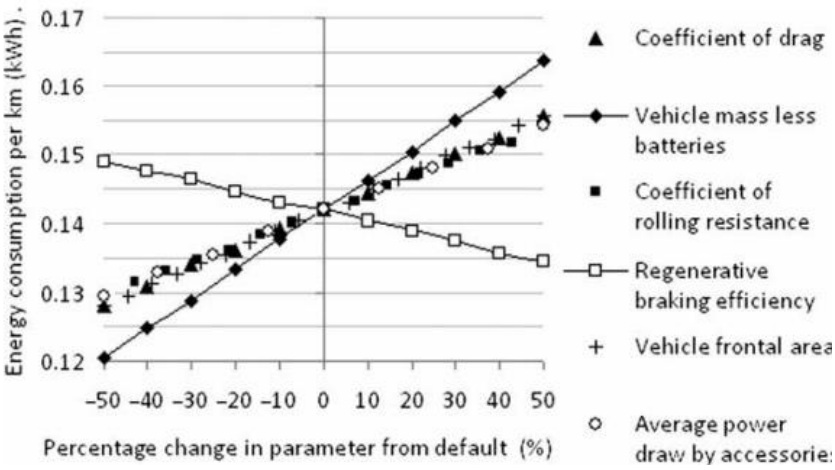


Figure 2.7- Variation of the different factors that may affect the energy consumption of the electric vehicle [21]

### 2.5.3 Influence of Drive Cycle Conditions

A group of investigators, from Chiang Mai University [22], studied the factors that can play a major role in the energy consumption of the BEVs: acceleration, ventilation, extra load, and others. It was performed real-world driving tests with different terrains, using two light passenger BEV. The tests were controlled by speed ranges and applying different "extra" loads (between 100 kg and 300 kg). Also, a comparable study that used machine learning algorithms to predict energy consumption from the same driving tests, was used too to have "solid" conclusions. Some of the results can be observed in Table 2.2.

Table 2.2- Minimum, and maximum consumption and the consumption difference between the minimum, and the maximum load in the vehicle from the study of Chiang Mai University [22]

| Min. Consumption Wh/km | Max. Consumption Wh/km | Consumption Difference Between Min. and Max. Load (100 km/h) Wh/km |
|---|---|---|
| 85 | 168 | 3 |

As it is possible to see from Table 2.2, the load did not have a major role in this consumption. The difference between the minimum and the maximum loads was only 3 Wh/km. Velocity presented a high influence in the energy consumption. The speed ranges between 0 km/h and 30 km/h, as well as above 80 km/h, were identified as high energy consumption speed ratings. The road slope may or may not have a high influence on energy consumption. Observing the graph from the Figure 2.8, where the energy consumption varies according to the road slope, the red curve has a low inclination, which means that the road slope does not have a high influence in the energy consumption of the vehicle. However, the regenerative braking allows to recover energy, and the authors of the study didn't clarify how much energy charged the battery through this process.

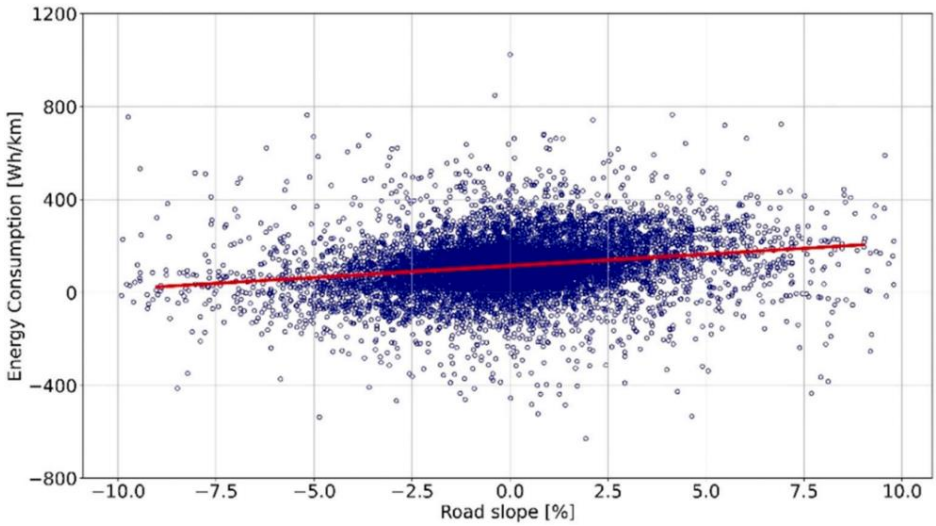


Figure 2.8- Dependence of the energy consumption on the slope of the road [22]

Regarding the powertrain, a team from Sweden [23] used a small light-duty vehicle, and based on the available data on its dimensions and performance, the vehicle was modeled and simulated in MATLAB/Simulink. To simplify the study, auxiliary loads were not considered, as well as thermal effects. In this simulation were used 19 official drive cycles, including Worldwide Harmonized Light Vehicles Test Procedure (WLTP) and the New European Driving Cycle (NEDC). It was concluded that the powertrain of a car can differ in its performance according to the driving cycles. As it is possible to see from the graph represented in the Figure 2.9, the rolling resistance energy consumption was, approximately, the same for every cycles. This justifies because it did not depend on the speed or in the acceleration of the car. Also depending on the test cycle, the total wheel energy consumption was between 40 Wh/km and 129 Wh/km. The battery efficiency was higher in the slow-speed tests and lower in the high-speed tests. When the car performed the high-speed tests, most of losses occurred in the electric machine and in the transmission. And for the low-speed tests, the losses occurred also in the electric machine, and in the inverter. This case prove that the electric machine should be improve to a better performance.

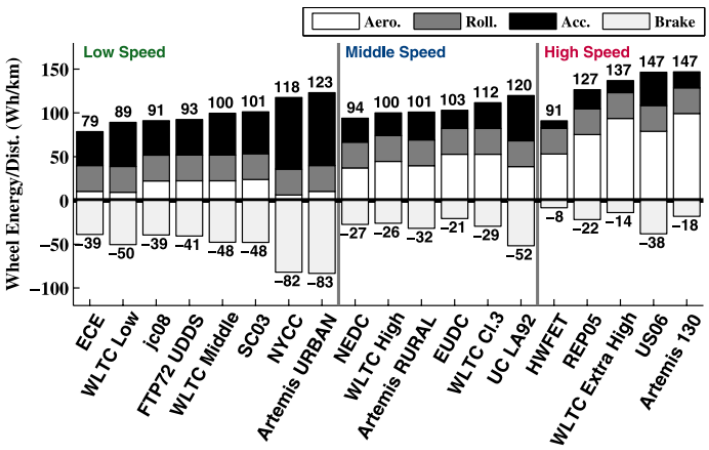


Figure 2.9- Wheel energy consumption for the different driving cycles [23]

The drivetrain can be optimized to decrease the energy consumption of the vehicles, allowing the vehicle to travel longer distances. To study the performance of the electric drivetrains, a group of

investigators [24] modelled and implemented a passenger car in MATLAB/Simulink. Six different transmission layouts were tested and are presented in the Table 2.3. The first test implemented was a constant speed drive, where the vehicle travelled at 10, 20, 30, 40 and 50 km/h (five different tests). The other two were driving cycles: the Urban Driving Cycle (UDC) and the Japanese 10-15 driving cycle (J10-15).

Table 2.3- Energy consumption (Wh/km) for the constant speed drive test for each typ of transmission [24]

| Test Type / Transmission Layouts | Constant Speed Drive km/h | | | | |
|---|---|---|---|---|---|
| | 10 | 20 | 30 | 40 | 50 |
| Single-speed gear drives (1G) | 25.5 | 27.0 | 31.5 | 35.5 | 45.5 |
| Two-speed gear drives (2G) | 25.5 | 27.0 | 31.0 | 36.0 | 45 |
| Half toroidal CVT (HT) continuously variable transmissions (CVTs) | 26.5 | 28.5 | 32.5 | 38 | 45 |
| Full toroidal (FT) continuously variable transmissions (CVTs) | 28 | 29.5 | 33.5 | 40.0 | 47.5 |
| Infinitely variable transmissions (IVTs)- Type I | 25.5 | 27.0 | 31.0 | 35.5 | 44.5 |
| Infinitely variable transmissions (IVTs)- Type II | 26 | 28.0 | 32.0 | 38 | 46 |

From Table 2.3, the FT contributed to the highest energy consumption: about 30 Wh/km, at 10 km/h, and about 50 Wh/km, at 50 km/h. While the speed tests increased, the IVT-I tended to be the transmission that contributed to the lowest energy consumption: about 25 Wh/km, at 10 km/h, and about 45 Wh/km, at 50 km/h. Also, in the other two tests, IVT-I was the one that contributed to less total energy consumption: about 187 Wh, in the UDC, and about 330 Wh, in the J10-15. However, the HT was the second lowest “consumer” in the UDC and in the J10-15 respectively with 187 Wh and 342 Wh.

The analysis of driving performance is important to investigate the potential optimizations that can be applied to a vehicle. An electric Peugeot iOn, and an electric version of the Ford Transit Connect (AGV) were tested in a chassis dynamometer testing with constant speeds, and in real life on-road conditions, which covered a total distance of 50 km in a trajectory of an urban, sub-urban and highway traffic roads [25]. For the chassis dynamometer tests, the results are represented in the Figure 2.10 for both cars.

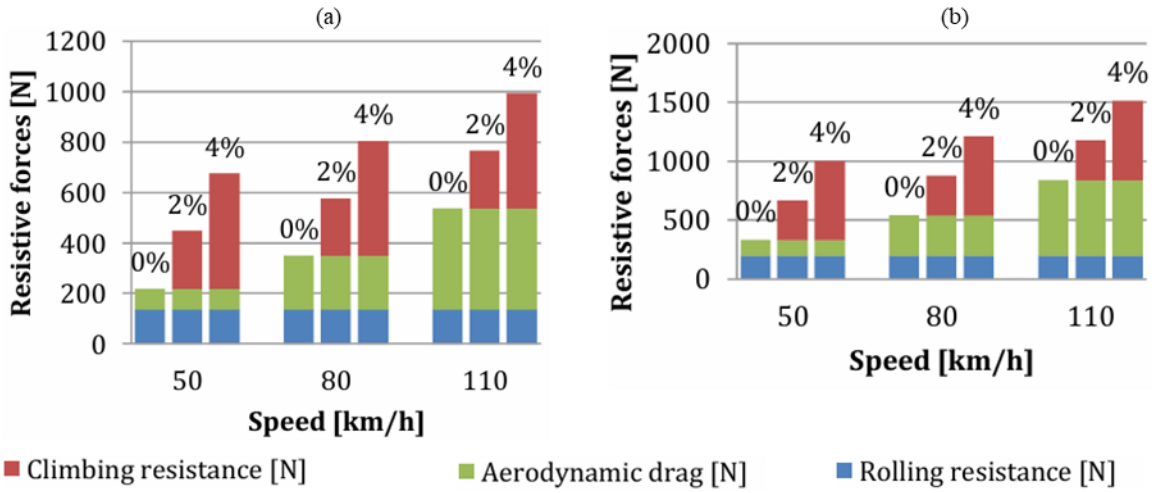


Figure 2.10- Climbing resistance, aerodynamic drag and rolling resistance for different climbing gradients (0%, 2% and 4%) and different speeds for the Peugeot iOn (a) and for the AGV (b) [25]

From Figure 2.10 (a), for a straight road the relative rolling resistance contribution decreases with the speed, while the aerodynamic drag is increasingly highlighted. With a 2% slope, the value of the climbing resistance is not null, and it's approximately the same for the speeds tested. However, its relative value is smaller and smaller with increasing slope. In a straight road, the rolling resistance is the most important factor to be optimised, but for a 2% and a 4% slope and for speeds higher, or equal, than 80 km/h, the climbing resistance is, relatively, the highest between the three. The same approach can be done for the AVG (Figure 2.10 (b)). However, its values are higher than the Peugeot. One of the causes could be that its curb weight (1625 kg) is greater than that of the Peugeot (1080 kg). In the real life road conditions, the consumption was 138 Wh/km and 192 Wh/km for the Peugeot and AVG, respectively, and the SOC was 53% and 40%, respectively. The autonomy of the Peugeot and the AVG, according to NEDC, was 150 km, and 160 km, respectively. However, with this test performed, the range decreased 50 km, and 40 km, respectively.

### 2.5.4 KIT Research on EV Testing

The Institute of Vehicle System Technology (FAST) at Karlsruhe Institute of Technology (KIT) has focused on vehicle performance by analysing factors such as tire characteristics. This research comprises several tire tests and benches focused on different vehicle types (car and/or truck) and specializes in different parameters related to tire dynamics.

Most of the existing driving cycles are not made specifically for electrical vehicles. Using conventional cycles, like NEDC and WLTP, the difference between simulated and real energy consumption can be considerably high in BEV. This does not allow to draw a good conclusion about the results. For this, three driving cycles were developed at KIT with a focus on BEV [26]: urban road (Fleet-BEV-Urban-Cycle), rural driving (Fleet-BEV-Rural-Cycle), and a mix of the previous cycles (Fleet-BEV-Cycle). Travel data from 80 vehicles was collected over three years, which allowed for the development of these types of BEV tests.

One of the test cars that the institute possesses is a fully electric Mercedes Benz A-Class (Figure 2.11). This car was originally powered by a fuel cell, but developments were carried out to turn it into a BEV.

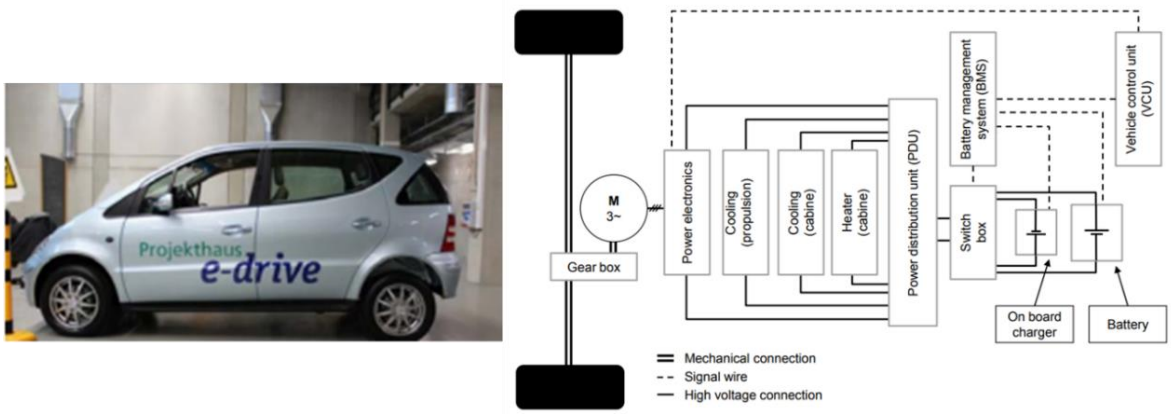


Figure 2.11- Test-vehicle, Mercedes Benz A-Class (left) and its drive train topology (right) [27,28]

The electric motor is installed by the manufacturer and is a 3-phase induction motor with a single gear transmission with a maximum power of 65 kW and a rated one of 45 kW. The car is constituted by a front wheel driven electric drive train. The direct current (DC) coming from the storage system is converted by the power electronics to alternate current (AC). This process is controlled by the motor control unit (MCU). Besides this function, the MCU has the work to maintain the good operation of the electric motor and preserve it by controlling the over current, the over speed and to take of the temperature protection. In the Figure 2.11 it is represented the configuration of the basis drive train of the vehicle [28].

The vehicle under test (VUT) is equipped with a battery with 21 UEV-18XP modules. However, to preserve the capacity of the battery, only 19 modules capacity is used. Due to the cathode type ($LiFeMgPO_4$) this battery provides an almost constant cell voltage over the complete state of charge range. Also, it is more efficient and fast charging. Like the electric motor has the MCU, the battery pack has the battery management system (BMS). In overall, this system allows to deliver the targeted range of current and voltage during a certain time. The main function of the BMS is to protect the battery so, even if the vehicle control unit (VCU) requires the system excessive energy, the BMS system will act independently. When the vehicle starts the battery has a current pick which can affect its performance. The vehicle must have a smooth start, so a resistor is added. After the electric motor starts, the resistor is removed, and the battery is connected directly to the high-voltage (HV) consumers. All these electronic control units, and others, are connected to the original controller area network (CAN bus). Most of the electronic control units had to be modified to ensure the safety of the vehicle and of the occupants [28].

# 3 Methodology

## 3.1 Simulation details

The simulations were carried out using the CarMaker software- a product designed by IPG Automotive that is used for virtual testing and simulation of cars and light-duty vehicles in all development stages. It allows to combine a virtual prototype with an adaptive driver model, as well as a detailed road and environment model, all pre-designed or designed by the user. In some cases, it was necessary to use the CarMaker for Simulink from MATLAB. It is a tool that allows the integration of the software into the MATLAB and SIMULINK environments. The research vehicle was modelled in this software and part of it was developed by J. Paul in [29].

All the parameters that will not be described were left as default by the system. The structure of the car was already designed, so some characteristic component values were left the same and according to its own coordinate system:

- Position, mass, and moment of inertia of the body and of the wheels (Table 3.1 and Table 3.2, respectively).
- All components related to the suspensions- spring, damper, buffer, and others.
- The forces and torque due to external wind loads.
- Brake torque amplification axle and how the pedal acts in a brake situation (Table 3.3).

Table 3.1- Important values defined as default for the vehicle and the engine defined in CarMaker

| **Vehicle Position** (x, y, z) m | **Vehicle Mass** kg | **Vehicle Moment of Inertia** (x, y, z) $kg \cdot m^2$ | **Engine Position** (x, y, z) m | **Engine Orientation** (x, y, z) deg |
|---|---|---|---|---|
| (0, 0, 0) | 1358 | (360, 1800, 1800) | (0, 0, 0) | (0, 0, 0) |

Table 3.2- Important values defined as default for the wheel position, mass and moment of inertia defined in CarMaker

| **Wheel Side** | **Wheel Position** (x, y, z) m | **Wheel Mass** kg | **Wheel Moment of Inertia** (x, y, z) $kg \cdot m^2$ |
|---|---|---|---|
| FL | (3.208, 0.778, 0.298) | 12.142 | (0.26, 0.459, 0.26) |
| FR | (3.208, -0.778, 0.298) | | |
| RL | (0.640, 0.7755, 0.293) | | |
| RR | (0.640, 0.7755, 0.293) | | |

Table 3.3- Important values of the parameterization of the brake model defined in CarMaker

| **Regenerative Brake Model** | **Brake Torque Recuperative Margin** Nm | Brake System Model and Mode | **Pressure to Brake Torque** Nm/ bar | | | | **Parkbrake Torque at Wheel** Nm | | | |
|---|---|---|---|---|---|---|---|---|---|---|
| Serial | 10 | Pressure Distribution by Pedal Actuation | FL | FR | RL | RR | FL | FR | RL | RR |
| | | | 10 | 10 | 5 | 5 | 0 | 0 | 1000 | 1000 |

The model was defined as a completely electrical one, with one electric motor coupled to the front axle (Figure 3.1). The control brake was defined as a regenerative serial which allows to charge the battery while the car is braking. The high voltage battery (HV) was modelled according to the Chen model (Figure 3.2) and the capacity, and total energy stored were defined as 69 Ah [30], and 25.17 kWh, respectively. Also, the charge profile of the battery modelled in the software was extrapolated from the Figure 3.3.

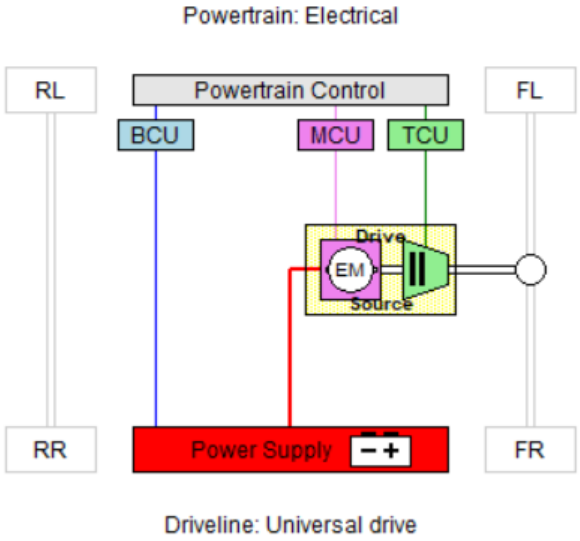


Figure 3.1- Powertrain of the model

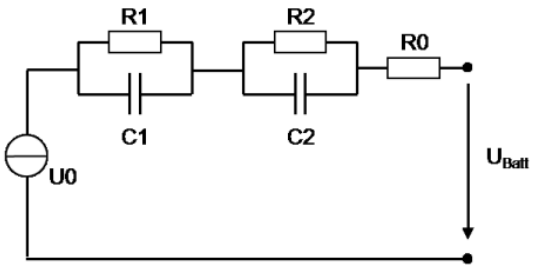


Figure 3.2- Equivalent circuit of the Chen battery [31]

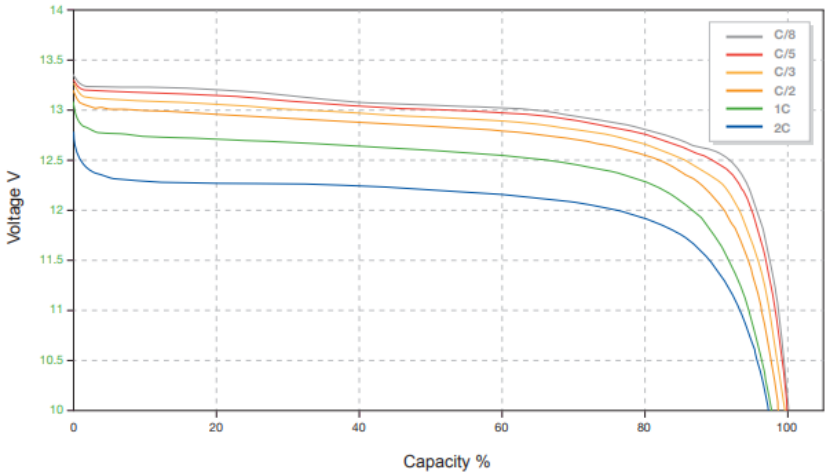


Figure 3.3- voltage profiles of the battery module previously described at various rates at the environment temperature of 23º C [30]

Some simulations could not be concluded due to the battery's low capacity for the test case. So, it was modelled a battery with the same capacity as the *Fiat 500e Cabrio 42 kWh* [32] due to its dimensions and equivalent structure, and data provided from the *U24-12XP battery*. The relevant data can be consulted in Table 3.4, and the respective voltage profile in the Figure 3.4 [32]. Also, the mass of the car was adapted to the new battery weight.

Table 3.4- Data of one module of the battery and the results obtained for the battery dimensioned from the *Fiat 500e Cabrio 42 kWh* [33]

| **Each Module** | | **Battery** (28 modules) | |
|---|---|---|---|
| **Nominal Module Voltage**<br>V | 12.8 | **Nominal Module Voltage**<br>V | 358.40 |
| **Nominal Capacity** (C/5, 25º C)<br>Ah | 118 | **Nominal Capacity** (C/5, 25º C)<br>Ah | 3304 |
| **Maximum Continuous Load Current**<br>A | 150 | **Maximum Continuous Load Current**<br>A | 150 |
| | | **Power**<br>kW | 53.25 |
| | | **Energy**<br>kWh | 42.29 |

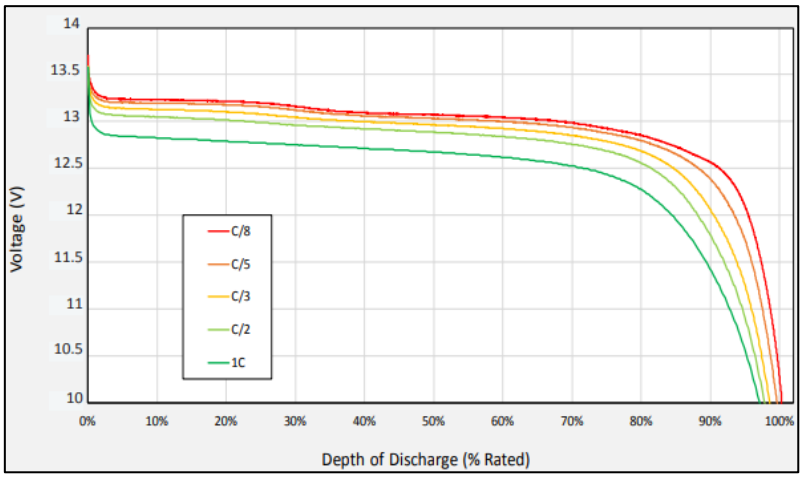


Figure 3.4- Voltage profiles of the battery module with a capacity of 42.29 kWh at various rates at the environment temperature of 23º C [33]

## 3.2 Tire Model and Parametrization

In this work, the most relevant car's elemental is the tire. It was used a pre-defined tire model which is based on tire measurements provided in Tyre Data Exchange Format (TYDEX): *RT_195_50R15*.

- Tire nominal width of 0.195 m.
- The nominal height to width ratio is 0.50.
- 15 inches of wheel rim diameter

The rolling resistance model was changed from a *Force by Load*, where it is only possible to define the rolling resistance factor, to a *Force by Load + Velocity*, where the force is defined according to the Eq. 3.1 [34].

$$F_{RR} = P^{\alpha} F_z^{\beta} \left(a + b \cdot v_{belt} + c \cdot v_{belt}^2\right) [N] \qquad \text{Eq. 3.1}$$

The parameters *a*, *b*, *c*, α, and β are dimensionless and P and $F_z$ stands for inflation pressure, in kilopascal (kPa), and applied load for vehicle weight in newton (N), respectively. The tire belt speed (km/h), $v_{belt}$, can be assumed as the vehicle speed.

It was set that the most relevant variables that could be variable in the software were: tire rolling resistance, tire pressure and vehicle weight. So, it was defined two major tire pressures: 2.2 bar and 2.9 bar. For each pressure, the vertical wheel load is different: if consider 100 % ETRTO (European Tire & Rim Technical Organisation), the force is 6033 N, but if it is only 80 % ETRTO, the force is 4826.40 N. For the next steps, the factor between these two units was calculated through the graph, circumferential force (Umfangskraft) vs. speed (Geschwindigkeit), in the Figure 3.5.

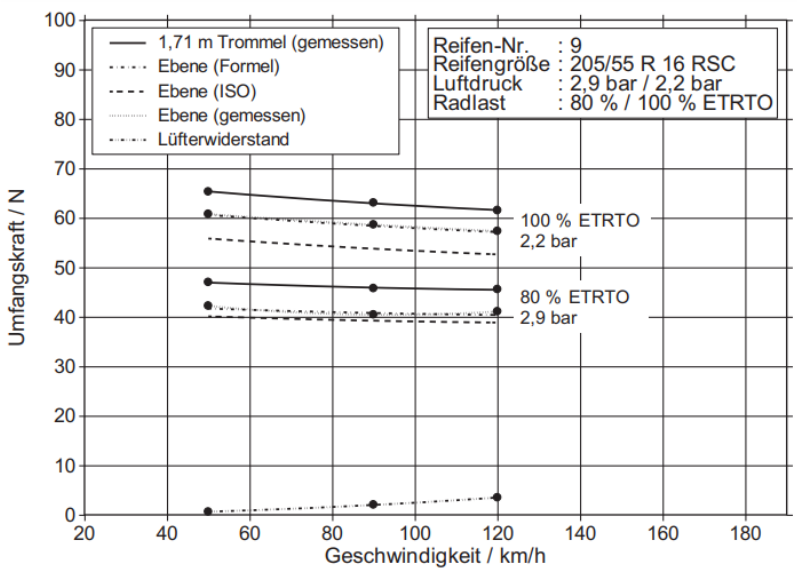


Figure 3.5- Representation of the circumferential force (Umfangskraft) vs. speed (Geschwindigkeit) and the rolling resistance of a tire converted to the flat (formula (Formel) based on the HBV and ISO formula) and measured on the flat [35]

In the Figure 3.5, the three points were extracted from *Ebene (Formel)* for both pressure curves, and the factor between 2.9 bar and 2.2 bar was calculated for each point. The average of the three results was 1.4, which was considered the factor between the two pressure values.

After defining the tire pressures, the values for two different curves of rolling resistance were calculated. First, the maximum speed the tire can safely handle (speed rating) for each curve was Q and H. The speed rating for a tire with a Q is 160 km/h, and with a H is 210 km/h. In the Figure 3.6, the symbol 'Q-M+S' means that the tire is designed to mud and snow conditions. V and T are also symbols that represents the speed rating: up to 240 km/ h and 190 km/ h, respectively. For each fill patterns that represent different speed symbol of the graph of the Figure 3.6, it was considering the average between the curve below (minimum values) and the curve above (maximum values) of that pattern. The rolling resistance coefficient varies according to the desirable maximum speed and must be as small as possible.

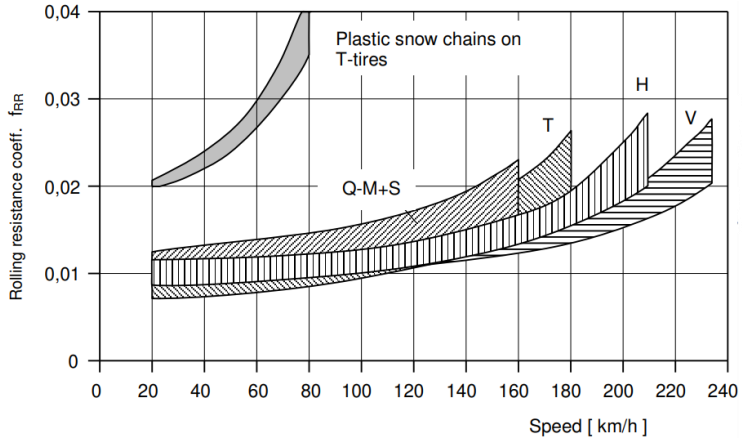


Figure 3.6- Rolling resistance coefficient dependence on the rating speed so the achieved speed must be accomplished. The maximum speed of V, H, and T are 240 km/ h, 210 km/ h, and 190 km/ h, respectively. Q-M+S means that Q is the speed rating symbol, so wheels can go up to 160 km/ h and is designed for mud (M) and snow (S) [36]

However, the results shown in the figure do not consider the different tire pressure. So, it was assumed that the values represented in Figure 3.6 were for 2.9 bar and, for each value, it was multiplied

by 1.4, which allowed us to obtain the rolling resistance coefficient relative to the 2.2 bar. The Eq. 2.2, was used to convert the rolling resistance coefficient, $k_r$, into rolling resistance, $F_r$. According to Figure 3.6, the behaviour of the curve is the same as a polynomial of degree two so, to represent the rolling resistance calculated to the vehicle speed, it was fitted a polynomial tendency line of degree two.

To analyse the influence of the tire pressure, it was used only the Q speed rating regime. In Eq. 3.1, was assumed that the pressure and the vertical load force would be constant during travel in the different simulations, which implies that $\alpha = 1$, and $\beta = 1$. So, 80 % ETRTO will be linked to 2.9 bar and 100 % ETRTO with 2.2 bar. For constant pressure and constant vertical force, a new equation is obtained:

$$F_{RR} = P \cdot F_z(a + b \cdot v_{belt} + c \cdot v_{belt}^2)\ [N] \quad \text{Eq. 3.2}$$

The two equations that describe the rolling resistance behaviour for the Q type are:

$$y = 0.004x^2 - 0.2702x + 107.18\ [N], \text{ for 2.2 bar} \quad \text{Eq. 3.3}$$

$$y = 0.0023x^2 - 0.1548x + 61.386\ [N], \text{ for 2.9 bar} \quad \text{Eq. 3.4}$$

The variable *y* represents the rolling resistance, and the variable *x* represents the vehicle speed. According to the Eq. 3.1 and the two previous equations:

- For 2.2 bar, $a = \frac{107.18}{P \cdot F_z}$, $b = \frac{-0.2702}{P \cdot F_z}$, and $c = \frac{0.004}{P \cdot F_z}$
- For 2.9 bar, $a = \frac{61.386}{P \cdot F_z}$, $b = \frac{-0.1548}{P \cdot F_z}$, and $c = \frac{0.0023}{P \cdot F_z}$

In order to analyse the influence of the tire rolling resistance, it was used the Q and H rating speed type. Comparing the same tire pressure, the H type has less rolling resistance coefficient than the Q type. In Eq. 3.1, it was assumed that the rolling resistance would be independent of the tire which implied α = 0. And the vertical load force would be constant during travel in the different simulations, which implied β = 1. Thus, the equation for the rolling resistance is obtained, and is independent of the tire pressure:

$$F_{RR} = F_z\left(a + b \cdot v_{belt} + c \cdot v_{belt}^2\right)[N] \quad \text{Eq. 3.5}$$

The two equations that describe the rolling resistance behaviour for the H type are:

$$y = 0.0047x^2 - 0.5506x + 100.18\ [N], \text{ for 2.2 bar} \quad \text{Eq. 3.6}$$

$$y = 0.0027x^2 - 0.3153x + 57.374\ [N], \text{ for 2.9 bar} \quad \text{Eq. 3.7}$$

According to Eq. 3.5 and the two previous equations:

- For 2.2 bar, $a = \frac{100.18}{F_z}$, $b = \frac{-0.5506}{F_z}$, and $c = \frac{0.0047}{F_z}$
- For 2.9 bar, $a = \frac{57.374}{F_z}$, $b = \frac{-0.3153}{F_z}$, and $c = \frac{0.0027}{F_z}$

## 3.3 Case Studies

The main goal of the work was to optimize the energy consumption of a fully electric vehicle. However, this optimization can only be achieved if the driving dynamics and driving comfort are also improved. Therefore, simulations were performed to analyse how driving dynamics influence vehicle movement (dynamic driving tests) and to identify factors that can enhance vehicle safety (safety driving dynamics).

For the safety driving dynamics tests, the influence of the autonomous emergency brake (AEB), and the anti-lock braking system (ABS) as systems that can avoid accidents or mitigate the damages. For the AEB evaluation, were considered two vehicles: the test one (Mercedes) and an obstacle one. The objective was to understand if the AEB was able to avoid a collision between both vehicles, or not, and what was the time response. The three tests (Test 1.1.1., Test 1.1.2. and Test 1.1.3.) were adapted from [37]. For the ABS, two tests (Test 1.2.1., Test 1.2.2.) were performed with the same road and vehicle conditions, except the presence of the ABS: in one test the ABS was on, and in the other was off. The idea was to compare the braking distance, the braking torque and the braking slip with, and without the ABS. These two tests were a suggestion of the CarMaker software.

For the dynamic driving tests, one of the tests performed was a circular drive test (Test 2.1.), with constant radius, adapted from the ISO 4138:2004(E). The car increased the speed until its trajectory was different from the vehicle route. By analysing the steering wheel angle, it is possible to conclude if the car suffered understeer or oversteer and determine the vehicle maximum speed for that radius. The electronic stability program (ESP) helps the vehicle to strengthen the loss of traction on the road, so its presence was evaluated in two different tests (Test 2.2. and Test 2.3.) based on the Double Lane Change (ISO 3888-1:2018(E)) and in the Moose Test, which is more evasive than the Double Lane Change. Both tests were preformed twice: one with the ESP on, and the other one with the ESP off. The objective was to analyse the speed steering wheel angle behaviour during the total of four tests (Test 2.2.1. and Test 2.2.2., Test 2.3.1. and Test 2.3.2.).

To analyse the economic driving, different types of tests were performed, and different parameters were analysed. First, were defined two (Test 3.1. and Test 3.2.) ‘aggressive’ tests where the vehicle had to push to its limit: rectangle speed profile and slowly increasing the speed. The first was adapted from US06 Supplemental Federal Test Procedure (SFTP) [38]. The third test (Test 3.3.) was adapted from the Worldwide harmonized Light vehicles Test Cycles (WLTC) that allows to determine the energy consumption of light duty vehicles. The other group of four tests were based on real roads: the Real Driving Emissions (RDE) track (Test 3.4.), where the car is exposed to different conditions; a straight road with the speed profile extracted from the RDE test (Test 3.5.); the travel of a person from his home to the university (Test 3.6.), and the way back (Test 3.7.). Were three the parameters selected: the tire pressure (2.2 bar vs. 2.9 bar), the rolling resistance by changing the speed rating of the tire (Q vs. H), and the extra load using the users (70 kg vs. 280 kg). The objectives were to compare the energy consumption of the vehicle and its energy loss through the tires. Seven tests were chosen for six variables, what gives a total of 28 tests realized in this sector. Plus, the twelve tests where the battery needed to be dimensioned with a higher capacity. Which results in 40 tests.

All case studies were run on dry roads under sunny conditions.

### 3.3.1 Case Study 1- Safety Driving Dynamics

In this case, the objective was to evaluate the influence of the autonomous emergency brake (AEB), and the anti-lock braking system (ABS). The AEB consists of a combination of *RADAR* and sensors that establish a range of potential obstacles that, if a collision is identified, the system will be warning the user and/or brake the car to prevent the collision or to reduce the severity. During a break,

the ABS allows to prevent the four wheels from locking, and it will reduce the braking distance. For both tests, the vehicle was considered occupied by four passengers (including the driver), weighing 70 kg each. Also, all tests were performed on a straight road.

For the AEB test, the range of the sensor was defined as 50 m, which means that the obstacle is detected if the distance between the test-vehicle and the obstacle is between 0 and 50 m. It was defined that if a collision were detected, the simulation would stop immediately. The Figure 3.7 shows the AEB system installed in the car. Also, it was modelled an object which was a car with no specifications. According to the test, the initial conditions and the obstacle behaviour were adapted.

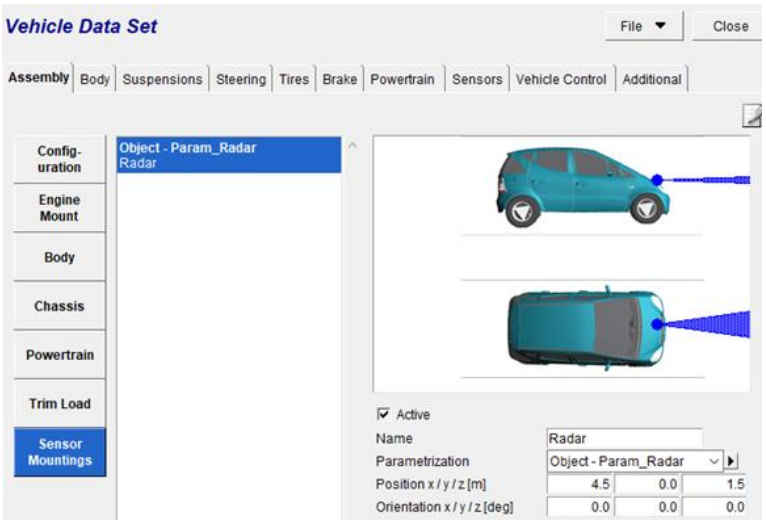


Figure 3.7- Illustration of the AEB system installed in the test-vehicle

To activate the ABS, it was necessary to open the file *SoftABS.mdl* in MATLAB and open the CarMaker GUI (graphical user interface). The file *SoftABS.mdl* is an example, provided by the software, of an ABS model where, in each wheel, the brake pressure is adjusted according to the slip.

The development of the three tests involving the AEB system took into consideration real-world characteristics adopted from [37]. The simplest test (test one) involved a second vehicle, which was immobilized, and the test-vehicle. The test-vehicle approach to the other vehicle with a speed of 50 km/h. The next test was similar to the previous one, but the speed of the test-vehicle increased to 80 km/h (test two). In the final simulation (test three), both objects are moving: the obstacle/ vehicle at 20 km/h, and the test-vehicle at 70 km/h. However, in the CarMaker software, it was possible to define the initial vehicle velocity, $v_i$, and so the test-vehicle and the object could start the simulation with 70 km/h and 20 km/h, respectively. The obstacle was defined at a considerable distance from the vehicle to avoid simulation errors regarding the speed of both vehicles. The Figure 3.8 illustrates the test condition.

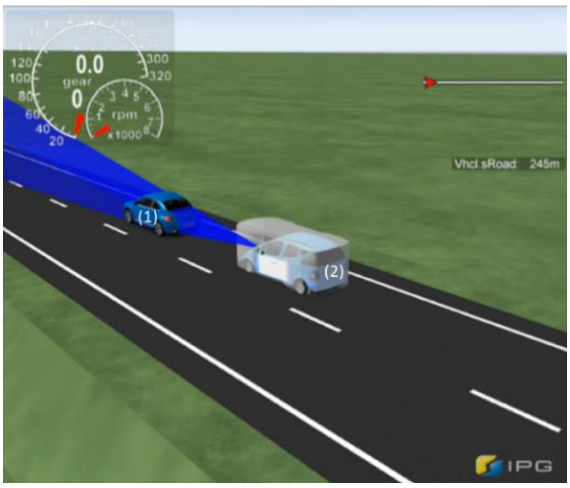


Figure 3.8- Illustration of the AEB test scenarios. (1)- obstacle; (2)- test-vehicle

Regarding the ABS, two tests were performed (Figure 3.9) and its conditions are resume in Table 4.1, where both speed conditions and braking time were the same for both tests. In one of the tests, the ABS system was installed in the vehicle, while in the second one, it was not. The car accelerates up to 120 km/h on a road with a friction coefficient of 1, then it changes to 0.4 1s before the vehicle reaches the desired speed. After it reaches the target speed, the acceleration pedal is released, and 1s after, the car applies full braking until the car stops.

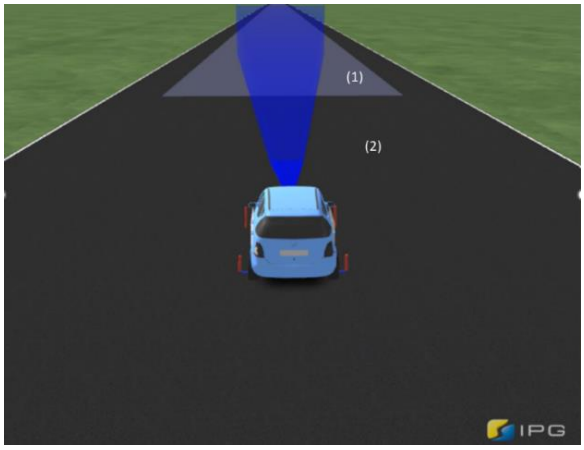


Figure 3.9- Illustration of the ABS test scenarios. (1) coefficient road friction of 0.4; (2)- coefficient road friction of 1

### 3.3.2 Case Study 2- Dynamic Driving Tests

The dynamic behaviour of the vehicle is challenging to evaluate due to the interaction between the driver, the car, and the environmental conditions. In order to obtain relevant data, three main tests (Test 2.1., Test 2.2., and Test 2.3.) were simulated. For the three tests, the vehicle was only occupied by the driver and all simulations were performed for a straight road. In two of these three testes, the influence of the electronic stability program (ESP) was evaluated by performing the same with and without the system (Test 2.1.1, and Test 2.2.2.). To activate the system, it was necessary to use the file *HydBrakeCU_ESP.mdl* in MATLAB and use the CarMaker GUI. After selecting the desired test, the brake control model had to be *CMASL User Model*, and the brake system model had to be changed to *HydESP*. The file *HydBrakeCU_ESP.mdl* is an example, provided by the software, of an ESP controller that can act even without the driver's brake pedal.

#### 3.3.2.1 Case Study 3- Circular Drive Test

In the circular drive test (Test 2.2.), the vehicle was driven on a straight road for 35 seconds (50 meters), approximately, to avoid issues related with simulation conversion, until it started to move in a counterclockwise direction at a continuous speed increase. The test only stopped when the vehicle stayed out of the desired vehicle. The radius of the circular path was 42 m. This test was based on [39] and allows us to understand when understeer or oversteer happens while driving. Increasing the toe slip angle, for example, can reduce the occurrence of one of the previous events, and so, energy losses will be lower, and the user's safety is guaranteed. The Figure 3.10 illustrates the test road conditions.

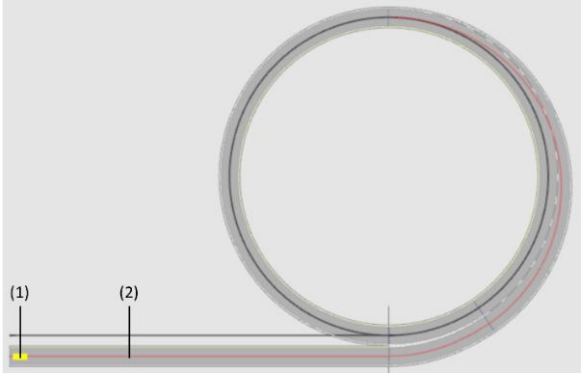


Figure 3.10- Illustration of the test road of the Circular Drive test. (1)- test-vehicle; (2)- in red, the vehicle route

#### 3.3.2.2 Case Study 3- ESP Test

In the real world, sometimes the vehicle needs to change its direction due to some obstacle in the road. The double lane change test evaluates these extreme scenarios where the car needs to be at its best performance to contour the obstacle and provide maximum safety. The most relevant parameters to be analyse were related with the steer-wheel and with lateral dynamics. The dimensions of the double lane change can be consult in the Table 3.5, whose illustration and sections are represented in the Figure 3.11. This test was adopted from [40] and, in CarMaker, the points represented in the Figure 3.11 were modelled as cones. The driver drove the car in a straight road to achieve a speed of 80 km/h and, at the exact moment he reaches the section 1, the accelerate pedal was released and the driver had to move the car through the track, as fast as possible.

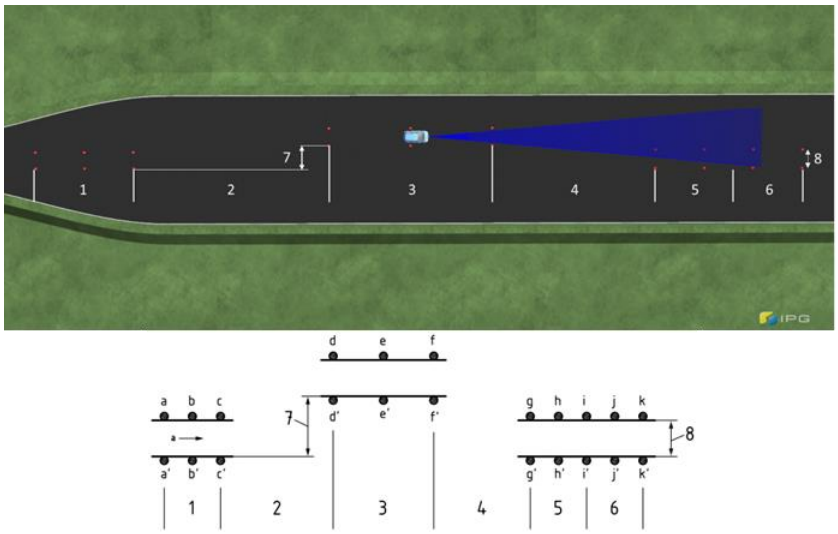


Figure 3.11- Illustration of the Double Lane Change track test and its sections. On top, the CarMaker image and, below, the standard measurements, where the 'a' with the arrow indicates the movement direction [40]

Table 3.5- Dimensions of the Double Lane Change test track [40]

| **Section** | **Length**<br>m | **Lane offset**<br>m | **Width**<br>m |
|---|---|---|---|
| **1** | 15 | - | 2.219 |
| **2** | 30 | - | - |
| **3** | 25 | 3.5 | 2.398 |
| **4** | 25 | - | - |
| **5** | 15 | - | 2.577 |
| **6** | 15 | - | 2.577 |

Equivalent to the previous test, the Moose Test (Test 2.3.1, and Test 2.3.2.) improves the safety of the vehicle's users, however, it is an evasive manoeuvre. In this test, and based on [41], the driver must enter the track at 60-65 km/h, keep a constant speed in all the track and do it as fast as possible. The track was modelled as the double lane change, but with track dimensions represented in the

Table 3.6. In CarMaker, the driver drove the car in a straight road to achieve a speed of 60 km/h, before entering in the track. Also, the ESP was tested in these simulations.

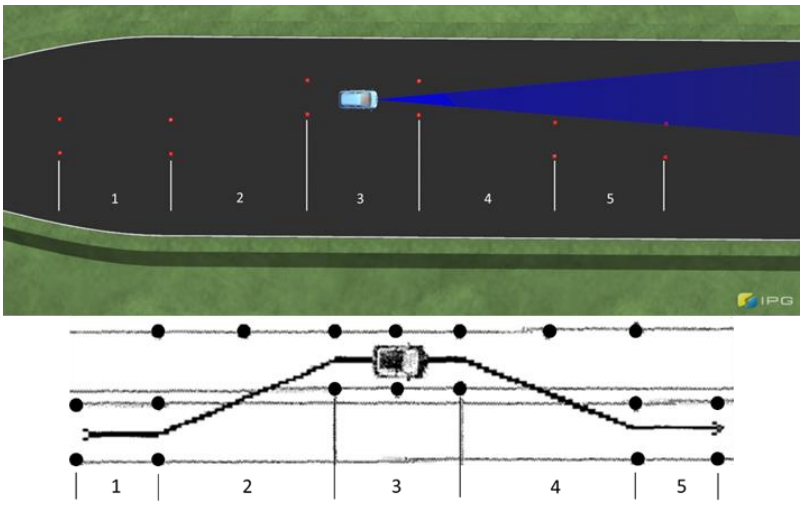


Figure 3.12- Illustration of the Moose Test track and its sections. On top, the CarMaker image and, below, the standard measurements [41]

Table 3.6- Dimensions of the Moose Test track [41]

| **Section** | **Length**<br>m | **Lane offset**<br>m | **Width**<br>m |
|---|---|---|---|
| **1** | 11 | - | 3 |
| **2** | 13.5 | - | 3 |
| **3** | 11 | 4 | 3 |
| **4** | 13.5 | - | 3 |
| **5** | 11 | - | 3 |

### 3.3.3 Case Study 3- Economic Driving Tests

The focus of these simulations was the influence of the energy losses through the tires and how it contributes to the energy consumption of the vehicle. For a comprehensive understanding of the problem, tire pressure, tire rolling resistance and the extra weight in the car were varied. The parameters that will be compare are summarized in Table 3.7:

Table 3.7- Summary of the components compared and the conditions of the other variables for the economic driving tests. *In this test the system was considered independent from the tire pressure

| **Comparison** | **Speed Rating** | **Tire Pressure**<br>bar | **Extra Load**<br>kg |
|---|---|---|---|
| Tire Pressure | Q | 2.2 | 280 kg |
| | | 2.9 | |
| Rolling Resistance | H | 2.2 | 280 kg |
| | Q | | |
| Rolling Resistance | H | 2.9 | 280 kg |
| | Q | | |
| Extra Load | Q | 2.2* | 70 kg |
| | | | 280 kg |

#### 3.3.3.1 Extreme Driving Tests

The two tests that simulated extreme driving conditions: a rectangle speed profile (Test 3.1.) and slowly increasing speed (Test 3.2.). In the first test, the driver increases the speed as fast as possible until 50 km/h, then maintains a constant speed for 20 seconds, and applies full braking until the car stops. The same process is repeated for 80 and 130 km/h. The second test type is similar to the previous one, but instead of braking, the driver increases the speed to 50, 80 and 130 km/h. Both tests were performed in the straight and dry road, so the only relevant tire force to analyse was the tire rolling resistance. To evaluate the cases from Table 3.7, each test was performed 8 times with the different variables present in the table.

#### 3.3.3.2 World Light vehicles Test Procedures

The European NEDC was a test cycle for the determination of emissions and the fuel consumption. However, NEDC needed an update, and so it was replaced by the World Light vehicles Test Procedures. This type of test is more similar to the actual travels and includes several Worldwide harmonized Light vehicles Test Cycles (WLTC). The cycle definitions depend on the vehicle maximum speed and the type of the vehicle. In the case of the pure electric vehicles, there is two type of tests that can be performed, according to the maximum speed: equal or higher than 120 km/h (class 3b) and lower than 120 km/ h (class 3a). To the case study, the test type choose was for the PEV and for the class 3b. The data were extracted from [42]. To evaluate the cases from Table 3.7, the test (Test 3.3.) was performed 8 times with the different variables present in the table.

#### 3.3.3.3 Driving Tests Based on Real Scenarios

Based on real roads, four different tests were modelled and simulated in the software. The first one, was a ride that fulfils the requirements of a Real Driving Emissions (RDE) track- from Karlsruhe, Germany, via Wörth am Rhein to Speyer and back (Test 3.4.). Then, the speed profile was collected and applied in a straight track (Test 3.5.). The other test was a typical track that a student ride from his home until the university (Test 3.6.)- from Cacém, Portugal, via IC19 to C8 Building of the Faculty of Sciences of the University of Lisbon. The opposite route was also simulated (Test 3.7.). To evaluate the cases from Table 3.7, each test was performed 8 times with the different variables present in the table.

For the first test (RDE), the GPS data was provided by the researchers from KIT, however, only longitude and latitude were possible to be modelled in the software. In the scenario editor of the CarMaker software, this file was inserted, and the track was automatically generated (Figure 3.13). The next step was to clean all the “interrupted” roads: due to some superposition of road points it was necessary to delete a certain number of branches. The desired speed profile contained in the file was not possible to associate to each point because some of the data was deleted and so, the time interval was irregular. To solve the issue, speed limits were defined with the help of *Google maps*, so the driver had to complete the track as fast as possible while respecting speed limits. It is also important to highlight that in all simulations of this section, road signs (stop signs, light signals, and others), road traffic, pedestrian traffic, and altitude were ignored.

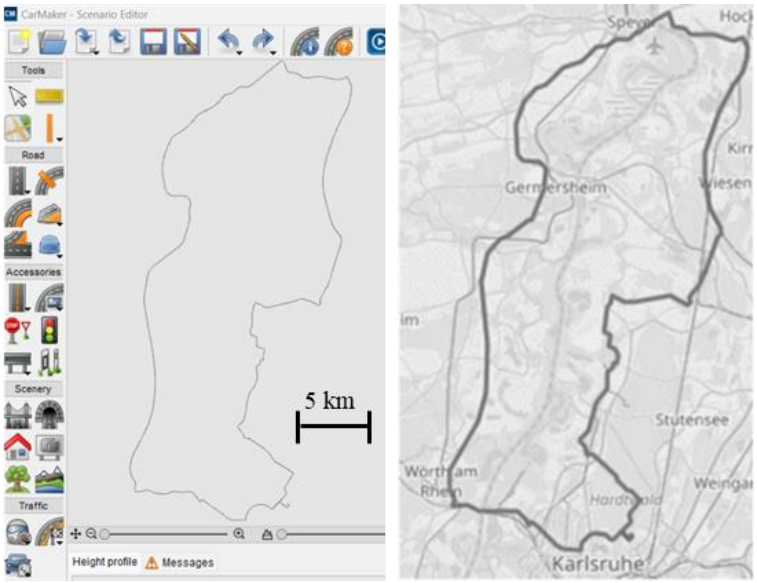


Figure 3.13- Illustration of the RDE track. On the left, the software results and, on the right, the real image of the ride around Karlsruhe [43]

The modulation of the last test (home to university and vice versa) was similar to the previous one: the GPS data were extracted from *Google My Maps* (*kml* file format). Here, the altitude was also neglected. Everything else about the process, from eliminating overlapping points to limiting speed, was the same as the previous test. The track is represented in the Figure 3.14.

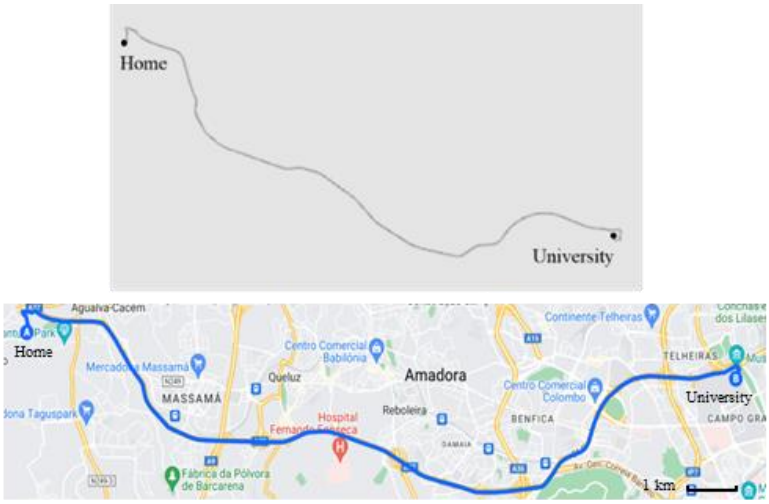


Figure 3.14- Illustration of the track from Cacém (Home) to C8 building/FCUL (University), and vice versa. On the top, are the software results and, below, an image from the real route obtained from the *Google My Maps*

# 4 Results and Discussion

## 4.1 Case Study 1- Safety Driving Dynamics

The results related to the AEB, and the ABS simulation tests are presented in this section, and its test conditions (Table 4.1).

Table 4.1- Resume of the conditions of the AEB tests (Test 1.1.1., Test 1.1.2., and Test 1.1.3.) and of the ABS tests (Test 1.2.1. and Test 1.2.2.)

| | **Test Car** $v_i$ km/ h | **Obstacle Car** $v_i$ km/ h | **Max. Test Car** $v_{max}$ km/ h | **Initial Friction Coefficient** [ ] | **Final Friction Coefficient** [ ] | **ABS System** | **AEB System** |
|---|---|---|---|---|---|---|---|
| **Test 1.1.1.** | 50 | 0 | - | - | - | Off | On |
| **Test 1.1.2.** | 80 | 0 | - | - | - | Off | On |
| **Test 1.1.3.** | 70 | 20 | - | - | - | Off | On |
| **Test 1.2.1.** | 0 | - | > 120 | 1 | 0.4 | Off | Off |
| **Test 1.2.2.** | 0 | - | > 120 | 1 | 0.4 | On | Off |

For each of the three AEB simulation tests, the speed of the test-vehicle and its distance to the obstacle were analysed. Figure 4.1, Figure 4.2, and Figure 4.3 show the results for test one, test two, and test three, respectively. All three tests involved a vehicle (obstacle). In Test 1.1.1., the test-vehicle approached to the other vehicle, which was immobilized, with a speed of 50 km/h. In Test 1.1.2., the approached speed was 80 km/h. In the last test, Test 1.1.3., the obstacle was moving at 20 km/h, and the test-vehicle at 70 km/h.

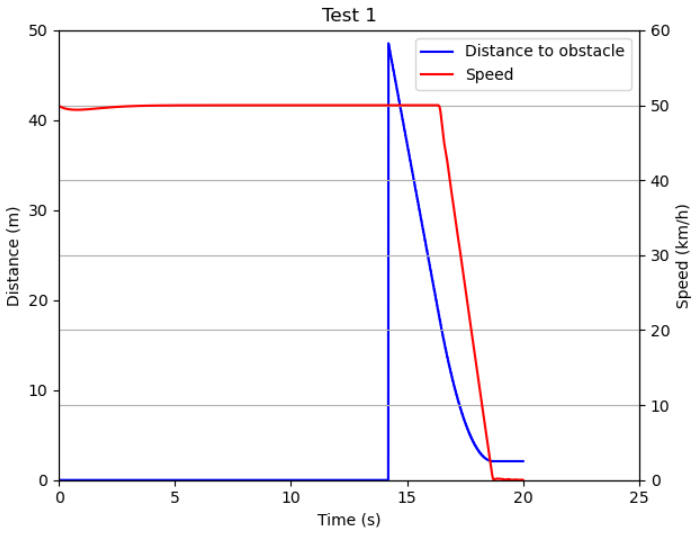


Figure 4.1- Distance between the test-vehicle and the obstacle and its speed during the AEB simulation of the test one

In the Figure 4.1, it's possible to conclude that the total time of the simulation was 20 s. At 50 m, approximately, the *RADAR* detected the obstacle, as defined, and it happened at the moment t = 14 s, approximately. The difference between the 50 m and the maximum of the blue curve is owed to the delay between the object detention and the approximation of the vehicle test to the obstacle. This also happened for the tests 1.1.2 and 1.1.3. The speed of the car started to decrease at t = 16 s, which means that 2 s after the detection of the obstacle, the AEB system started to brake the car. In the end, the car stopped, and the accident was avoided. The final distance between the two objects were 2.10 m, and he brake distance was 16.50 m.

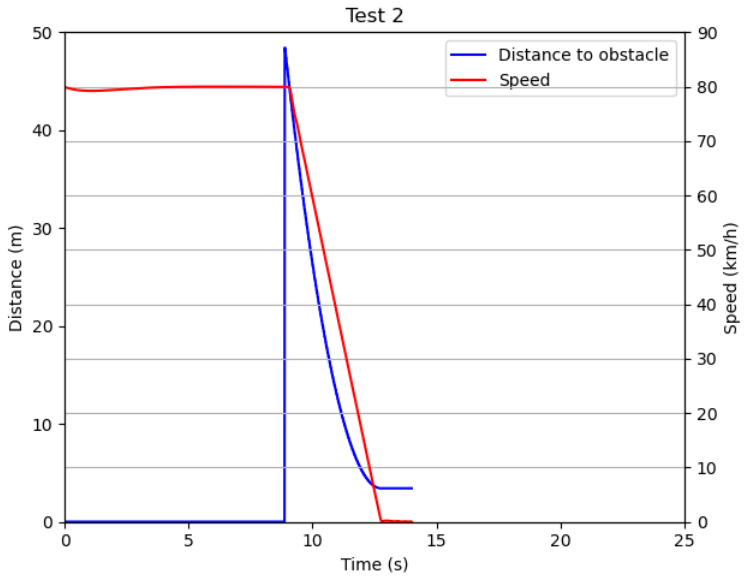


Figure 4.2- Distance between the test-vehicle and the obstacle and its speed during the AEB simulation of the test two

In the Figure 4.2, it is possible to conclude that the total time of the simulation was 14 s, approximately. At 50 m, the *RADAR* detected the obstacle, as defined, and it happened at the moment t = 9 s, approximately. The speed of the car started to decrease (braking activation) almost immediately after the obstacle detection. In the end, the car stopped, and the accident was avoided. The final distance between the two objects were 3.40 m, and he brake distance was 41.70 m.

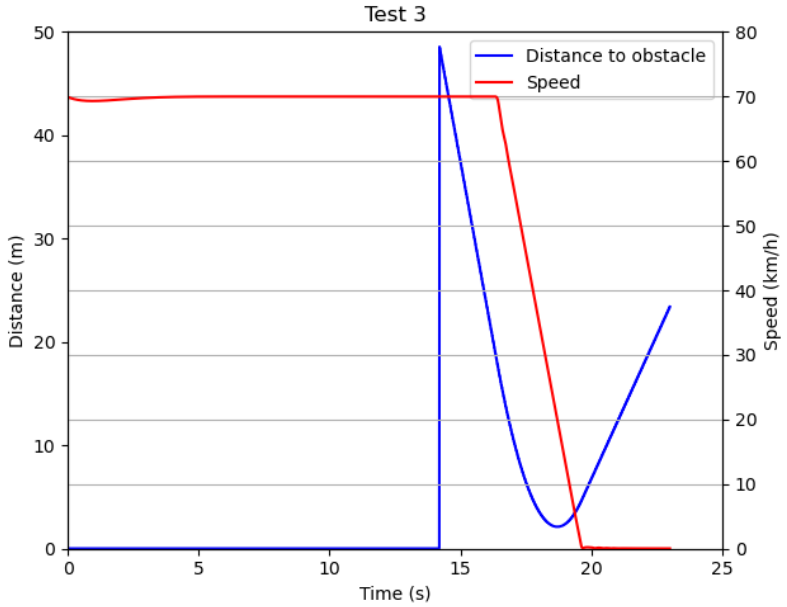


Figure 4.3- Distance between the test-vehicle and the obstacle and its speed during the AEB simulation of the test three

In Figure 4.3, it is possible to conclude that the total time of the simulation was 23 s, but the events of interest occurred until t = 19 s. At t = 14 s, the *RADAR* detected the obstacle, and the car started to brake two seconds after the previous event. After the minimum of the blue curve, the distance between the two objects started to increase because the obstacle kept its movement, which was 20 km/h. However, the minimum of the curve is equivalent to the shortest distance of the two cars- 2.10 m. This distance was reached when the two vehicles had the same velocity, 20 km/ h (t = 19 s). And the brake distance until the vehicle standstill and reached the minimum distance from the obstacle was 32.12 m and 29.50 m, respectively.

Table 4.2 summarizes the important data analysed in the previous figures.

Table 4.2- Initial speed, $v_i$, of the two objects, time when the AEB system detected the obstacle, and when it activated the brakes, the shortest distance between the two vehicles, and the brake distance from the moment the test car starts to brake until it reaches the minimum distance between it and the obstacle, for the three tests. All times are referring to the time t = 0 s

| | **Test Car** $v_i$ km/ h | **Obstacle Car** $v_i$ km/ h | **AEB Detection** s | **Brake Activation** s | **Minimum Distance between Obstacles** m | **Brake Distance until Shortest Distance** m |
|---|---|---|---|---|---|---|
| **Test 1.1.1.** | 50 | 0 | 14.20 | 16.35 | 2.10 | 16.50 |
| **Test 1.2.1.** | 80 | 0 | 8.88 | 9.03 | 3.40 | 41.70 |
| **Test 1.3.1.** | 70 | 20 | 14.20 | 16.35 | 2.10 | 29.50 |

From Table 4.2, it is possible to conclude that as high as the speed difference between the two vehicles, the response of the AEB system is faster to anticipates the brake distance, and avoid the accident, allowing a safe standstill of the test-vehicle.

The travelled distance and the vehicle speed in the ABS test simulations are shown in **Error! Reference source not found.**. For both tests, the car accelerates for, approximately, 43 seconds and

rolls during 1 second. At this moment, it is applying full braking, which leads to different speed and driving distances.

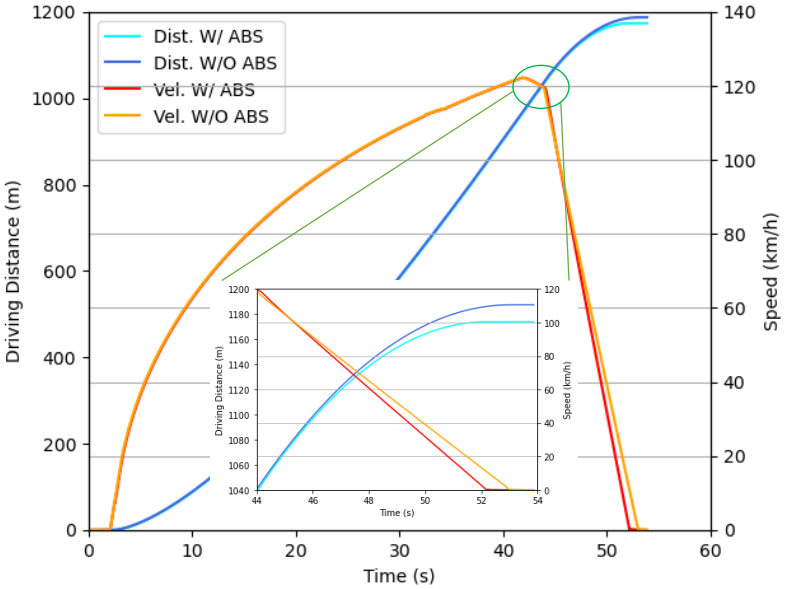


Figure 4.4-Representation of the vehicle driving distance with the ABS system (Dist. W/ ABS), and without the ABS system (Dist. W/O ABS), and the vehicle speed during the simulation with the ABS system (Vel. W/ ABS), and without the ABS system (Vel. W/O ABS)

In the Figure 4.4, the car starts to brake at, approximately, t = 44 s. It is possible to see the different speed values during the braking due to the presence of the ABS system. The simulation where the ABS system was not installed, the braking distance was 154 meters. With the activation of the ABS system, the braking distance was reduced to 140 meters. In Figure 4.4 it is possible to see a slight difference in the driving distance, from the moment t = 50 s until the end of the simulation. The activation of this automated system can be observed on the Figure 4.5, where it compares the total brake torque with the braking slip.

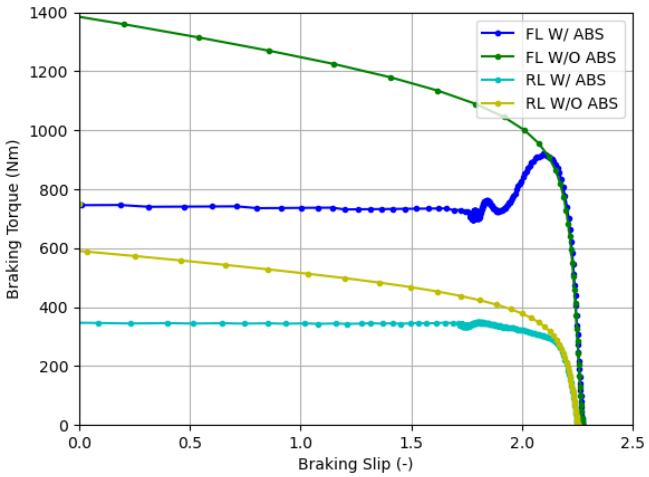


Figure 4.5- Comparison between the total braking torque and the braking slip, for both ABS simulations, during the braking part of the test. It is only shown the front left (FL) tire and the rear left (RL) tire, however, the behaviour of the tires from the same axle can be considered the same

As it is possible to see from Figure 4.5, the curves refer to the simulation without ABS, are always decreasing, which means, the only variable that is present in the brake is the brake pedal. In the other curves, when the values of braking slip are between 1.7 and 2.3, the fluctuations indicate the presence of an “external” source that is applied in the brakes- ABS. This helps to control the force that is applied in the brakes, to not block the rolling movement of the tires, so the car reduces its braking distance and, in case it needs to change its movement direction, it can do it.

With this work, it is possible to verify and quantify how both the AEB and ABS systems installed in an electric vehicle can prevent and/or mitigate accidents between the car and an obstacle. With the AEB it can help situations where the driver cannot see the obstacle, for example, at the call “death angles”, by brake and, possibly, avoid the accident. The ABS helps the driver to standstill the vehicle in a safety way by preventing the block to movement of the tires. This work can be replicated for an ICE light-duty vehicle.

## 4.2 Case Study 2- Dynamic Diving Tests

### 4.2.1 Circular Drive Test

Figure 4.6 represents the results regarding the speed profile and the steering wheel angle during the circular motion for the Circular Drive test,

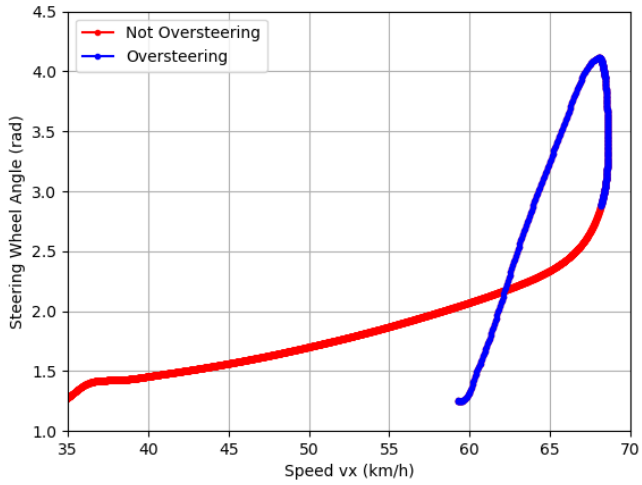


Figure 4.6- Representation of the dependence of the horizontal speed on the steering wheel angle in the Circular Drive test when the car is accelerating in the circular circuit

Figure 4.6- Representation of the dependence of the horizontal speed on the steering wheel angle in the Circular Drive test when the car is accelerating in the circular circuit it is possible to observe from the red curve the steering wheel angle increases as the speed also increases; however, at higher speeds, it develops more rapidly. When the speed reaches 68.7 km/h it stops decreasing and keeps constant until the breakdown (blue curve): oversteer. This means that the car test cannot perform a curve, with a radius of 42 meters, at a speed of 68 km/h or higher.

### 4.2.2 ESP Test

Table 4.3 summarizes the test conditions for each test presented in this section.

Table 4.3- Resume of the conditions of the Circular test (Test 2.1.), The Double Lane Change tests (Test 2.2.1. and Test 2.2.2.) and of the Moose tests (Test 2.3.1. and Test 2.3.2.)

| | **Track Radius** m | **ESP System** | **Tracker Input Speed** km/ h | **Speed During Track** |
|---|---|---|---|---|
| **Test 2.1.** | 42 | - | - | Accelerated |
| **Test 2.2.1.** | - | Off | 80 | Decelerated |
| **Test 2.2.2.** | - | On | 80 | Decelerated |
| **Test 2.3.1.** | - | Off | 60 | Constant |
| **Test 2.3.2.** | - | On | 60 | Constant |

For the Double Lane Change analysis, only the results regarding the track were subject to the study. The initial acceleration was to allow the reduction of the software errors in the final data. Figure 4.7 and Figure 4.8 show the speed profile and the steering wheel angle behaviour during the simulations for a vehicle with and without ESP system, respectively.

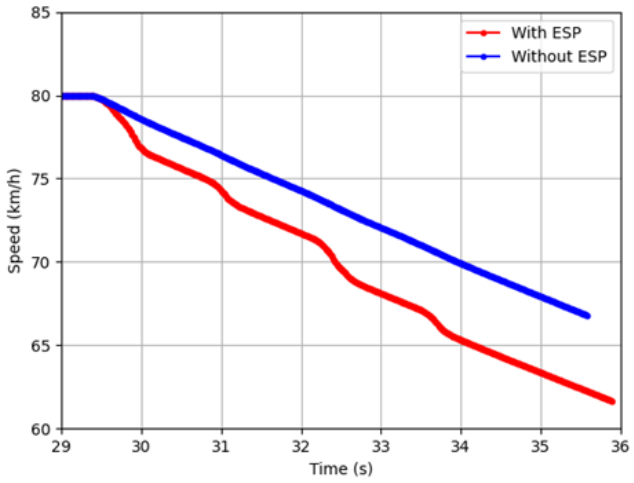


Figure 4.7- Speed profile of the Double Lane Change test track and for the simulations where ESP was and was not installed

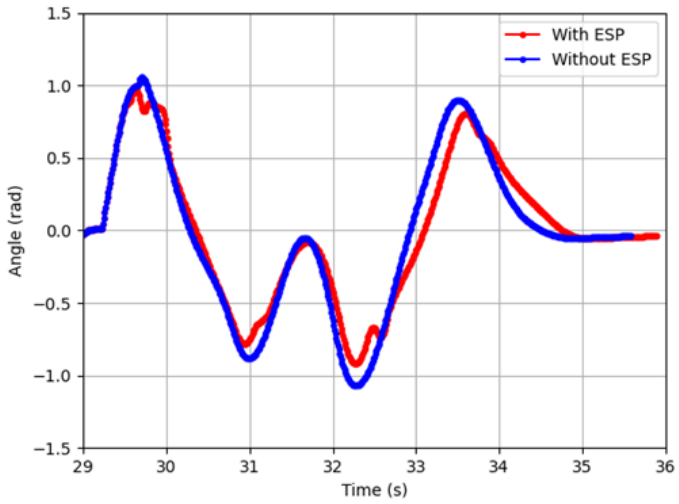


Figure 4.8- Steering wheel angle behaviour during the Double Lane Change test track and for the simulations where ESP was and was not installed

In Figure 4.7, the speed of the car equipped with ESP undergoes a sharper reduction when compared to the car without ESP installed. The system allows the reduction of the torque from the electric drive unit or activates the brakes individually to reduce the speed and rectify the position of the vehicle. In Figure 4.8, when the values increase, it is equivalent to the steering wheel turning to the left, and when it decreases it is equivalent to the steering wheel turning to the right. If the curve is constant, the steering wheel does not change its position, and when the derivative is zero, the steering wheel changes its position. Also, if the angle is zero radians, the steering wheel is in neutral position. As it is possible to see in Figure 4.8, the ESP allows for attenuation of the changes in the movement direction of the car preventing the understeer or the oversteer. Also, it is possible to identify the different sections of the track: zone 1, 29.2 to 29.8 s; zone 2, 29.8 to 31.0 s; zone 3, 31.0 to 31.6 s; zone 4, 31.6 to 33.5 s; and zone 5, 33.5 to 34.8 s. This proves that the system allows a safer travel and helps the driver to “control” the car in case of an emergency, where the movement direction of the vehicle must be, suddenly, changed.

As in the previous simulation, and for the Moose Test, only the results regarding the track were subject in the study. Figure 4.9 and Figure 4.10 show the speed profile and the steering wheel angle behaviour during the simulations for a vehicle with and without ESP, respectively.

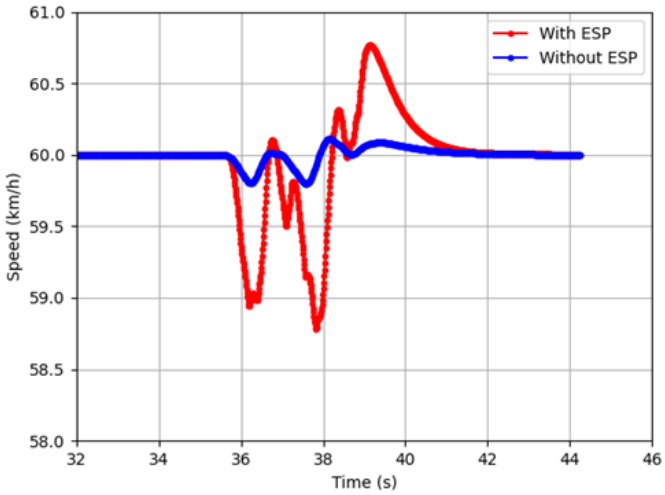


Figure 4.9- Speed profile of the Moose Test track and for the simulations where ESP was and was not installed

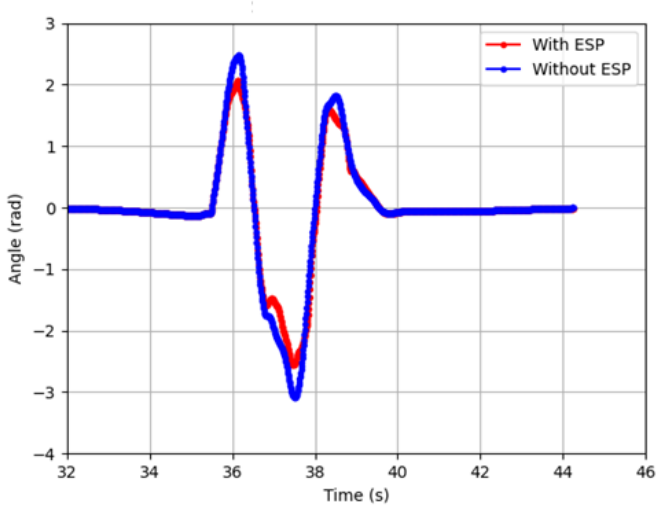


Figure 4.10- Steering wheel angle behaviour during the Moose Test track and for the simulations where ESP was and was not installed

The speed variation, in Figure 4.9, occurred in the simulation where the ESP was installed because this system reduced the car velocity and, to compensate for this loss, the system makes the car accelerate until reaches the desired speed; however, it may pass the desired speed in $t \in [38, 40]$ due to the excessive boost. In Figure 4.10, is possible to see the actuation of the system when the angle of the steering wheel is too high, or too low. Also, it is possible to identify the different sections of the track: zone 1, 35.8 to 36.1 s; zone 2, 36.1 to 37.8 s; zone 3, 37.8 to 38.8 s; zone 4, 38.8 to 39.9 s; and zone 5, 39.9 to 40.2 s.

## 4.3 Case Study 3- Economic Driving Tests

The test results concerning the vehicle's energy consumption are presented in this section. The tire energy losses due to the camber angle were not considered since the losses resulting from this force are nearly zero. Also, when the RDE test and the test that used the speed profile from the previous one involved a full passenger capacity, with a Q type tire using a pressure of 2.2 bar, the car did not finish

the circuit. Thus, and in addition to other factors under evaluation, such simulations were performed with a battery parameterization different from the original.

### 4.3.1 Extreme Driving Tests

The speed profile of the test which encompasses a gradual speed increase before a sharp speed reduction is, from now on, called “Different Speed”, and is represented in the graph in Figure 4.11. The maximums between each acceleration are due to the time the simulations needed to converge to the desired vehicle speed.

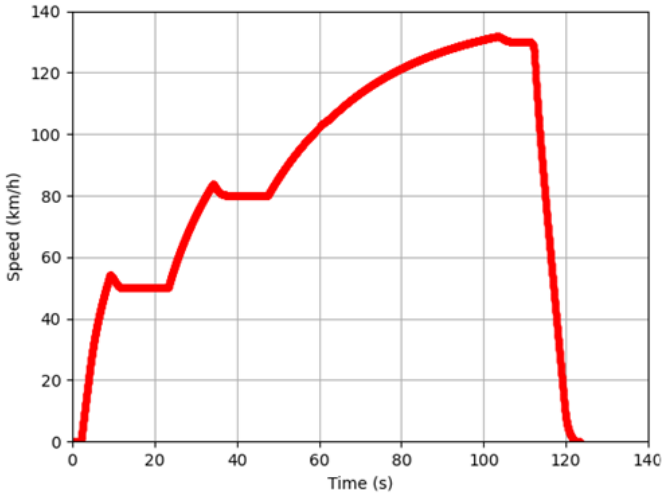


Figure 4.11- Speed profile of the Different Speed simulation. In this case, it corresponds to a Q tire type with 2.9 bar

During this simulation, the car travelled 3 km with a tire pressure of 2.9 bar, with a consumption of 0.33 kWh/ km. With a tire pressure of 2.2 bar, the car travelled 760 m more than the previous case, and vehicle consumption was 0.35 kWh/ km. With a high tire pressure, the vehicle achieved the desire speed faster than with a lower one.

The energy losses due to the tire rolling resistance in the Different Speed simulations are represented in the Figure 4.12 for the different vehicle tires.

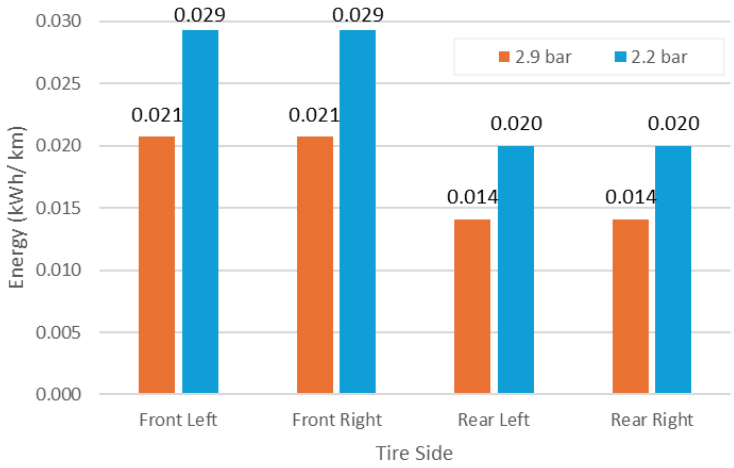


Figure 4.12- Energy losses per kilometre due to the tire rolling resistance for the tire pressure of 2.2 bar and 2.9 bar of the Q tire type in the Different Speed tests

In Figure 4.12 it is possible to see that the major energy losses occurred in the front tires. This occurred because the layout of the drive system is coupled to the front axle. The losses are higher with a lower tire pressure due to the contact area between the tire and the surface is higher than for the case of 2.9 bar tire pressure. The losses in the 2.2 bar tires were, approximately, 30 % higher than the losses in the 2.9 bar tire and contributed 28 % to the total energy consumption, while the tires with lower pressure contributed only 21 %.

The speed profile of the test that was described as Rectangle Speed is represented in the Figure 4.13.

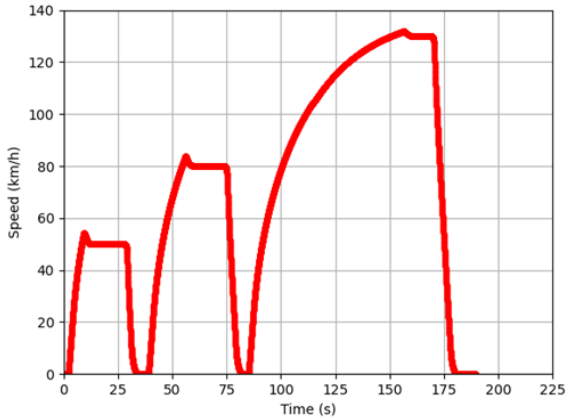


Figure 4.13- Speed profile of the Rectangle Speed simulation. In this case, for Q tire type with 2.9 bar

As in the previous test, the car travelled different distances with 2.2 bar and 2.9 bar tire pressure: 4.5 km and 3.7, respectively. With the higher tire pressure, the car takes less time to achieve the desire speed. The consumption per kilometre was, approximately, the same for the two cases, so 0.35 kWh/ km for 2.9 bar and 0.36 kWh/ km for 2.2 bar. The energy losses due to the tire rolling resistance in the Rectangle Speed simulations are represented in the Figure 4.14.

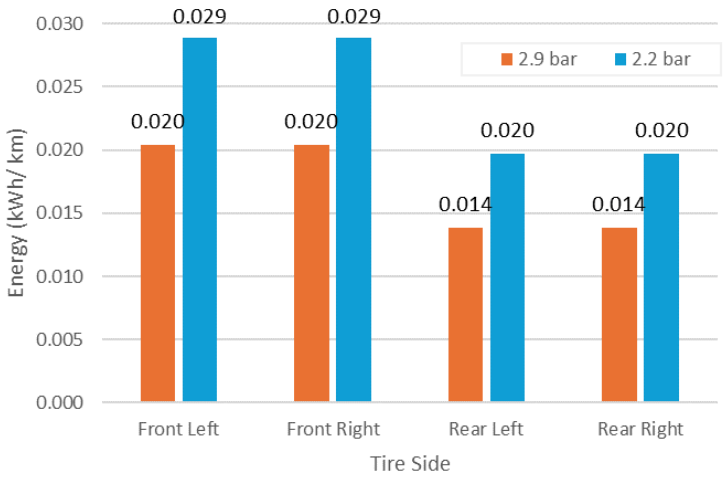


Figure 4.14- Energy losses per kilometre due to the tire rolling resistance for the tire pressure of 2.2 bar and 2.9 bar of the Q tire type in the Rectangle Speed tests

In Figure 4.14, it is possible to see that most energy losses occurred in the front tires, and the losses are higher with lower tire pressure. Comparing the losses in the 2.2 bar tire are, approximately, 30 % higher than the losses in the 2.9 bar tire and they contributed 27 % of total energy consumption, while the tires with higher pressure contributed only 20 %.

### 4.3.2 World Light Vehicles Test Procedures

In the WLTP test, the car travelled 23 km, with both tire pressure types, where its speed profile is represented in Figure 4.15.

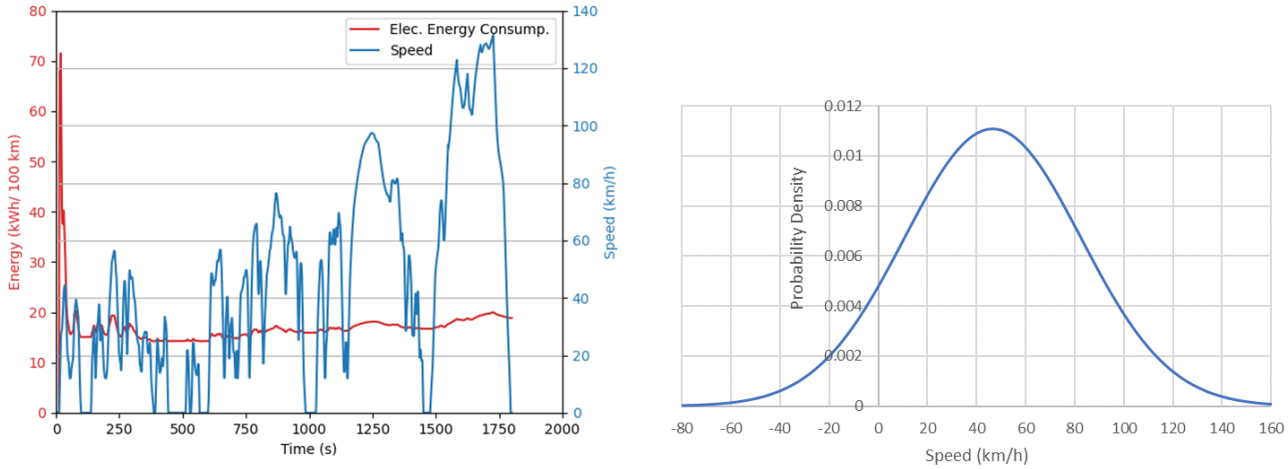


Figure 4.15- Speed profile of the WLTP simulation and its average energy consumption (left) and its normal distribution (right). In this case, for Q tire type with 2.9 bar and 280 kg extra load due to the presence of passengers. The average, median and 2 times the standard deviation (± 2σ) is 46.46 km/ h, 41.53 km /h, and ± 71.90 km/ h, respectively

The consumption per kilometre was, approximately, the same with 0.20 kWh/ km for 2.9 bar, and 0.22 kWh/ km for 2.2 bar. The energy losses due to the different forces applied in the tire that occurred in this simulations are represented in the Figure 4.16 and in Figure 4.17 for 2.2 and 2.9 bar, respectively.

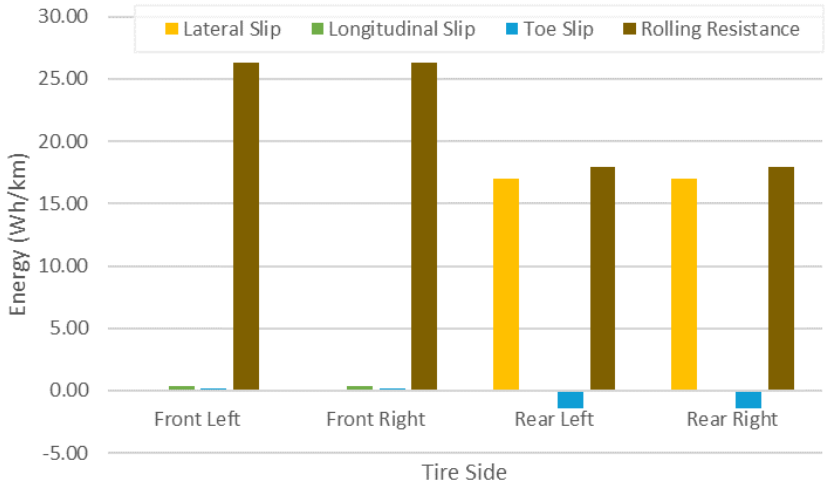


Figure 4.16- Energy losses per kilometre due to the lateral slip, the longitudinal slip, the toe slip and the rolling resistance for the tire pressure of 2.2 bar of the Q tire type in the WLTP test

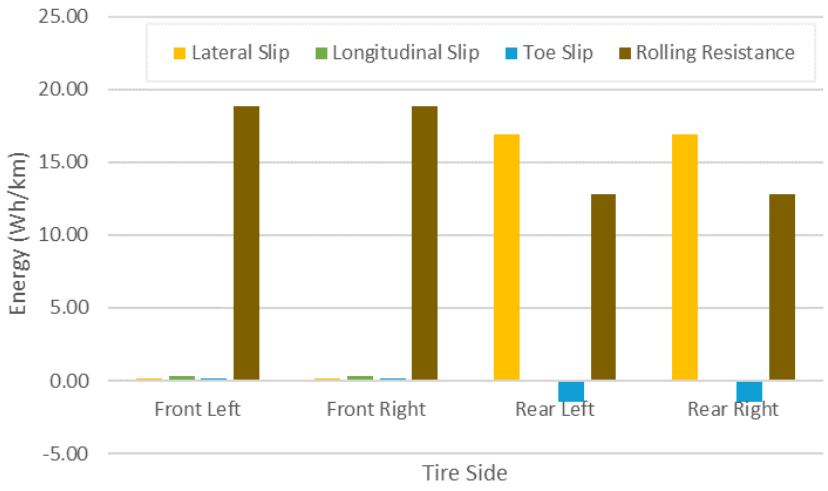


Figure 4.17- Energy losses per kilometre due to the lateral slip, the longitudinal slip, the toe slip and the rolling resistance for the tire pressure of 2.9 bar of the Q tire type in the WLTP test

The two forces that are highlighted in the graphs (Figure 4.16 and Figure 4.17) are the lateral slip for both rear tires and the rolling resistance for all the tires. The negative values indicates that, in overall, there was an energy gain by toe slip. This is possible when the tire is twisted and thus winds up like a spring- gain in potential energy. This gain was about the same for both pressures. The main differences are in the rolling resistance, where most losses occurred. The total energy losses in the 2.2 bar tire were about 21 % higher than the 2.9 bar tire. In these values, the gains were considered. However, for the total tire energy consumption this difference was not relevant since, with 2.9 bar, the tires lost about 0.100 kWh/ km, and contributed for 48 % of the vehicle energy consumption. With 2.2 bar, the tires lost 0.121 kWh/ km which contributed to 54 % of the final energy consumption of the car.

### 4.3.3 Driving Tests Based on Real Scenarios

The speed profile of the RDE simulation and the normal distribution are represented in Figure 4.18.

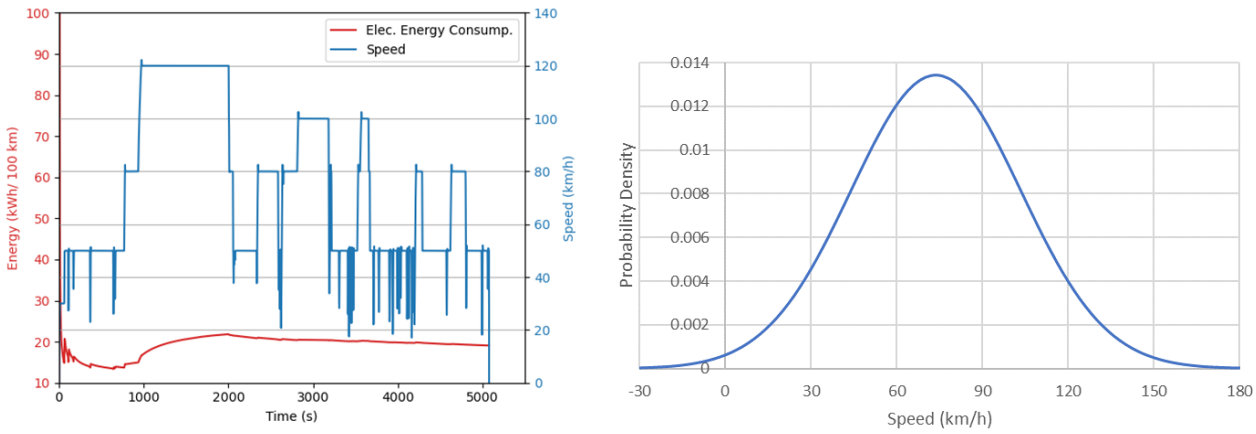


Figure 4.18- Speed profile of the RDE simulation, and its average energy consumption (left) and its normal distribution (right). In this case, for Q tire type with 2.9 bar and 280 kg extra load

The length of the circuit was 104 km, approximately, but in the simulation where the car was equipped with a tire pressure of 2.2 bar, it only travelled 94 km. Here, the capacity of the battery was not enough for the energy demand of the car. The consumption per kilometre was 0.21 kWh/ km for 2.9 bar, and 0.27 kWh/ km for 2.2 bar. The energy losses due to the different forces applied in the tire that occurred in these simulations are represented in the Figure 4.19 and in the Figure 4.20 for 2.2 and 2.9 bar, respectively.

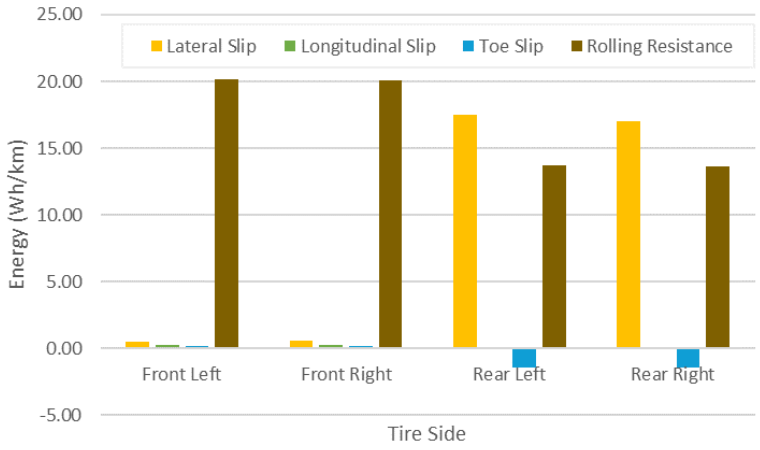


Figure 4.19- Energy losses per kilometre due to the lateral slip, the longitudinal slip, the toe slip and the rolling resistance for the tire pressure of 2.2 bar of the Q tire type in the RDE test

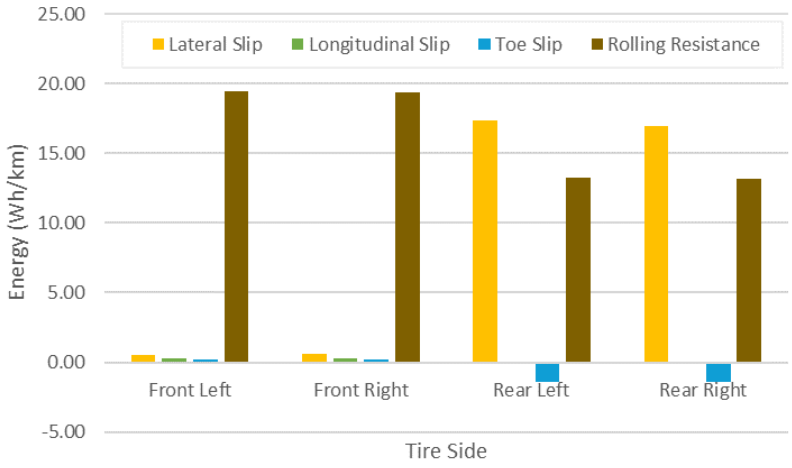


Figure 4.20- Energy losses per kilometre due to the lateral slip, the longitudinal slip, the toe slip and the rolling resistance for the tire pressure of 2.9 bar of the Q tire type in the RDE test. The average, median and 2 times the standard deviation ($\pm 2\sigma$) is 73.64 km/ h, 51.38 km /h and ± 59.39 km/ h, respectively

The total energy losses in the tires were 0.100 kWh/ km and 0.126 kWh/ km for 2.9 bar and 2.2 bar, respectively. Comparing the graph from Figure 4.19 and the graph from Figure 4.20, the main differences are in the lateral slip and the tire rolling resistance. However, both tire pressures contributed the same percentage, about 47 % of the total energy consumption of the vehicle. In these simulations, the tire pressure was the parameter that allowed the vehicle to finish the circuit, or not.

With a new battery design and the use of 2.2 bar tire pressure allowed the vehicle to concluded the stipulated circuit. The consumption per kilometre was higher than with the other battery, 0.24 kWh/ km for 2.9 bar, and 0.28 kWh/ km for 2.2 bar, that may be a result from the different weight of this new battery. The energy losses due to the different forces applied in the tire that occurred in this simulations are represented in the Figure 7.3 and in the Figure 7.4, in appendix, for 2.2 and 2.9 bar, respectively.

The total energy losses in the tires were 0.109 kWh/ km and 0.136 kWh/ km for 2.9 bar and 2.2 bar, respectively. The relevant losses are the same as the previous RDE test, as well as the differences between the two tire pressures. However, they are higher with the new battery, but its contribution for the total energy consumption was, approximately, the same- 46 % for 2.9 bar and 49 % for 2.2 bar.

In the simulation where the car moved along a straight road with the respective speed profile from the RDE will be, from now on, named “Straight RDE”. The travelled distance was the same as the previous simulation (RDE) for the 2.2 bar and 2.9 bar tire pressure. The consumption per kilometre was 0.21 kWh/ km for 2.9 bar, and 0.26 kWh/ km for 2.2 bar. The energy losses due to the different forces applied in the tire that occurred in these simulations are represented in the Figure 7.5 and in the Figure 7.6, in appendix, for 2.2 and 2.9 bar, respectively.

The total energy losses in the tires were about 0.100 kWh/ km and 0.124 kWh/ km for 2.9 bar and 2.2 bar, respectively. Comparing Figure 7.5 and Figure 7.6, in appendix, the main difference is in the tire rolling resistance. This is an important parameter because it consumes more energy than the other forces presented, until now. Both tire pressures contributed, approximately, with the same percentage to the total energy consumption of the vehicle- 46 % for 2.9 bar and 47 % for 2.2 bar. In these simulations, the tire pressure was the parameter that allowed the vehicle to finish the circuit.

The Straight RDE test was simulated with the new battery parameterization mentioned above. As it is possible to see in the Figure 4.21 and in the Figure 4.22, the predominant losses in the Straight RDE occurred by lateral slip and rolling resistance.

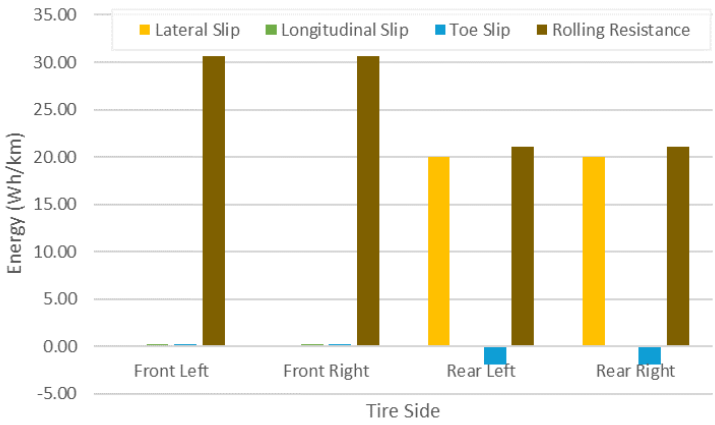


Figure 4.21- Energy losses per kilometre due to the lateral slip, the longitudinal slip, the toe slip and the rolling resistance for the tire pressure of 2.2 bar of the Q tire type in the Straight RDE test with the new battery

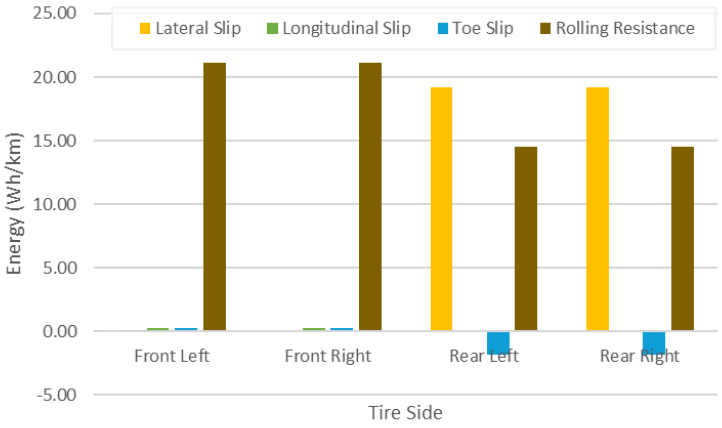


Figure 4.22- Energy losses per kilometre due to the lateral slip, the longitudinal slip, the toe slip and the rolling resistance for the tire pressure of 2.9 bar of the Q tire type in the Straight RDE test with the new battery

Observing the two previous figures, the lateral slip caused fewer energy losses than the RDE test (Figure 4.21 and Figure 4.22), however, the losses due to the rolling resistance are slightly high. This justifies the same total tire energy losses as the RDE test, approximately.

The round trip-type travel from home to the university (HU), and the way back (UH), covered 17 km and a distribution of the speed was also defined for the HU test (Figure 4.23) and the UH test (Figure 4.24). For both simulations, the consumption per kilometre was 0.21 kWh/ km for 2.9 bar, and 0.23 kWh/ km for 2.2 bar. The normal distribution curves of the two previous simulations are combined in Figure 4.25.

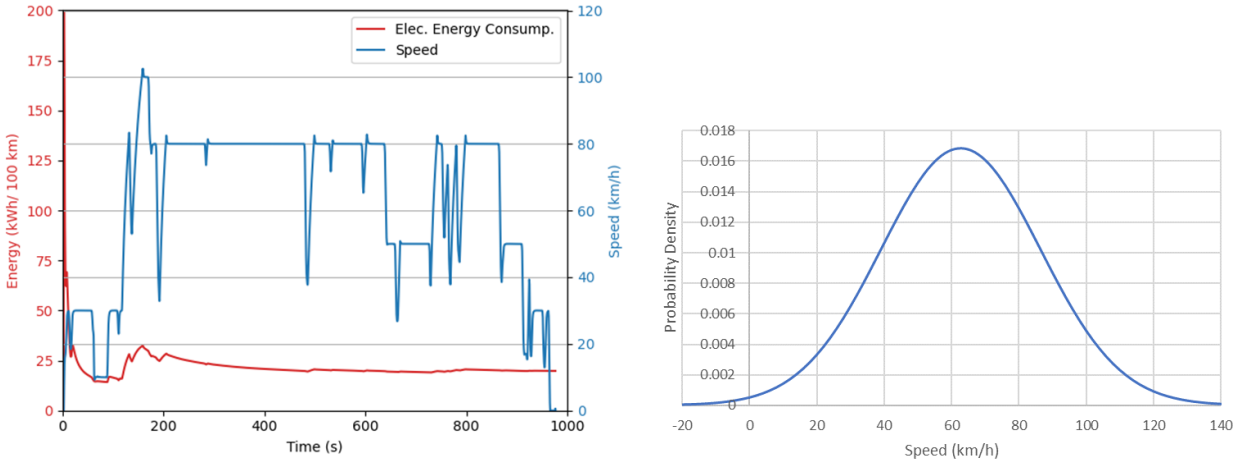


Figure 4.23- Speed profile of the Home to University simulation, and its average energy consumption (left) and its normal distribution (right). In this case, for Q tire type with 2.9 bar and 280 kg extra load. The average, median and 2 times the standard deviation (± 2σ) is 62.75 km/ h, 80.00 km /h and ± 47.36 km/ h, respectively

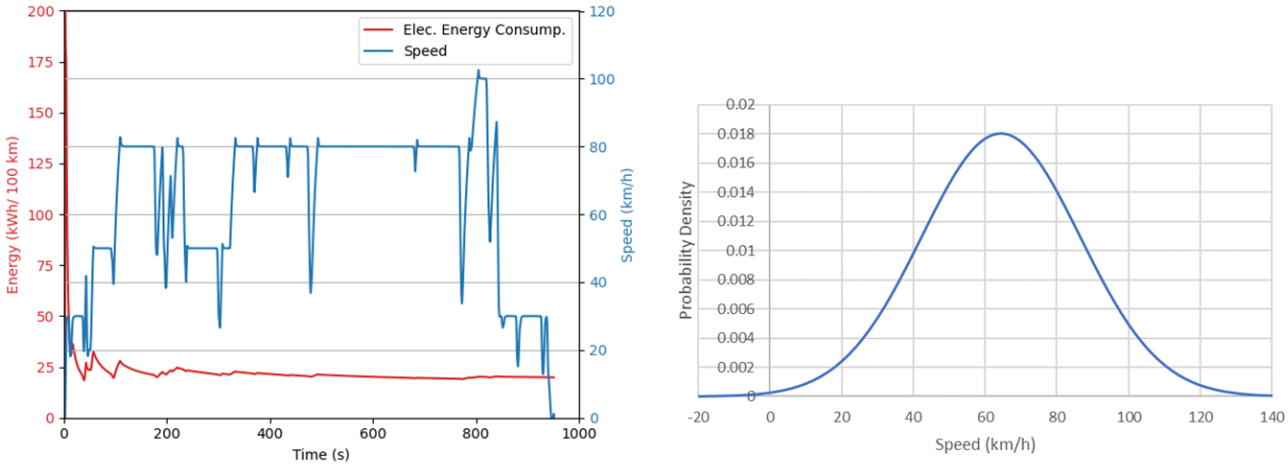


Figure 4.24- Speed profile of the University to Home simulation, and its average energy consumption (left) and its normal distribution (right). In this case, for Q tire type with 2.9 bar and 280 kg extra load. The average, the median and the 2 times the standard deviation (± 2σ) is 64.44 km/ h, 80.00 km /h and ± 44.26 km/ h, respectively

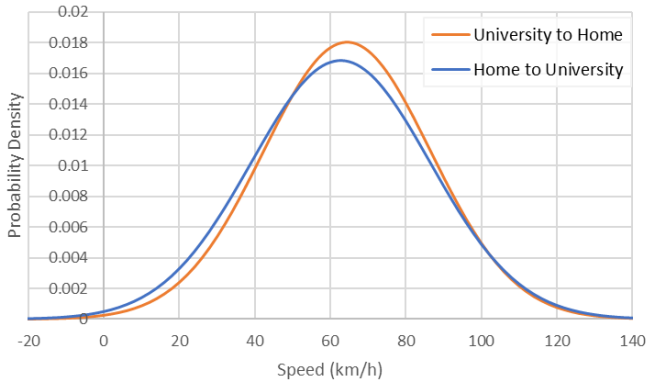


Figure 4.25- Normal distribution of the speed profile in the Home to University and in the University to Home simulations. For the Home to University test, the average, median and 2 times the standard deviation (± 2σ) is 62.75 km/ h, 80.00 km /h and ± 47.36 km/ h, respectively. For the University to Home test, the average, the median and the 2 times the standard deviation (± 2σ) is 64.44 km/ h, 80.00 km /h and ± 44.26 km/ h, respectively

The energy losses due to the different forces applied in the tire that occurred in HU simulations are represented in Figure 4.26 and in Figure 4.27 for 2.2 and 2.9 bar, respectively.

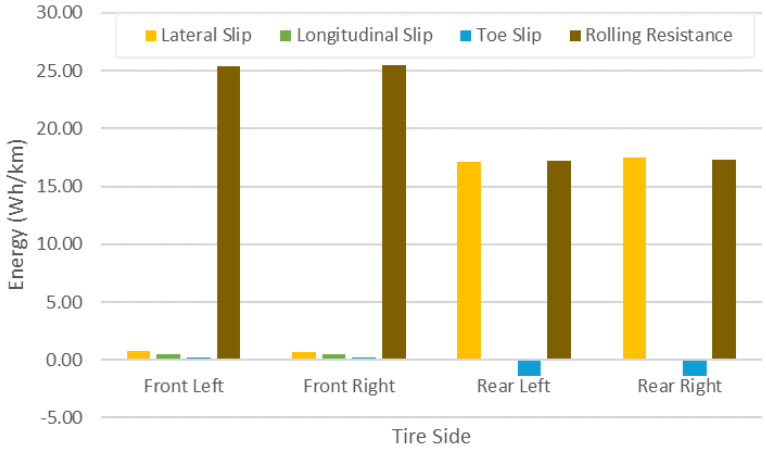

Figure 4.26- Energy losses per kilometre due to the lateral slip, the longitudinal slip, the toe slip and the rolling resistance for the tire pressure of 2.2 bar of the Q tire type in the HU test

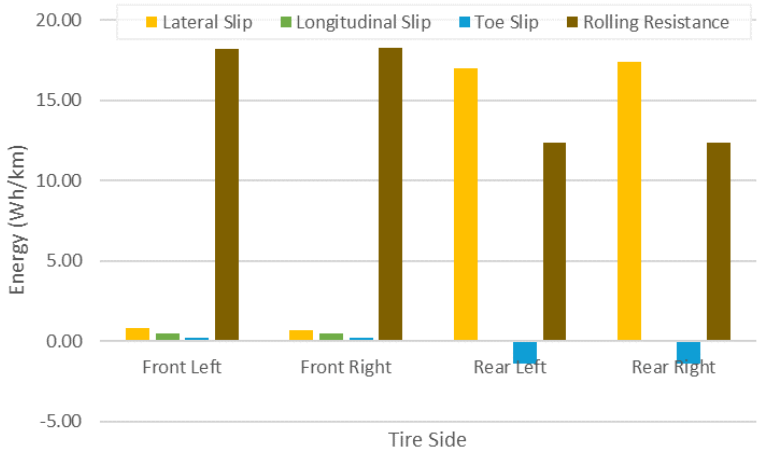


Figure 4.27- Energy losses per kilometre due to the lateral slip, the longitudinal slip, the toe slip and the rolling resistance for the tire pressure of 2.9 bar of the Q tire type in the HU test

The total energy losses in the tires were approximately 0.100 kWh/ km and 0.120 kWh/ km for 2.9 bar and for 2.2 bar, respectively. Comparing the graph from Figure 4.26 and the graph from Figure 4.27, the main difference is in the tire rolling resistance losses, where the energy losses of the 2.2 bar were about 30 % higher than the 2.9 bar losses. Both tire pressures contributed, approximately, with the same percentage to the total energy consumption of the vehicle- 46 % for 2.9 bar and 52 % for 2.2 bar.

The energy losses due to the different forces applied in the tire that occurred in UH simulations are represented in Figure 7.7 and in Figure 7.8, in appendix, for 2.2 and 2.9 bar, respectively.

The results in the UH simulation were, approximately, equal to the HU simulations as it is possible to see from both Figure 7.7 and Figure 7.8, in appendix. Also, the contributions of the total losses in the tires were the same as the previous HU simulations.

The Figure 4.28 and the Figure 4.29 summarizes the total energy losses in the tires, and its contribution to the battery energy consumption, respectively, for the analysis of the rolling resistance coefficient analysis, considering only the simulations with the original battery.

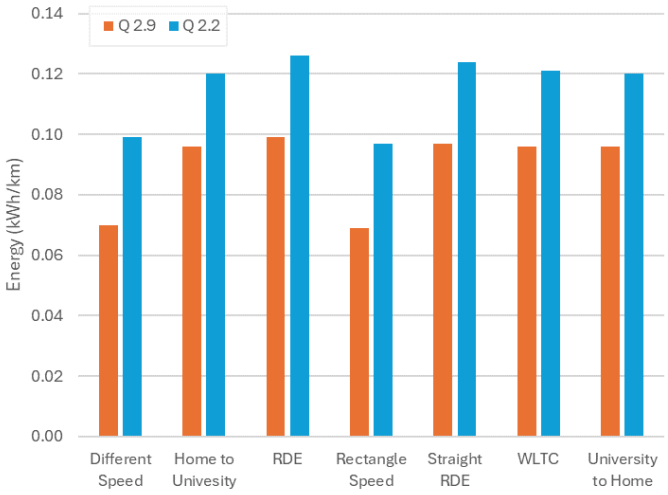


Figure 4.28- Total energy loss per kilometre in the tires in each simulation for the 2.9 bar and 2.2 bar, with Q tire type

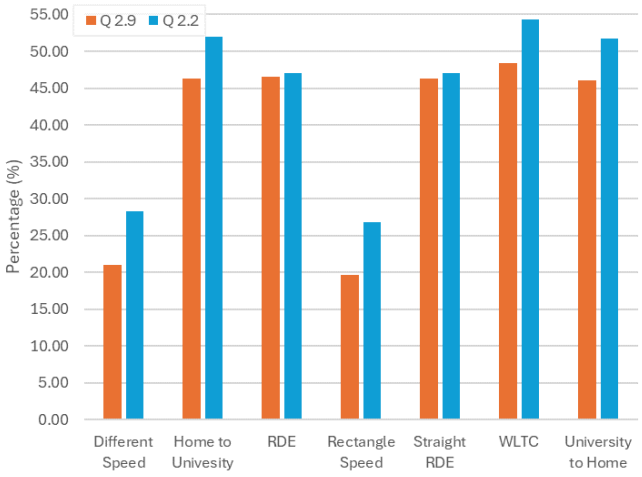


Figure 4.29- Percentage of the total energy lost through the tires that contributed to the total energy consumption of the battery in each simulation, for the 2.9 bar and 2.2 bar, with Q tire type

The highest losses occurred during simulations where a real world driving was modelled- HU, RDE, WLTP and UH. However, in the Figure 4.29Figure 4.29, the highest losses that more contributed to the energy consumption occurred in the HU, in the WLTP and in the UH simulations. The Straight RDE also had high losses, however, this is due to the rolling resistance being the force that reduces the tires performance. This can be concluded from the Figure 4.30, where the percentage of the energy lost in tires for the 2.2 bar tire pressure is always 15 % higher than the 2.9 bar, especially in the Different Speed test and in the Rectangle Speed test. In this simulations, the car travelled always in the straight road, where the rolling resistance was the predominant force in tire. This results show that the energy losses in the tire have high influence in the final consumption of the vehicle, and adapting the tire pressure can reduce the energy losses by 20%. and reduced the influence on the vehicle energy consumption by 10 %.

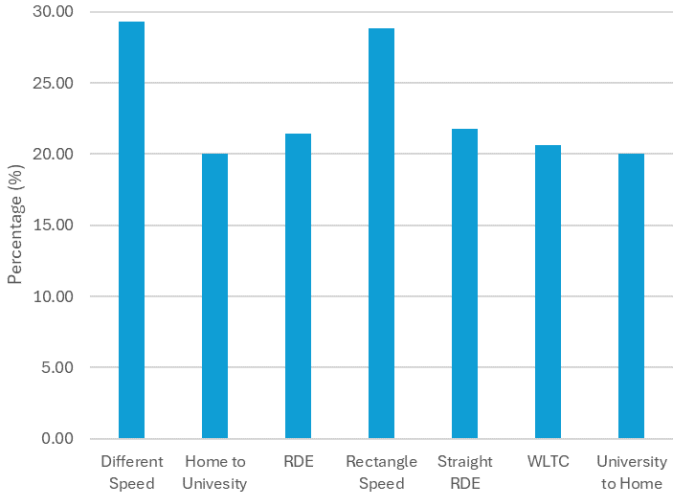


Figure 4.30- Percentage difference between the total tire energy loss per kilometre of 2.2 bar and 2.9 bar of the Q tire type

After the analyse of the influence of the tire pressure in the vehicle energy consumption, the rolling resistance influence will by evaluate in the next text, staring to compare the H type with the Q type, both with 2.2 bar tire pressure. Table 4.4 and Table 4.5 summary the results obtained from the tire pressure analysis.

Table 4.4- Representation of the tires total energy losses, the depth of discharge, the battery energy consumption, and the tire contribution for each driving cycle with respect to the tire pressure evaluation and the extra load evaluation, with the Q tire type with 2.9 bar tire pressure and with 280 kg of extra load

| **Tire Pressure Evaluation- Q 2.9 bar and Extra Load Evaluation- 280 kg** | | | | |
|---|---|---|---|---|
| **Driving Cycle** | **Tires Total Energy Loss** kWh/ km | **Depth of Discharge** % | **Battery Energy Consumption** kWh/ km | **Tire Contribution to the Energy Consumption** % |
| Different Speed | 0.070 | 3.96 | 0.33 | 20.97 |
| Home to University | 0.096 | 14.00 | 0.21 | 46.29 |
| Real Driving Emissions | 0.099 | 87.59 | 0.21 | 46.54 |
| Rectangle Speed | 0.069 | 5.16 | 0.35 | 19.71 |
| Straight Real Driving Emissions | 0.097 | 86.63 | 0.21 | 46.32 |
| WLTC | 0.096 | 18.21 | 0.20 | 48.44 |
| University to Home | 0.096 | 14.06 | 0.21 | 46.06 |

Table 4.5- Representation of the tires total energy losses, the depth of discharge, the battery energy consumption, and the tire contribution for each driving cycle with respect to the tire pressure evaluation with the Q tire type with 2.2 bar tire pressure and with 280 kg of extra load.

| **Tire Pressure Evaluation- Q 2.2 bar and 280 kg** | | | | |
|---|---|---|---|---|
| **Driving Cycle** | **Tires Total Energy Loss** kWh/ km | **Depth of Discharge** % | **Battery Energy Consumption** kWh/ km | **Tire Contribution to the Energy Consumption** % |
| Different Speed | 0.099 | 5.21 | 0.35 | 28.29 |
| Home to University | 0.12 | 15.67 | 0.23 | 51.98 |
| Real Driving Emissions | 0.126 | 100 | 0.27 | 47.08 |
| Rectangle Speed | 0.097 | 6.50 | 0.36 | 26.83 |
| Straight Real Driving Emissions | 0.126 | 100 | 0.27 | 47.08 |
| WLTC | 0.121 | 20.49 | 0.22 | 54.29 |
| University to Home | 0.12 | 15.76 | 0.23 | 51.68 |

In the Different Speed simulation, with the H type, the car travelled 3 km, and with Q type, the car needed more time to achieve the desire speed, which took it to travelled, almost, one more kilometre. The vehicle energy consumption was, approximately, the same: 0.34 kWh/ km with H type and 0.35

kWh/ km with Q type. The Figure 7.9, in appendix, represents the tire energy loss due to rolling resistance, for the Q and the H type.

In the Figure 7.9, it is possible to see that the most energy losses occurred in the front tires, as in the previous Different Speed simulations, when compared the tire pressures. The losses are higher with a higher tire rolling resistance coefficient, due to the higher friction between the tires and the surface. The losses in the Q were, approximately, 23 % higher than the losses in the H type and they contributed 28 % of total energy consumption, while the tires with lower rolling resistance coefficient contributed 23 %.

In the Rectangle Speed simulation, with the H type, the car travelled about 4 km, and with Q type, the car travelled 4.5 km. The vehicle energy consumption was, approximately, the same: 0.35 kWh/ km with H type and 0.36 kWh/ km with Q type. The Figure 7.10, in appendix, represents the tire energy loss due to rolling resistance, for the Q and the H type.

Base on the previous figure, and as the same happened in the previous test, a higher rolling resistance coefficient implied higher tire losses. The losses in the Q were, approximately, 24 % higher than the losses in the H type and they contributed 27 % of the total energy consumption, while the tires with lower rolling resistance coefficient contributed 21 %.

In the WLTP test the car travelled 23 km, with both tire types. The consumption per kilometre was, approximately, the same with 0.20 kWh/ km for H type, and 0.22 kWh/ km Q type. The energy losses due to the different forces applied in the tire that occurred in this simulations are represented in the Figure 4.31 and in the Figure 4.32 for Q and H type, respectively.

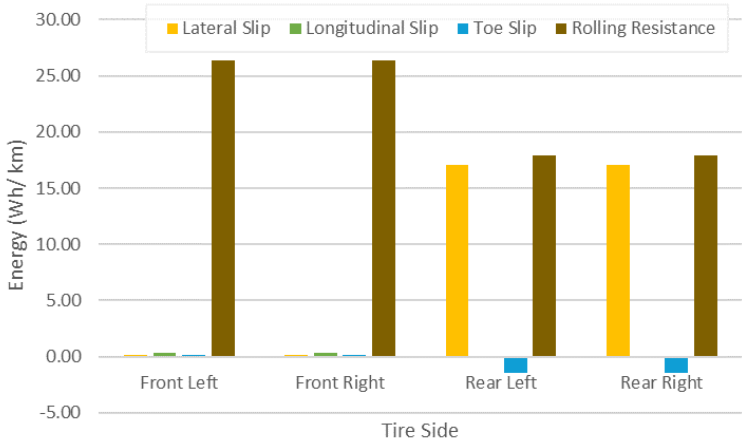


Figure 4.31- Energy losses per kilometre due to the lateral slip, the longitudinal slip, the toe slip and the rolling resistance for Q tire type, with 2.2 bar tire pressure, in the WLTP test

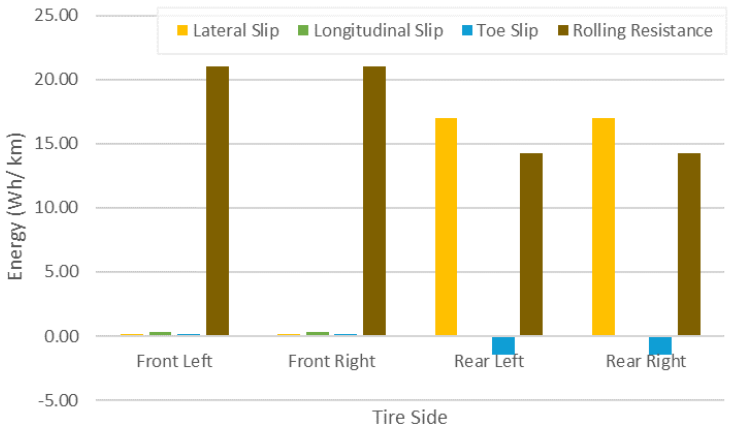


Figure 4.32- Energy losses per kilometre due to the lateral slip, the longitudinal slip, the toe slip and the rolling resistance for H tire type, with 2.2 bar tire pressure, in the WLTP test

Also, the two forces that highlight are the lateral slip for both rear tires, and the rolling resistance for all the tires. The total energy losses in the Q type were about 15 % higher than the H type. However, for the total tire energy consumption this difference was not relevant because, with H type the tires lost 0.103 kWh/ km which contributed for 51 % of the vehicle energy consumption. And with Q type, the tires lost 0.121 kWh/ km which contributed for 55 % for the final energy consumption of the car.

As in the previous simulation that involved the RDE circuit, the Q type only travelled 94 km. The consumption per kilometre was 0.22 kWh/ km for H type, and 0.27 kWh/ km for Q type. The energy losses due to the different forces applied in the tire that occurred in this simulations are represented in the Figure 7.11 and in the Figure 7.12, in appendix, for Q and H type, respectively.

The total energy losses in the tires were 0.105 kWh/ km and 0.126 kWh/ km for H and Q type, respectively. Comparing the graph from the Figure 7.12 and the graph from the Figure 7.13, in appendix, the main difference is in the tire rolling resistance. However, both tire pressures contributed with the same percentage, about 47 %, to the total energy consumption of the vehicle.

In the “new” RDE, the consumption per kilometre was higher than with the other battery, 0.25 kWh/ km for H type, and 0.28 kWh/ km for Q type, that may be a result from the different weight of this new battery. The Figure 4.33 and Figure 4.34 shows the tire energy losses for the different forces that are applied in the tire.

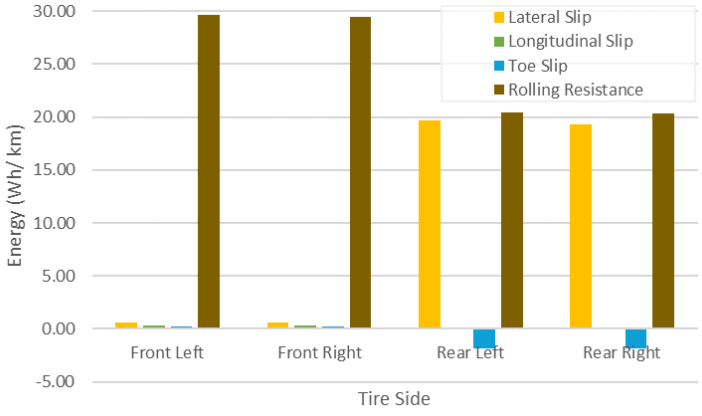


Figure 4.33- Energy losses per kilometre due to the lateral slip, the longitudinal slip, the toe slip and the rolling resistance for Q tire type, with 2.2 bar tire pressure, in the RDE test with the new battery

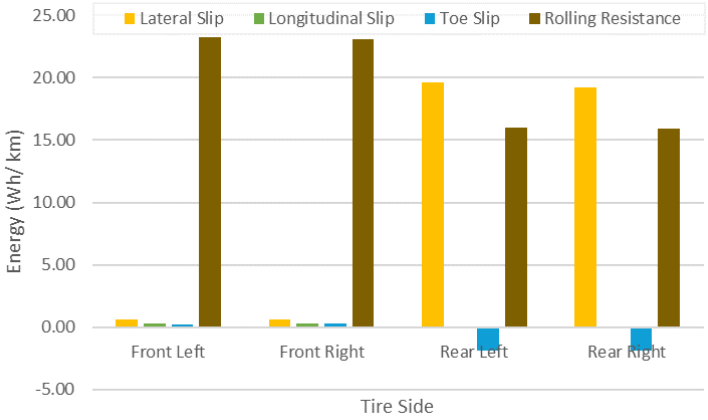


Figure 4.34- Energy losses per kilometre due to the lateral slip, the longitudinal slip, the toe slip and the rolling resistance for H tire type, with 2.2 bar tire pressure, in the RDE test with the new battery

The total energy losses in the tires were 0.116 kWh/ km and 0.137 kWh/ km for H and Q type, respectively. Both tire pressures contributed, approximately, with the same percentage to the total energy consumption of the vehicle- 47 % for H type and 49 % for Q type. Analysing the graphs from the Figure 4.33 and Figure 4.34, the lateral slip and the rolling resistance are the forces that most influence the energy consumption of the vehicle. The main difference between the two tire types is the rolling resistance, which was predictable due to the different rolling resistance coefficient if both types.

In the Straight RDE simulation, the consumption per kilometre was 0.22 kWh/ km H type, and 0.26 kWh/ km for Q type. The energy losses due to the different forces applied in the tire that occurred in this simulations are represented in the Figure 7.13 and Figure 7.14, in appendix, for Q type and H type, respectively.

The total energy losses in the tires were 0.104 kWh/ km and 0.124 kWh/ km for H type and Q type, respectively. Comparing the graph from the Figure 7.13 and the graph from the Figure 7.14, in appendix, the main differences are in the lateral slip and in the tire rolling resistance. However, both tire pressures contributed with the same percentage, about 47 %, to the total energy consumption of the vehicle. Also, the total energy losses in the Q tire type were about 16 % higher than the H tire type.

The Figure 7.15 and the Figure 7.16, in appendix, shows the energy losses for the same previous test, however, with the battery that is capable of respond to the demand. The consumption per kilometre was 0.24 kWh/ km for H type, and 0.27 kWh/ km for Q type.

From the Figure 7.15 and the Figure 7.16, in appendix, and as in the previous same type of tests, the two forces that highlight are the lateral slip for both rear tires, and the rolling resistance for all the tires. The main difference is in the rolling resistance, and where most losses occurred. The total energy losses in the Q type were about 16 % higher than the H type. The total tire energy consumption for the H type were 0.114 kWh/ km, which contributed for 49 % of the vehicle energy consumption. And with Q type, the total tires lost were 0.136 kWh/ km which contributed for 49.5 % for the final energy consumption of the car.

The energy losses due to the different forces applied in the tire that occurred in HU simulations are represented in the Figure 4.35 and the Figure 4.36 for Q type and H type, respectively. The consumption per kilometre was 0.210 kWh/ km for H tire type, and 0.230 kWh/ km for Q tire type.

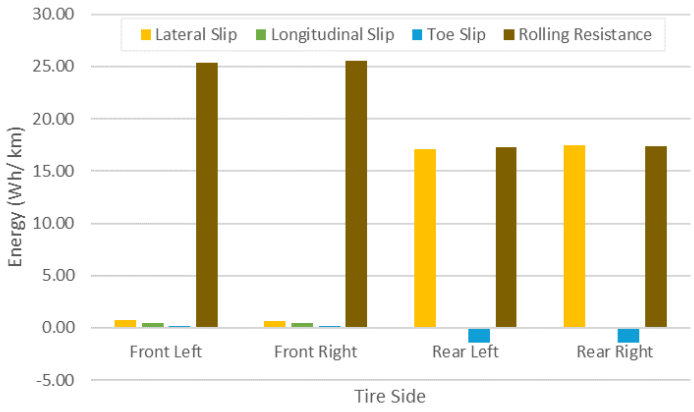


Figure 4.35- Energy losses per kilometre due to the lateral slip, the longitudinal slip, the toe slip and the rolling resistance for Q tire type, with 2.2 bar tire pressure, in the HU test

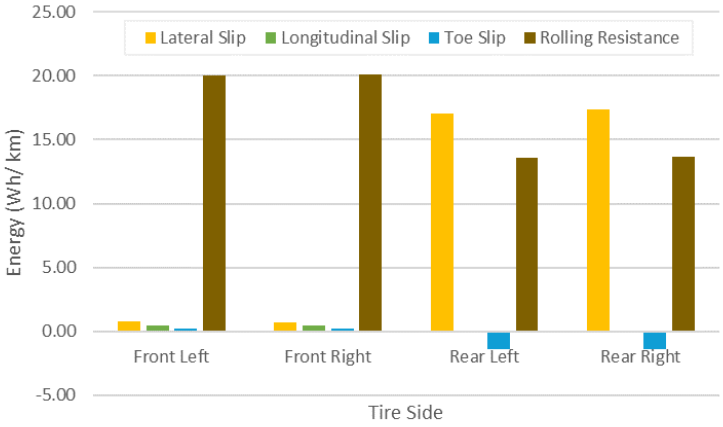


Figure 4.36- Energy losses per kilometre due to the lateral slip, the longitudinal slip, the toe slip and the rolling resistance for H tire type, with 2.2 bar tire pressure, in the HU test

The total energy losses in the tires were 0.102 kWh/ km and 0.120 kWh/ km for H and Q tire type, respectively. Comparing the graph from the Figure 4.35 and the graph from the Figure 4.36, the main difference is in the tire rolling resistance losses, where the energy losses of the Q type were about 15 % higher than the H tire type energy losses. Both tire pressures contributed, approximately, with the same percentage to the total energy consumption of the vehicle- 48 % for H type and 52 % for Q type.

In the UH tests, the results were, approximately, the same as the HU tests for the respective tire types. Also, the energy differences between the Figure 7.17 and the Figure 7.18, in appendix, are the same as the two previous figures.

The total energy losses in the tires for each simulation is represented in the Figure 7.19, in appendix, where the battery considered was the original one, and its contribution for the total energy consumption of the vehicle is represented in the Figure 7.20, in appendix. Also, for each simulation and to highlight the percentage of the energy losses in the tires in the Q type is higher than the H type, the graph from the Figure 4.37 was created.

Analysing the graph from the Figure 7.19, in appendix, it is possible to conclude that the losses were, approximately, the same between the real driving simulations, and the same between the simulations that represented extreme drive conditions. In the Figure 7.20, in appendix, the highest losses that more contributed to the energy consumption occurred in real driving simulations, especially in the

WLTP, HU and UH. The contribution of the losses in the Different Speed and the Rectangle Speed simulations were about 20 % lower than the other simulations. From the Figure 4.37, the percentage of the energy lost in tires for the Q tire type pressure is always 10 % higher than the H tire type, especially in the Different Speed test and in the Rectangle Speed test. In this simulations, the car travelled always in the straight road, where the rolling resistance was the predominant force in tire. This results show that the energy losses in the tire have high influence in the final consumption of the vehicle, and adapting the tire rolling resistance coefficient can reduced the energy losses by 18 % and reduced the influence on the vehicle energy consumption by 5 %.

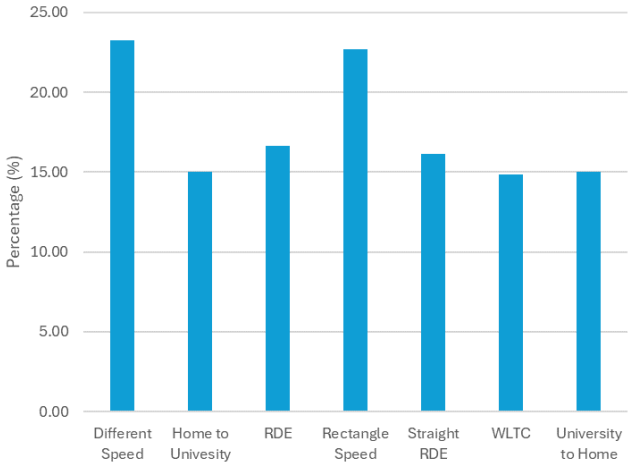


Figure 4.37- Percentage difference between the total tire energy loss per kilometre of Q and H tire type, with 2.2 bar tire pressure

Still within the rolling resistance analysis, the comparison between the two different tire speed rating, Q and H, will be made with a different tire pressure - 2.9 bar. Table 4.6 and Table 4.7 summarizes the results obtained from the Q and H tire type, with 2.2 bar tire pressure.

Table 4.6- Representation of the tires total energy losses, the depth of discharge, the battery energy consumption, and the tire contribution for each driving cycle with respect to the tire rolling resistance evaluation with the H tire type with 2.2 bar tire pressure and with 280 kg of extra load

| **Rolling Resistance Evaluation- H 2.2 bar and 280 kg** | | | | |
|---|---|---|---|---|
| **Driving Cycle** | **Tires Total Energy Loss** kWh/ km | **Depth of Discharge** % | **Battery Energy Consumption** kWh/ km | **Tire Contribution to the Energy Consumption** % |
| Different Speed | 0.076 | 4.13 | 0.34 | 22.51 |
| Home to University | 0.102 | 14.4 | 0.21 | 47.87 |
| Real Driving Emissions | 0.105 | 91.4 | 0.22 | 47.42 |
| Rectangle Speed | 0.075 | 5.36 | 0.35 | 21.20 |
| Straight Real Driving Emissions | 0.104 | 90.31 | 0.22 | 47.31 |
| WLTC | 0.103 | 18.84 | 0.20 | 50.61 |
| University to Home | 0.102 | 14.48 | 0.21 | 47.74 |

Table 4.7- Representation of the tires total energy losses, the depth of discharge, the battery energy consumption, and the tire contribution for each driving cycle with respect to the tire rolling resistance evaluation with the Q tire type with 2.2 bar tire pressure and with 280 kg of extra load

| **Rolling Resistance Evaluation- Q 2.2 bar** | | | | |
|---|---|---|---|---|
| **Driving Cycle** | **Tires Total Energy Loss** kWh/ km | **Depth of Discharge** % | **Battery Energy Consumption** kWh/ km | **Tire Contribution to the Energy Consumption** % |
| Different Speed | 0.099 | 5.21 | 0.35 | 28.29 |
| Home to University | 0.12 | 15.68 | 0.23 | 51.87 |
| Real Driving Emissions | 0.126 | 100 | 0.27 | 47.08 |
| Rectangle Speed | 0.097 | 6.51 | 0.36 | 26.79 |
| Straight Real Driving Emissions | 0.124 | 100 | 0.26 | 47.08 |
| WLTC | 0.121 | 20.50 | 0.22 | 54.46 |
| University to Home | 0.120 | 15.77 | 0.23 | 51.65 |

In the Different Speed simulation, the travelled distance for 2.9 bar was different from the 2.2 bar. With a H type, the car travelled 2.8 km, almost 200 m less than the Q type. The vehicle energy consumption was, approximately, the same: 0.32 kWh/ km with H type and 0.33 kWh/ km with Q type.

The Figure 7.20, in appendix, represents the tire energy loss due to rolling resistance, for the Q and the H type.

For a high tire pressure, Figure 7.21, in appendix, shows the remaining differences between the energy losses of each tire type. The losses in the Q were, approximately, 23 % higher than the losses in the H type, the same as 2.2 bar. Also, the losses occurred in the Q type contributed 21 % of total energy consumption, while the tires with lower rolling resistance coefficient contributed 17 %

As expected in the Rectangle Speed simulation, the distance travelled was also lower then with 2.2 bar. With the H type, the car travelled about 3.5 km, and with Q type, the car travelled 3.7 km. The vehicle energy consumption was, approximately, the same: 0.34 kWh/ km with H type and 0.35 kWh/ km with Q type. The Figure 7.22, in appendix, represents the tire energy loss due to rolling resistance, for the Q and the H type.

Observing the Figure 7.22, in appendix, the differences between each tires are not significant. The losses in the Q (0.068 kWh/ km) were, approximately, 22 % higher than the losses in the H type (0.053 kWh/ km) and they contributed 20 % of the total energy consumption, while the tires with lower rolling resistance coefficient contributed 16 %.

In the WLTP test, the consumption per kilometre was 0.18 kWh/ km and 0.20 kWh/ km for the H and Q type, respectively. The energy losses due to the different forces applied in the tire that occurred in this simulations are represented in the Figure 4.38 and in the Figure 4.39 for Q and H type, respectively.

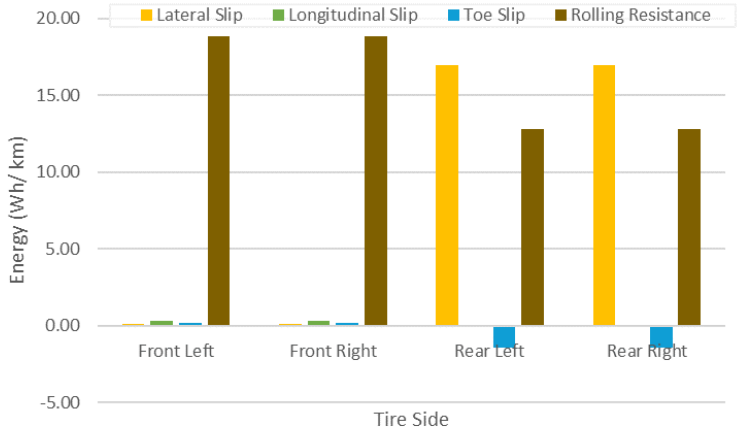


Figure 4.38- Energy losses per kilometre due to the lateral slip, the longitudinal slip, the toe slip and the rolling resistance for Q tire type, with 2.9 bar tire pressure, in the WLTP test

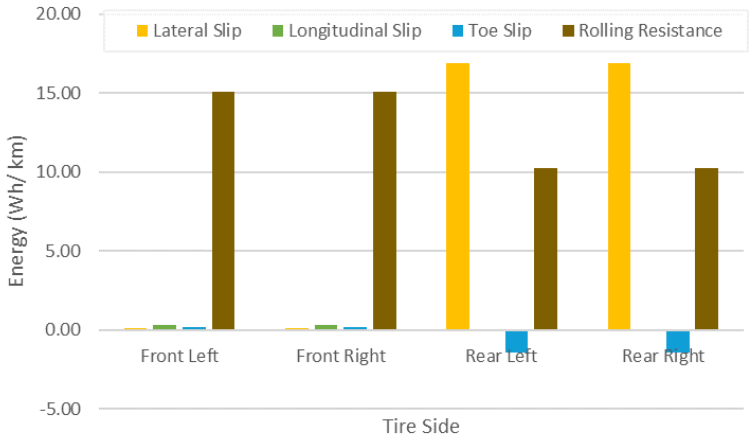


Figure 4.39- Energy losses per kilometre due to the lateral slip, the longitudinal slip, the toe slip and the rolling resistance for H tire type, with 2.9 bar tire pressure, in the WLTP test

In the Figure 4.39, the two forces that highlight is the lateral slip for both rear tires, and the rolling resistance for all the tires. The total energy losses in the Q type were about 14 % higher than the H type. With H type the tires lost 0.083 kWh/km which contributed for 45 % of the vehicle energy consumption. And with Q type, the tires lost 0.096 kWh/km which contributed for 49 % for the final energy consumption of the car.

In the RDE simulations, the car completed the circuit when using each one of the previous tire types. The consumption per kilometre was 0.19 kWh/km for H type, and 0.21 kWh/km for Q type. The energy losses due to the different forces applied in the tire that occurred in this simulations are represented in the Figure 4.40 and in the Figure 4.41 for Q and H type, respectively.

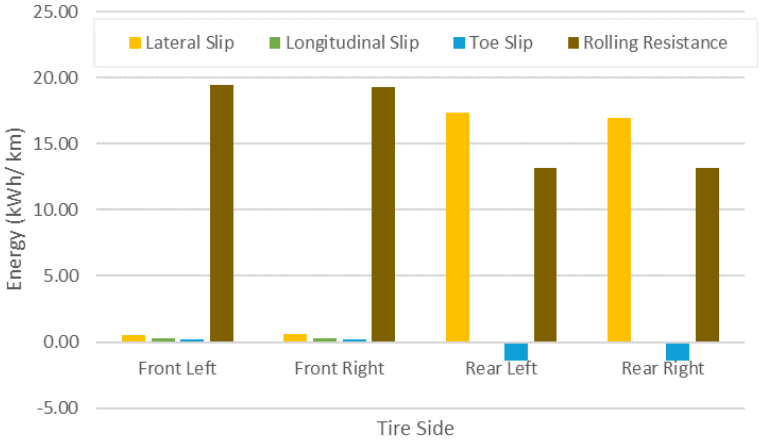


Figure 4.40- Energy losses per kilometre due to the lateral slip, the longitudinal slip, the toe slip and the rolling resistance for Q tire type, with 2.9 bar tire pressure, in the RDE test

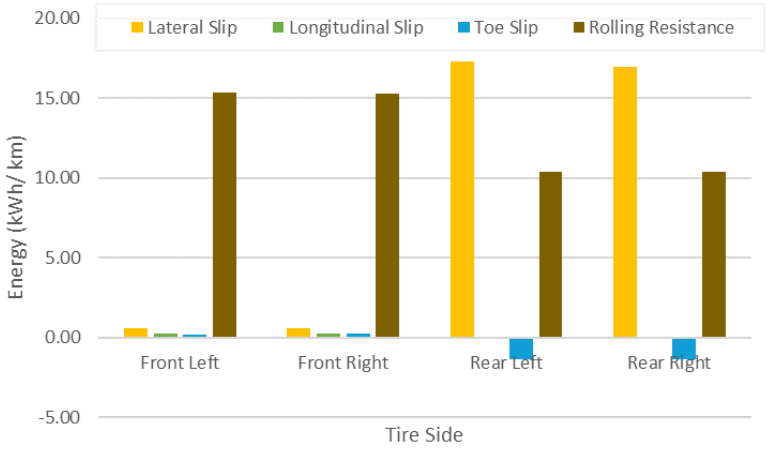


Figure 4.41- Energy losses per kilometre due to the lateral slip, the longitudinal slip, the toe slip and the rolling resistance for H tire type, with 2.9 bar tire pressure, in the RDE test

The two forces that highlight from the graphs, represented in the Figure 4.40 and in the Figure 4.41, are the lateral slip for both rear tires, and the rolling resistance for all the tires. In opposite what happened in the previous data, the forces that has most influence in the energy losses are the rolling resistance, for the Q type, and the lateral slip, for the H type. The total energy losses in the Q type tire were about 15 % higher than the H tire type. In this values, the gains were considered. However, for the total tire energy consumption this difference was not relevant because, with the H type the losses were 0.085 kWh/km, which contributed for 44 % of the vehicle energy consumption. And with the Q type the tires lost 0.100 kWh/ km which contributed for 46.50 % for the final energy consumption of the car.

In the Straight RDE, the consumption per kilometre was 0.19 kWh/km for H tire speed rating, and 0.21 kWh/km for Q tire speed rating. The energy losses due to the different forces applied in the tire that occurred in this simulations are represented in the Figure 4.42 and in the Figure 4.43 for Q and H, respectively.

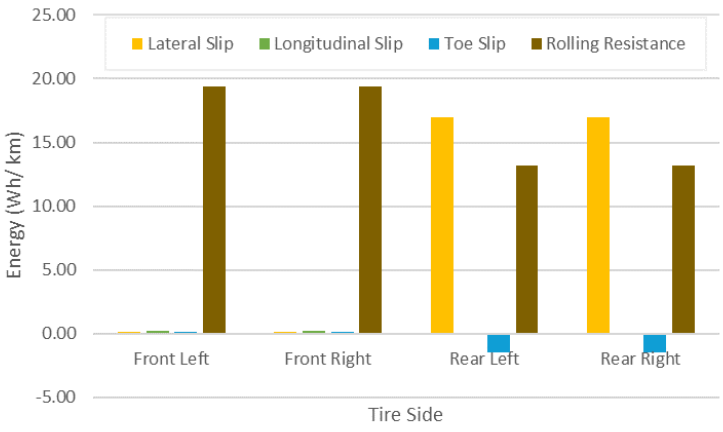


Figure 4.42- Energy losses per kilometre due to the lateral slip, the longitudinal slip, the toe slip and the rolling resistance for Q tire type, with 2.9 bar tire pressure, in the Straight RDE test

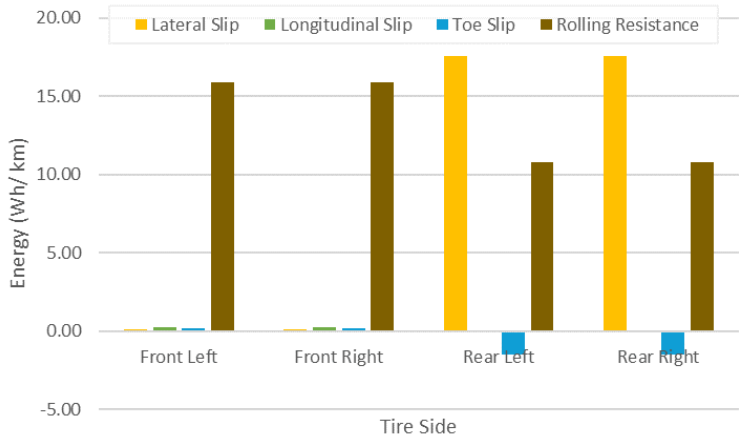


Figure 4.43- Energy losses per kilometre due to the lateral slip, the longitudinal slip, the toe slip and the rolling resistance for H tire type, with 2.9 bar tire pressure, in the Straight RDE test

The total energy losses in the tires were 0.083 kWh/km and 0.097 kWh/km for H type and Q type, respectively. Comparing the graph from the Figure 4.42 and the graph from the Figure 4.43, the main differences are in the lateral slip and in the tire rolling resistance. Both tire pressures contributed, approximately, with the same percentage to the total energy consumption of the vehicle- 44 % for H type and 46 % for Q type. Also, the total energy losses in the Q tire type were about 14 % higher than the H tire type.

The energy losses due to the different forces applied in the tire that occurred in HU simulations are represented in the Figure 4.44 and in the Figure 4.45 for Q type and H type, respectively. The consumption per kilometre was 0.190 kWh/km for H tire type, and 0.210 kWh/km for Q tire type.

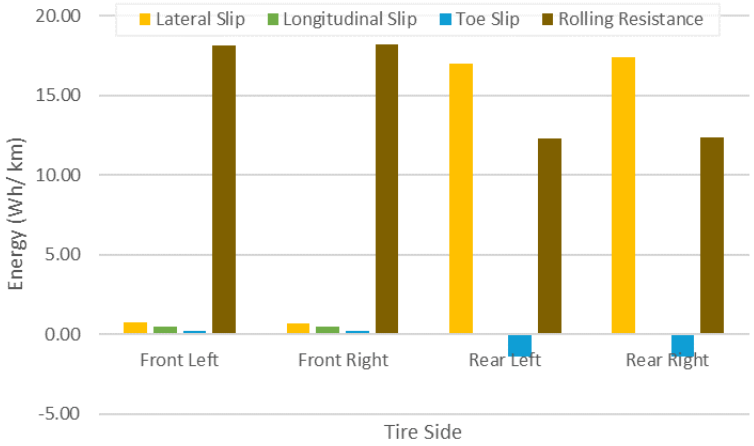


Figure 4.44- Energy losses per kilometre due to the lateral slip, the longitudinal slip, the toe slip and the rolling resistance for Q tire type, with 2.9 bar tire pressure, in the HU test

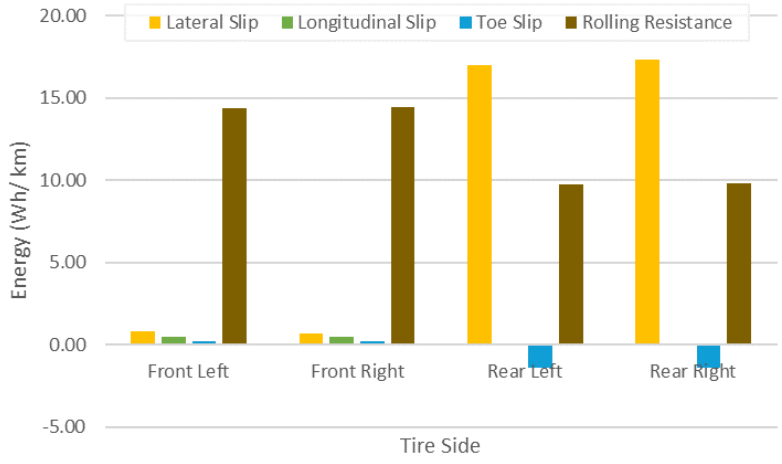


Figure 4.45- Energy losses per kilometre due to the lateral slip, the longitudinal slip, the toe slip and the rolling resistance for H tire type, with 2.9 bar tire pressure, in the HU test

The total energy losses in the tires were 0.083 kWh/km and 0.096 kWh/km for H and Q tire type, respectively. Comparing the graph from the Figure 4.44 and the graph from the Figure 4.45, the main difference is in the tire rolling resistance losses, where the energy losses of the Q type were about 13.50 % higher than the H tire type energy losses. Both tire pressures contributed, approximately, with the same percentage to the total energy consumption of the vehicle- 43 % for H type and 46 % for Q type.

In the UH tests, the results were, approximately, the same as the HU tests for the respective tire types. Also, the energy differences between the Figure 7.23 and the Figure 7.24, in appendix, are the same as the two previous figures. The consumption per kilometre was 0.190 kWh/km for H tire type, and 0.210 kWh/km for Q tire type.

The total energy losses in the tires for each simulation is represented in the Figure 7.25, in appendix, where the battery considered was the original one, and its contribution for the total energy consumption of the vehicle is represented in the Figure 7.26, in appendix. Also, for each simulation and to highlight the percentage of the energy losses in the tires in the Q type is higher than the H type, the graph from the Figure 4.46 was created.

Analysing the graph from the Figure 7.25, in appendix, it is possible to conclude that the losses were consistent between the real driving simulations, and between the simulations that represented extreme drive conditions. In the Figure 7.26, in appendix, the highest losses that more contributed to the energy consumption occurred in real driving simulations. The maximum contribution of the losses in the total energy consumption were about 50 %, with the Q type, and about minus 5 % with H type. From the Figure 4.46, the percentage of the energy lost in tires for the Q tire type pressure is always 10 % higher than the H tire type, and lower than 25 %. The same happened when the two types were compared with 2.2 bar tire pressure.

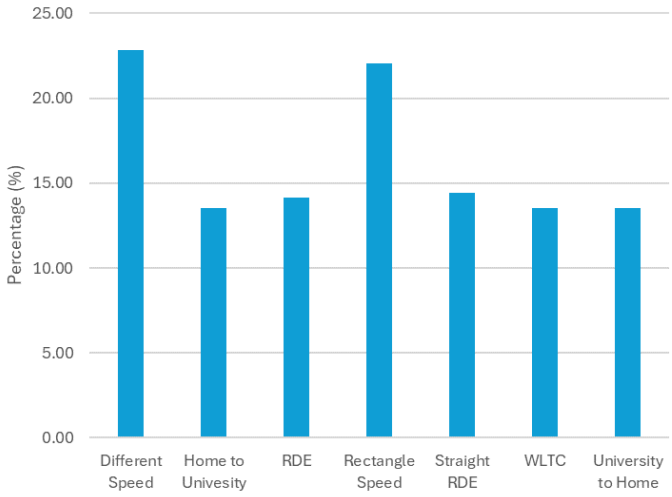


Figure 4.46- Percentage difference between the total tire energy loss per kilometre of Q and H tire type, with 2.9 bar tire pressure

Table 4.8 and Table 4.9 summarizes the results obtained from the Q and H tire type, with 2.9 bar tire pressure.

Table 4.8- Representation of the tires total energy losses, the depth of discharge, the battery energy consumption, and the tire contribution for each driving cycle with respect to the tire rolling resistance evaluation with the H tire type with 2.9 bar tire pressure and with 280 kg of extra load

| **Rolling Resistance Evaluation- H 2.9 bar and 280 kg** | | | | |
|---|---|---|---|---|
| **Driving Cycle** | **Tires Total Energy Loss** kWh/ km | **Depth of Discharge** % | **Battery Energy Consumption** kWh/ km | **Tire Contribution to the Energy Consumption** % |
| Different Speed | 0.054 | 3.57 | 0.32 | 16.80 |
| Home to University | 0.083 | 13.08 | 0.19 | 42.83 |
| Real Driving Emissions | 0.085 | 79.62 | 0.19 | 43.96 |
| Rectangle Speed | 0.053 | 4.73 | 0.34 | 15.79 |
| Straight Real Driving Emissions | 0.083 | 78.76 | 0.19 | 43.68 |
| WLTC | 0.083 | 17.00 | 0.18 | 45.11 |
| University to Home | 0.083 | 13.16 | 0.19 | 42.57 |

Table 4.9- Representation of the tires total energy losses, the depth of discharge, the battery energy consumption, and the tire contribution for each driving cycle with respect to the tire rolling resistance evaluation with the Q tire type with 2.9 bar tire pressure and with 280 kg of extra load

| **Rolling Resistance Evaluation- Q 2.9 bar and 280 kg** | | | | |
|---|---|---|---|---|
| **Driving Cycle** | **Tires Total Energy Loss** kWh/ km | **Depth of Discharge** % | **Battery Energy Consumption** kWh/ km | **Tire Contribution to the Energy Consumption** % |
| Different Speed | 0.07 | 14.05 | 0.33 | 20.87 |
| Home to University | 0.096 | 18.20 | 0.21 | 46.32 |
| Real Driving Emissions | 0.099 | 86.57 | 0.21 | 46.52 |
| Rectangle Speed | 0.068 | 5.16 | 0.35 | 19.63 |
| Straight Real Driving Emissions | 0.097 | 87.54 | 0.21 | 46.31 |
| WLTC | 0.096 | 13.98 | 0.20 | 48.46 |
| University to Home | 0.096 | 3.96 | 0.21 | 46.09 |

To finish this section, the last results presented will be about the different load applied in the vehicle. The previous results were obtained by simulating the tests roads with a vehicle occupied by four users. So, the values related with the tire speed rating Q with 2.2 bar tire pressure, and with the tire rolling resistance independent from the tire pressure, will not be repeated in the next analysis. Only the values regarding the occupation of the vehicle with the driver.

In the Different Speed simulation, the car occupied only by the driver (70 kg) covered about one less kilometre than the car with full capacity (280 kg). Its consumption was 0.33 kWh/ km. The energy losses due to the tire rolling resistance are represented in the Figure 7.27, in appendix.

Observing the Figure 7.27, in appendix, the energy losses between the front left and the front right tires it is because the “extra “weight” is in the same plane as the front left tire. The total energy losses in tire for the 70 kg extra load were 0.083 kWh/ km- 16 % lower than the 280 kg extra load. Also, its contribution for the total energy consumption were 5 % lower than the car full capacity.

The Rectangle Speed tests results were not too different from the previous test. With one occupant, the car battery spent 0.280 kWh/ km. Also, it travelled distance were one kilometre less than the car equipped with 280 kg extra load. The results from the energy losses can be consult in the graph of the Figure 7.28, in appendix.

The differences between each load represented in the Figure 7.28, in appendix, are not significant for the total energy losses. With 280 kg, the losses were 12 % higher than with 70 kg, with 0.085 kWh/ km of losses for the 70 kg part. Also, each contribution were, approximately, the same- 30 %.

In the WLTP test, the car travelled the same distance in both simulations, as in the previous WLTP simulations. And the energy consumption of the car with 70 kg extra load was 0.200 kWh/ km. To analyse the energy losses through the tires for 280 kg and 70 kg extra load, the Figure 4.47 and the Figure 4.48 were created, respectively.

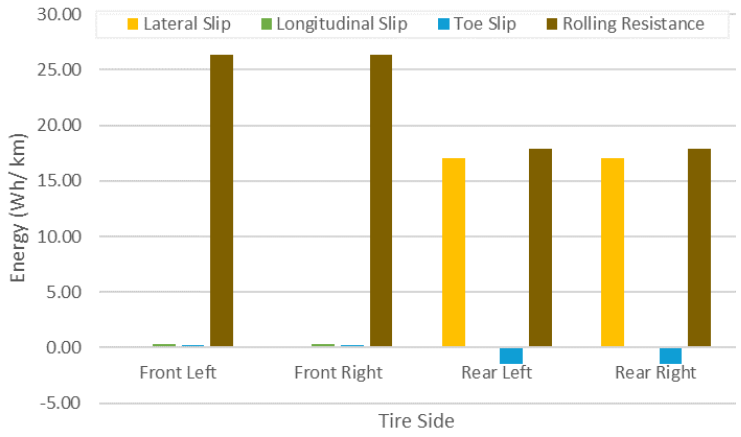


Figure 4.47- Energy losses per kilometre due to the lateral slip, the longitudinal slip, the toe slip and the rolling resistance for 280 kg extra load in the WLTP tests

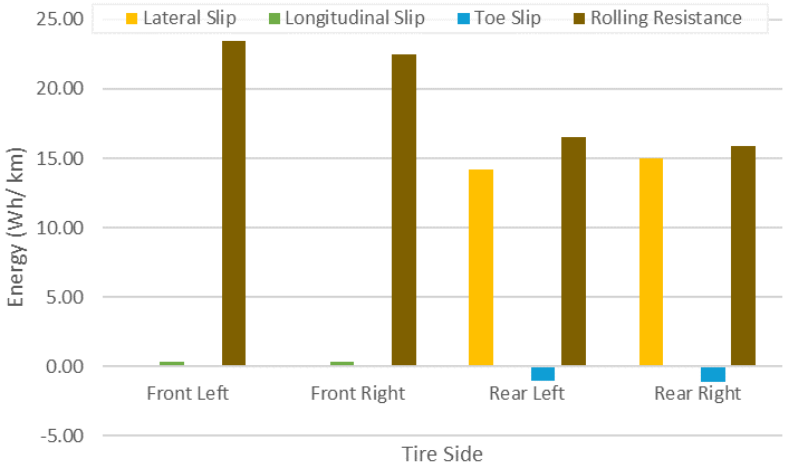


Figure 4.48- Energy losses per kilometre due to the lateral slip, the longitudinal slip, the toe slip and the rolling resistance for 70 kg extra load in the WLTP tests

The two forces that highlight from the graphs, represented in the Figure 4.47 and in the Figure 4.48, are the lateral slip for both rear tires, and the rolling resistance for all the tires. The total energy losses in the car with 70 kg load were about 12 % higher than the car with 280 kg load. With 70 kg extra, the tires lost 0.106 kWh/km, which contributed for 53 % of the vehicle energy consumption.

For the RDE simulations, it is important to remember that the simulation was repeated, with the new battery, for the car when equipped with a 2.2 bar tire pressure and with 280 kg of extra weight. The consumption per kilometre was 0.23 kWh/km for the 70 kg load. The energy losses due to the different forces applied in the tire that occurred in this simulations are represented in the Figure 4.49 and in the Figure 4.50 for 280 kg and 70 kg load, respectively.

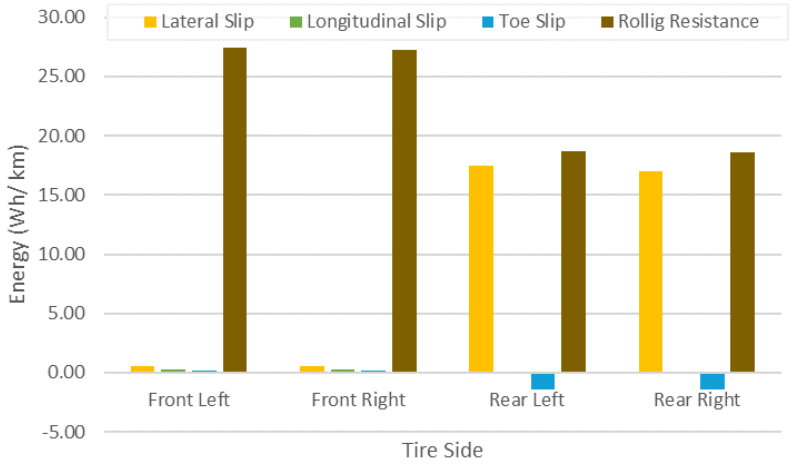


Figure 4.49- Energy losses per kilometre due to the lateral slip, the longitudinal slip, the toe slip, and the rolling resistance for 280 kg extra load in the RDE tests

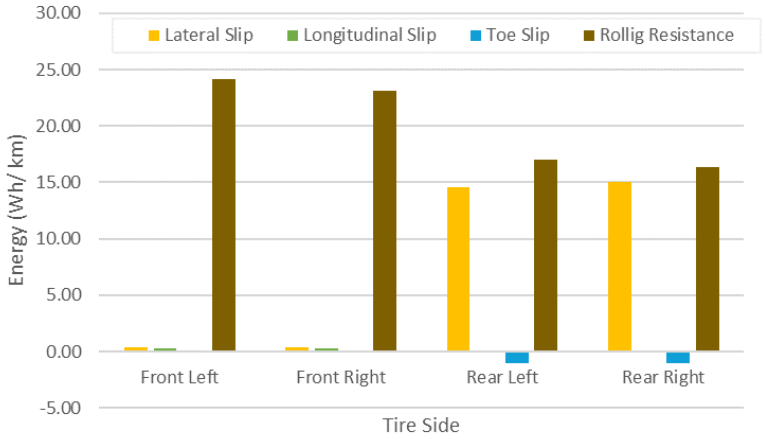


Figure 4.50- Energy losses per kilometre due to the lateral slip, the longitudinal slip, the toe slip, and the rolling resistance for 70 kg extra load in the RDE tests

The total energy losses in the tires were 0.110 kWh/km for 70 kg load, respectively. Comparing the graph from the Figure 4.49 and the graph from the Figure 4.50, the main differences are in the lateral slip and in the tire rolling resistance. However, both tire pressures contributed with the same percentage, about 48 %, to the total energy consumption of the vehicle. In this simulations, the weight difference was the parameter that allowed the vehicle to finish the circuit, or not.

With the new battery, the car equipped with 2.2 bar tire pressure, and 280 kg extra load, concluded the RDE circuit. The consumption per kilometre was higher than with the other battery, 0.250 kWh/km for 2.9 bar that may be a result from the different weight of this new battery. The energy losses due to the different forces applied in the tire that occurred in this simulations are represented in the Figure 7.29 and in Figure 7.30, in appendix, for 280 kg and 70 kg, respectively.

Observing the Figure 7.29 and the Figure 7.30, in appendix, the front tires are the ones how present a major difference, where comparing with the rear tires. The total tire energy losses in the car occupied only with the driver was 0.123 kWh/ km- 10 % less than the fully occupied vehicle. In both simulations, the tires contributed about 50 % for the total energy consumption.

In the Straight RDE test, the simulations were, also, performed with the original battery, and with the one that was adapted. With the original battery, the total energy consumption with the 70 kg load were 0.220 kWh/ km. The energy losses due to the different forces applied in the tire that occurred in this simulations are represented in the Figure 7.31 and in the Figure 7.32, in appendix, for 280 kg and 70 kg, respectively.

Analysing the Figure 7.31 and the Figure 7.32, in appendix, the lateral slip and the rolling resistance still be the highlight forces. It's due to this forces in the tires that makes the difference between the two typologies in the tire energy losses- 12 % of the losses with a load of 280 kg are higher than with a 70 kg load in the car.

With the adapted battery, the Figure 7.33 and the Figure 7.34, in appendix, were defined to represent the energy losses through the tires in the "adapted" Straight RDE tests for 280 kg and 70 kg load, respectively. The energy consumption of the vehicle constituted with a 70 kg load, 0.250 kWh/ km, was lower than with a 280 kg load.

Even in the new simulation, the values based on the Figure 7.33 and in the Figure 7.34, in appendix, still not have high differences between the 70 kg and the 280 kg load. There were only 10 % difference between the energy losses of the load analysis. Also, in both simulations the tires contributed about 50 % for the total energy consumption.

The travel from home until the university (HU), and the way back (UH), were the last simulations to be performed. For both simulations, the consumption per kilometre was 0.21 kWh/km for 70 kg load. The energy losses due to the different forces applied in the tire that occurred in HU simulations are represented in the Figure 7.35 and in the Figure 7.36, in appendix, for 280 kg and 70 kg, respectively.

As it is possible to conclude from the two previous figures, the differences between the 70 kg and the 280 kg load are practically inexistent- 12 % in total energy losses. Also, the losses in the front tires are not so different as in the previous tests.

In order to analyse the behaviour of the vehicle in the opposite direction of the HU, the Figure 7.37 and the Figure 7.38, in appendix, were created with the tire energy losses from the UH simulations with the car full capacity, and only with the drive, respectively.

The results in the UH simulation were, approximately, equal to the HU simulations as it is possible to see from the Figure 7.37 and the Figure 7.38, in appendix. Also, the contributions of the total losses in the tires were the same as the previous HU simulations.

The Figure 7.39 and the Figure 7.40, in appendix, summarizes the total energy losses in the tires, and its contribution to the battery energy consumption, respectively, for the extra load analysis, considering only the simulations with the original battery.

Analysing the graph from the Figure 7.39, in appendix, it is possible to conclude that the losses were, approximately, the same between all simulations- the maximum difference is 0.02 kWh/ km. Which translates in a low influence on the energy losses by different loads applied in the vehicle. In the Figure 7.40, in appendix, the highest losses that more contributed to the energy consumption occurred in real driving simulations. The contribution of the losses in the Different Speed and the Rectangle Speed simulations were about 20 % lower than the other simulations. From the Figure 4.51, the percentage of the energy lost in tires when the car is occupied by the driver is always 10 % higher than its full capacity, and lower than 15 %. Except in the Different Speed test case. However, the is almost no variation in the simulation tests

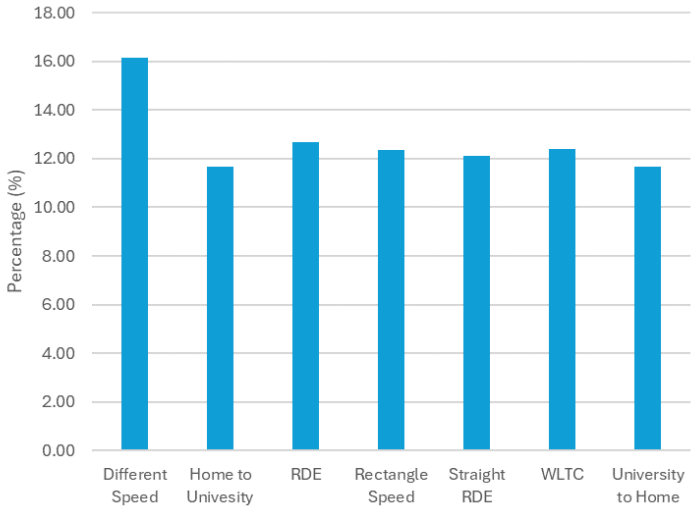


Figure 4.51- Percentage difference between the total tire energy loss per kilometre for 70 kg and 280 kg vehicle load, with the Q tire type and 2.2 bar tire pressure, where the rolling resistance of the vehicle is independent from the tire pressure

Table 4.10 and Table 4.11 summarizes the results obtained from the extra load evaluation.

Table 4.10- Representation of the tires total energy losses, the depth of discharge, the battery energy consumption, and the tire contribution for each driving cycle with respect to the tire pressure evaluation and the extra load evaluation, with 280 kg of extra load

| **Extra Load Evaluation- 280 kg** | | | | |
|---|---|---|---|---|
| **Driving Cycle** | **Tires Total Energy Loss** kWh/ km | **Depth of Discharge** % | **Battery Energy Consumption** kWh/ km | **Tire Contribution to the Energy Consumption** % |
| Different Speed | 0.070 | 3.96 | 0.33 | 20.97 |
| Home to University | 0.096 | 14.00 | 0.21 | 46.29 |
| Real Driving Emissions | 0.099 | 87.59 | 0.21 | 46.54 |
| Rectangle Speed | 0.069 | 5.16 | 0.35 | 19.71 |
| Straight Real Driving Emissions | 0.097 | 86.63 | 0.21 | 46.32 |
| WLTC | 0.096 | 18.21 | 0.20 | 48.44 |
| University to Home | 0.096 | 14.06 | 0.21 | 46.06 |

Table 4.11- Representation of the tires total energy losses, the depth of discharge, the battery energy consumption, and the tire contribution for each driving cycle with respect to the extra load evaluation with 70 kg of extra load

| **Extra Load Evaluation- 70 kg** | | | | |
|---|---|---|---|---|
| **Driving Cycle** | **Tires Total Energy Loss** kWh/ km | **Depth of Discharge** % | **Battery Energy Consumption** kWh/ km | **Tire Contribution to the Energy Consumption** % |
| Different Speed | 0.083 | 3.97 | 0.33 | 25.02 |
| Home to University | 0.106 | 14.22 | 0.21 | 50.29 |
| Real Driving Emissions | 0.11 | 93.40 | 0.23 | 48.49 |
| Rectangle Speed | 0.085 | 4.10 | 0.28 | 30.62 |
| Straight Real Driving Emissions | 0.109 | 92.62 | 0.22 | 48.34 |
| WLTC | 0.106 | 18.60 | 0.20 | 52.76 |
| University to Home | 0.106 | 14.29 | 0.21 | 50.04 |

The tires have a high influence in the vehicle energy consumption. The tire energy losses can reach at 50 % of the total consumption of the battery.

All the results obtained for this study, can be compared with other values obtained in other works. This serves, mainly, to understand if the results can translate real world driven data. The total energy consumption varied between 0.190 kWh/ km and 0.360 kWh for real world driven cycles, which average was 0.220 kWh. The average energy consumption is between 0.168 kWh and 0.225 kWh, which was obtained in [44]. Also, the WLTC was a mixture between the different the different levels of this type of test (low, middle and high). In [23] the tire losses varied between 0.089 kWh/ km and 0.100 kWh/ km in the three different WLTC. In this dissertation, the tire losses varied between 0.083 kWh/ km and 0.121 kWh/ km, for the best-case scenario and for the worst-case scenario, respectively. The differences between the extreme values are not relevant due to what has been present. With this, it is possible to prove that IPG CarMaker can replicate real scenarios, so the analysis regarding the mobility sector can be simpler and cheap.

# 5 Conclusions and Future Suggestions

The aims of this work were to evaluate the tire influence on energy consumption and its influence in the driving dynamics of an electric driven vehicle. To achieve this, one of the test cars that KIT possesses, a fully electric Mercedes Benz A-Class, was modelled in the CarMaker software and different simulations were carried out using this software.

The car model was already defined in other works, so some characteristic component values were left the same and according to its own coordinate system, for example, position, mass, and moment of inertia of the body and of the wheels, spring, damper, buffer, and others. The important parameters that were defined in more detail were the high voltage battery, and the tire model.

The battery was defined based on the Chen model, and on literature with a capacity of 69 Ah, and a total energy stored of 25.17 kWh. However, some of the simulations were not concluded due to the battery's low capacity. So, it was necessary to dimension a battery with a higher capacity, capable of performed the simulation. *Fiat 500e Cabrio 42 kWh* has dimensions and structure similar to the Mercedes Benz A-Class (test car), so the new battery of the Mercedes was modelled based on the battery of the Fiat, with a total energy stored of 42.29 kWh.

For the tire model it was used a pre-defined tire model in CarMaker. Tire rolling resistance, and tire pressure were defined according to the Eq. 3.1. So, it was defined two major tire pressures, 2.2 bar and 2.9 bar, and for the tire rolling resistance were defined two speed rating, Q and H, due to its different rolling resistance coefficient. To evaluate the extra load on the vehicle, the occupancy by four users, including the driver, and by only the driver was tested. Each user counted with 70 kg.

After the car been defined, it was set up three major tests: safety driving dynamics, dynamic driving, and economic driving. In the first one, the AEB and the ABS were evaluated by defining a total of five tests and the car was occupied by only the driver. The three tests involving the AEB system took into consideration real-world characteristics adopted from [37]. The other tests involving the ABS were based on scenarios pre-defined in the CarMaker software. For the dynamic driving tests, were defined five tests, in which four of them, included the ESP analysis. The one where the ESP was not testes was the Circular Test (Test 2.1.), of constant radius, according to ISO 4138. The other two main tests were the Double Lane Change (Test 2.2.1., and Test 2.2.2.), and the Moose Test (Test 2.3.1., and Test 2.3.2) based on ISO 3888-2, and based on [41], respectively. In the last case, which involved analyse the influence of the variables before mentioned, the economic driving tests were divided into extreme driving tests (Test 3.1. and Test 3.2.), where the two tests (rectangle speed profile, and slowly increasing speed) simulated extreme driving conditions; world light vehicles test procedures (Test 3.3.), based on [42], represents real travels and it is used for determination of energy consumption; in the tests based on real scenarios, a ride that fulfils the requirements of a Real Driving Emissions (RDE) track- from Karlsruhe, Germany, via Wörth am Rhein to Speyer and back was defined (Test 3.4.), and its speed profile was then applied in a straight road (Test 3.5.). The other two tests in this section were a typical track that a student ride from his home until the university- from Cacém, Portugal, via IC19 to C8 Building of the Faculty of Sciences of the University of Lisbon (Test 3.6.), and the last test included its way back (Test 3.7.)

The tire pressure was the parameter that showed how high it can affect the energy losses verified in a vehicle tire and the impact on its consumption. However, increasing the tire pressure may not be safe when rolling on surfaces where the contact area between the tire and the road is reduced (dry roads or the presence of ice in the road) since it may allow instability in the vehicle. In this context, the average tire losses were 0.089 kWh/ km and 0.115 kWh/ km for 2.9 bar and 2.2 bar, representing a difference of 0.026 kWh/ km. On a surface with a high temperature, high tire pressure does not justify due to the

deterioration of the rubber. So, the tire pressure must be adapted to the vehicle, the road, and the weather conditions.

The extra load applied in the vehicle (only the vehicle driver, or the car at its full capacity) does not have a relevant influence on the tire energy losses. The average tire losses were 0.101 kWh/ km and 0.115 kWh/ km for only the driver and car's full capacity, respectively, representing a difference of 0.014 kWh/ km. This small difference is justified by the total vehicle weight: the total mass of the vehicle is 1358 kg and both loads, 70 kg and 280 kg, are relatively small when compared with the vehicle mass. However, the tire pressure must be adapted to the total vehicle mass to provide a safe trip, and the tire does not create asymmetries in its body which may provide an unstable vehicle body.

The rolling resistance coefficient of the tires was revealed to be a parameter that has some influence on the energy losses. In average, the tire energy losses were 0.095 kWh/ km and 0.115 kWh/ km for the H and Q-rated speeds, respectively, using 2.2 bar as the tire pressure. As of 2.9 bar tires, 0.075 kWh/ km and 0.089 kWh/ km were obtained for the H and Q-rated speeds, respectively. This represents a difference of 0.020 kWh/ km for 2.2 bar and 0.014 kWh/ km for 2.9 bar. This means that the difference is higher for the lower pressure. However, in roads where the friction coefficient is too low (wet roads), a tire with a high rolling resistance coefficient may be necessary to allow comfort and safety in travel. Both tire pressure and tire rolling resistance coefficient may be adapted to the conditions, so the energy losses by tires may be as low as possible.

In future works, and regarding the simulations where real conditions were modelled, it would be interesting to include traffic, traffic signs (signals, road marks, and others), the altitude, and the slope of the road for a more realistic approach and determination of the losses due to tires and breaking. Also, perform the simulations in a typical winter season and compare them with the results from this work. Would be of relevance to analyse the influence of the battery and the tires' temperature on the vehicle energy consumption using the simulations methodologies developed in this work. Also, the experimental validation of the simulated data should be done by mimicking the test cycles in an appropriate test bench.

# 6 References


1. Range of Full Electric Vehicles Available online: https://ev-database.org/cheatsheet/range-electric-car (accessed on 11 December 2023).
2. EV Sales, Cars, World, STEPS Scenario 2020-2030 Available online: https://www.iea.org/data-and-statistics/data-tools/global-ev-data-explorer (accessed on 11 December 2023).
3. EV Sales, Cars, World, 2010-2022 Available online: https://www.iea.org/data-and-statistics/data-tools/global-ev-data-explorer (accessed on 11 December 2023).
4. Resolution Adopted by the General Assembly on 25 September 2015 2015.
5. *Sustainability Driven: Accelerating Impact with the Tire Sector SDG Roadmap*; 2021;
6. Heißing, B. *Chassis Handbook*;
7. ISO 8855:2011(En) Road Vehicles — Vehicle Dynamics and Road-Holding Ability — Vocabulary Available online: https://www.iso.org/obp/ui/en/#iso:std:iso:8855:ed-2:v1:en (accessed on 30 November 2023).
8. How Do All-Electric Cars Work? Available online: https://afdc.energy.gov/vehicles/how-do-all-electric-cars-work (accessed on 12 December 2023).
9. The Various Types of Electric Motors for Your Sustainable Mobility 2023.
10. Nissan LEAF Available online: https://www.nissan.pt/veiculos/novos-veiculos/leaf.html.
11. Model S Owner's Manual Available online: https://www.tesla.com/ownersmanual/models/en_eu/ (accessed on 3 December 2024).
12. Narang, U. Differences between Various Types of Motors Used in EVs. *THE TIMES OF INDIA* **2023**.
13. What's the Difference Between Brushed and Brushless Motors? Available online: https://ibtinc.com/difference-between-brushed-brushless-motors/#:~:text=Brushless%20motors%20operate%20more%20efficiently,energy%20lost%20to%20heat%20generation.
14. Pelonis, S. Comparing the Efficiency of Different Electric Motor Types Available online: https://www.pelonistechnologies.com/blog/comparing-the-efficiency-of-different-electric-motor-types.
15. Dambrauskas, K.; Vanagas, J.; Zimnickas, T.; Kalvaitis, A.; Ažubalis, M. A Method for Efficiency Determination of Permanent Magnet Synchronous Motor. *Energies (Basel)* **2020**, *13*, 1004, doi:10.3390/en13041004.
16. MIT Electric Vehicle Team *A Guide to Understanding Battery Specifications*; 2008;
17. *Handbook of Batteries*; Linden, D., B. Reddy, T., Eds.; Third.; McGraw-Hill;
18. Xiong, R.; Li, L.; Tian, J. Towards a Smarter Battery Management System: A Critical Review on Battery State of Health Monitoring Methods. *J Power Sources* **2018**, *405*, 18–29, doi:10.1016/j.jpowsour.2018.10.019.
19. Lin, Z.; Li, D.; Zou, Y. Energy Efficiency of Lithium-Ion Batteries: Influential Factors and Long-Term Degradation. *J Energy Storage* **2023**, *74*, 109386, doi:10.1016/j.est.2023.109386.
20. Vasiljević, S.; Aleksandrović, B.; Glišović, J.; Maslać, M. Regenerative Braking on Electric Vehicles: Working Principles and Benefits of Application. **2022**, 012025, doi:10.1088/1757-899X/1271/1/012025.
21. Sweeting, W.J.; Hutchinson, A.R.; Savage, S.D. Factors Affecting Electric Vehicle Energy Consumption. *International Journal of Sustainable Engineering* **2011**, *4*, 192–201, doi:10.1080/19397038.2011.592956.

22. Janpoom, K.; Suttakul, P.; Achariyaviriya, W.; Fongsamootr, T.; Katongtung, T.; Tippayawong, N. Investigating the Influential Factors in Real-World Energy Consumption of Battery Electric Vehicles. *Energy Reports* **2023**, *9*, 316–320, doi:10.1016/j.egyr.2023.10.012.
23. Grunditz, E.; Thiringer, T. *Characterizing BEV Powertrain Energy Consumption, Efficiency, and Range During Official and Drive Cycles From Gothenburg, Sweden*; 2016;
24. Bottiglione, F.; De Pinto, S.; Mantriota, G.; Sorniotti, A. Energy Consumption of a Battery Electric Vehicle with Infinitely Variable Transmission. *Energies (Basel)* **2014**, *7*, 8317–8337, doi:10.3390/en7128317.
25. El Baghdadi, M.; De Vroey, L.; Coosemans, T.; Van Mierlo, J.; Foubert, W.; Jahn, R. Electric Vehicle Performance and Consumption Evaluation. *World Electric Vehicle Journal* **2013**, *6*, 30–37, doi:10.3390/wevj6010030.
26. Pfriem, M.; Gauterin, F. Development of Real-World Driving Cycles for Battery Electric Vehicles. *World Electric Vehicle Journal* **2016**, *8*, 14–24, doi:10.3390/wevj8010014.
27. Dr.-Ing.Gießle, M.; Dr.-Ing Sander, O.; Dr.-Ing. Müller-Glaser, K.; Prof. Dr. rer. nat. Gauterin, F. Converted Vehicle for Battery Electric Drive: Aspects on the Design of the Software-Driven Vehicle Control Unit.; 2nd Energy Efficienct Vehicle Conference (EEVC 2012), June 2012.
28. Gießler, M.; Fritz, A.; Paul, J.; Sander, O.; Gauterin, F.; Glaser, K. *Converted Vehicle for Battery Electric Drive: Aspects on the Design of the Software-Driven Vehicle Control Unit.*; Karlsruher;
29. Paul, J. Aufbau Eines Fahrzeugsimulationsmodells Für Untersuchungen Zum Batterieelektrischen Fahrbetrieb (Building a Vehicle Simulation Model for Studies on Battery-Electric Driving). PhD thesis, Karlsruher Institut für Technologie: Karlsruhe, 2012.
30. UEV-18XP Available online: www.valence.com (accessed on 4 October 2023).
31. CarMaker User's Guide Version 11.1.
32. Useable Battery Capacity of Full Electric Vehicles Available online: https://ev-database.org/cheatsheet/useable-battery-capacity-electric-car.
33. Group 24, 12 Volt, 118 Ah Lithium Ion Battery Module Available online: https://www.lithionbattery.com/wp-content/uploads/2019/12/Valence-U24-12XP-Data-Sheet-210623.pdf.
34. CarMaker Reference Manual Version 11.1.
35. Unrau, H.-J. Der Einfluss Der Fahrbahnoberflächenkrümmung Auf Den Rollwiderstand, Die Cornering Stiffness Und Die Aligning Stiffness von Pkw-Reifen (The Influence of Road Surface Curvature on the Rolling Resistance, Cornering Stiffness and Aligning Stiffness of Passenger Car Tires). PhD. Dissertation, Karlsruher Institut für Technologie (KIT): Karlsruher, 2012.
36. Prof. Dr. rer. nat. Gauterin. F.; Dr.-Ing. Gießler, M.; Prof. Dr.-Ing. Gnadler, R. Automotive Engineering I 2022.
37. Hulshof, W.; Knight, I.; Edwards, A.; Avery, M.; Grover, C. *AUTONOMOUS EMERGENCY BRAKING TEST RESULTS*;
38. SFTP-US06 Available online: https://dieselnet.com/standards/cycles/ftp_us06.php (accessed on 26 August 2024).
39. Passenger Cars — Steady-State Circular Driving Behaviour — Open-Loop Test Methods 2004, *ISO 4138:2004(E)*.
40. Passenger Cars — Test Track for a Severe Lane-Change Manoeuvre — Part 1: Double Lane-Change 2018, *ISO 3888-1:2018(E)*.
41. Breuer, J.J. *ANALYSIS OF DRIVER-VEHICLE-INTERACTIONS IN AN EVASIVE MANOUEUVRE - RESULTS OF "MOOSE TEST" STUDIES*;

42. Worldwide Harmonized Light Vehicles Test Cycle (WLTC) Available online: https://dieselnet.com/standards/cycles/wltp.php#cycles.
43. Wagner, C.; Keskin, M.-T.; Grill, M.; Bargende, M.; Cai, L.; Pitsch, H.; Blochum, S. Potential Analysis and Virtual Development of SI Engines Operated with DMC+. In *20. Internationales Stuttgarter Symposium*; 2020; pp. 49–74.
44. Fetene, G.M.; Kaplan, S.; Mabit, S.L.; Jensen, A.F.; Prato, C.G. Harnessing Big Data for Estimating the Energy Consumption and Driving Range of Electric Vehicles. *Transp Res D Transp Environ* **2017**, *54*, 1–11, doi:10.1016/j.trd.2017.04.013.

# 7 Annexes

## 7.1 Simulation Details

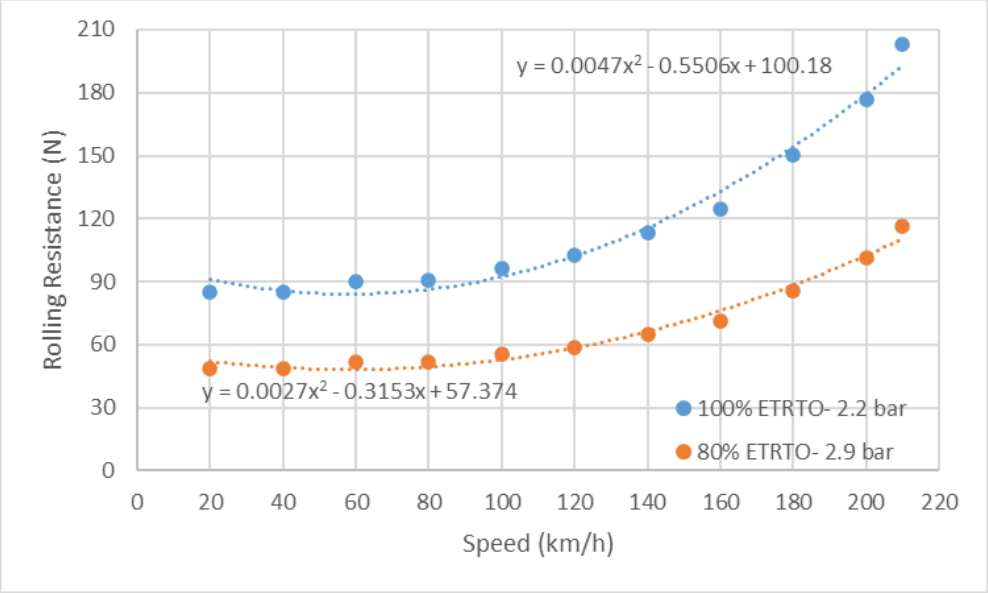


Figure 7.1- Calculated rolling resistance of the H speed rating for 2.2 bar and 2.9 bar tire pressure

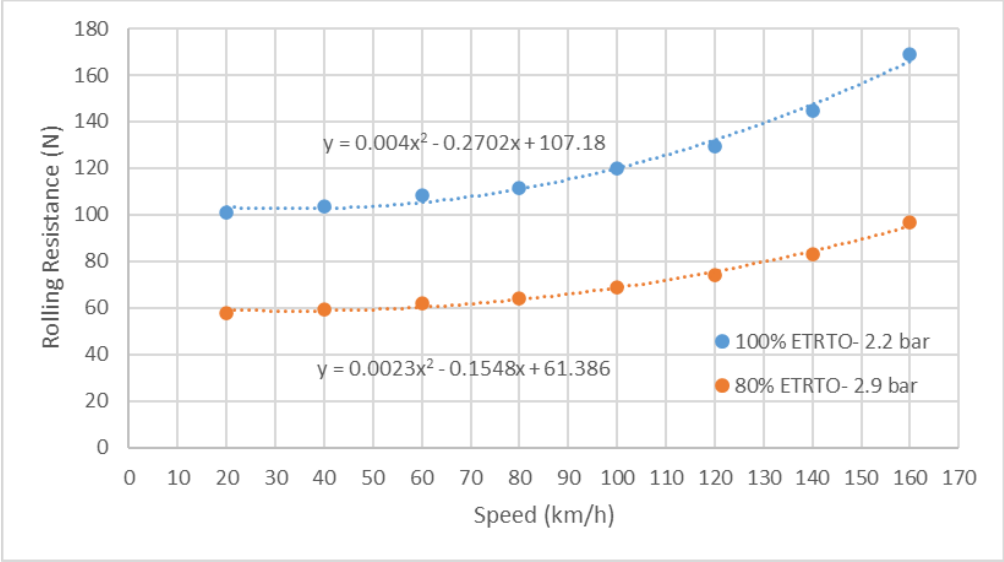


Figure 7.2- Calculated rolling resistance of the Q speed rating for 2.2 bar and 2.9 bar tire pressure

## 7.2 Summary of the Results of the Economic Driving Tests

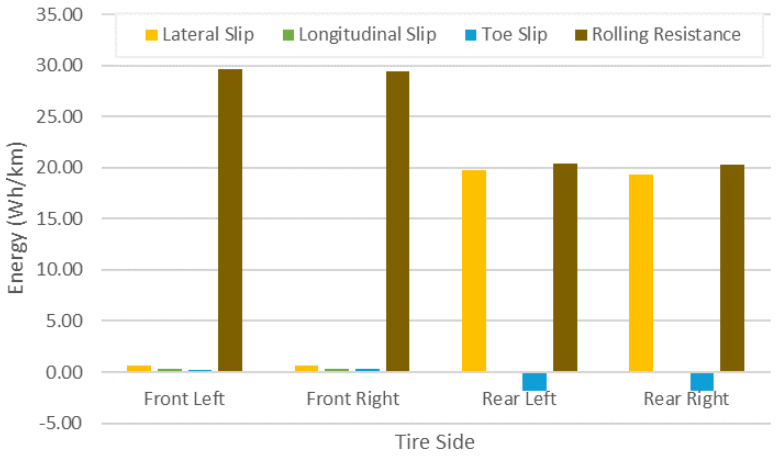


Figure 7.3- Energy losses per kilometre due to the lateral slip, the longitudinal slip, the toe slip and the rolling resistance for the tire pressure of 2.2 bar of the Q tire type in the RDE test with the new battery

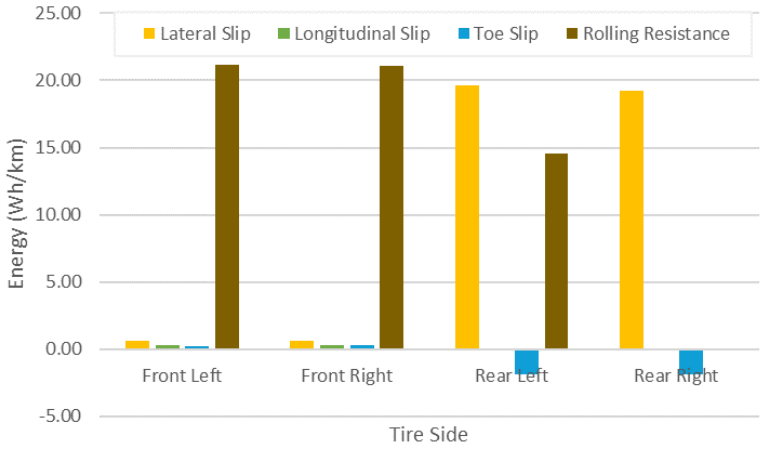


Figure 7.4- Energy losses per kilometre due to the lateral slip, the longitudinal slip, the toe slip and the rolling resistance for the tire pressure of 2.9 bar of the Q tire type in the RDE test with the new battery

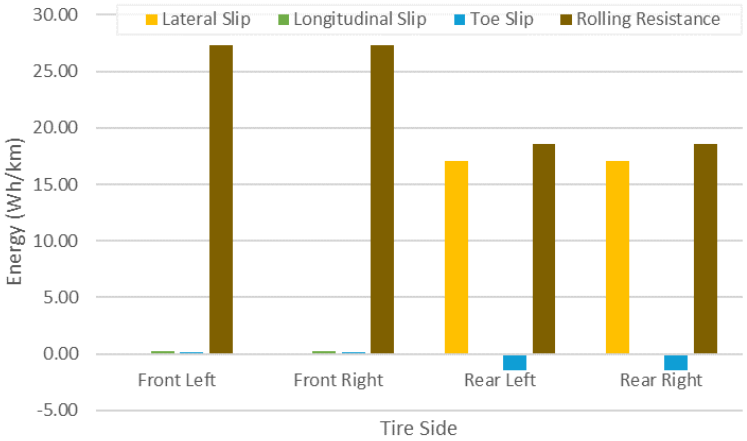

Figure 7.5- Energy losses per kilometre due to the lateral slip, the longitudinal slip, the toe slip and the rolling resistance for the tire pressure of 2.2 bar of the Q tire type in the Straight RDE test

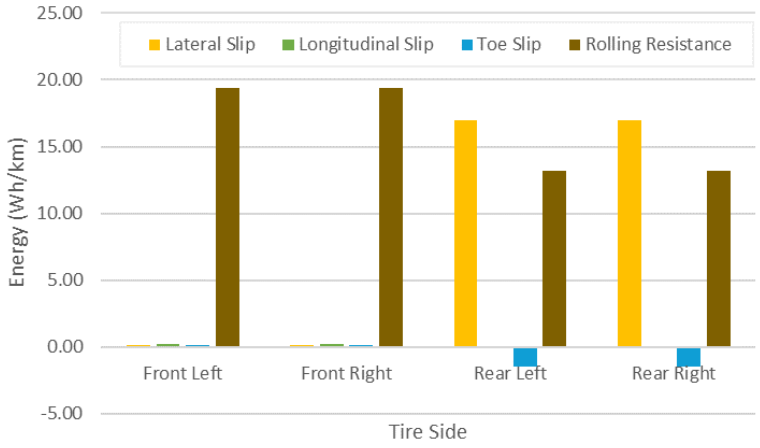


Figure 7.6- Energy losses per kilometre due to the lateral slip, the longitudinal slip, the toe slip and the rolling resistance for the tire pressure of 2.9 bar of the Q tire type in the Straight RDE test

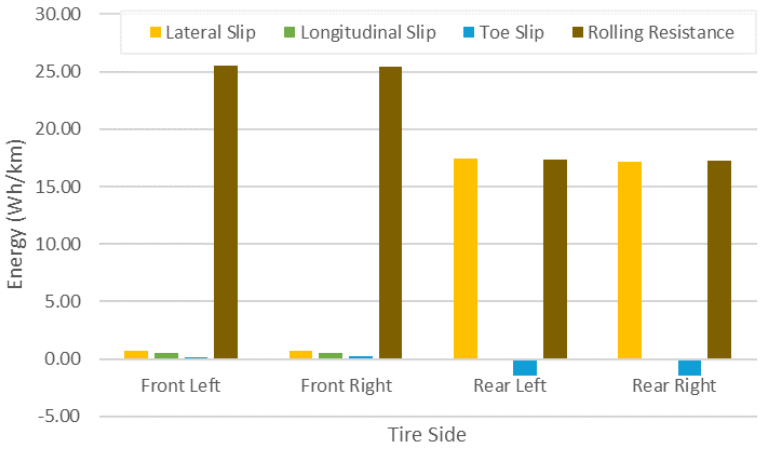


Figure 7.7- Energy losses per kilometre due to the lateral slip, the longitudinal slip, the toe slip, and the rolling resistance for the tire pressure of 2.2 bar of the Q tire type in the UH test

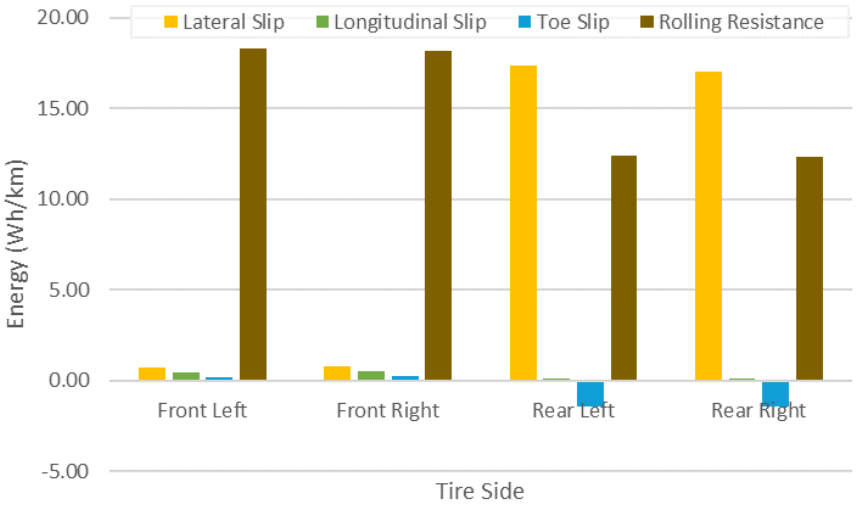


Figure 7.8- Energy losses per kilometre due to the lateral slip, the longitudinal slip, the toe slip and the rolling resistance for the tire pressure of 2.9 bar of the Q tire type in the UH test

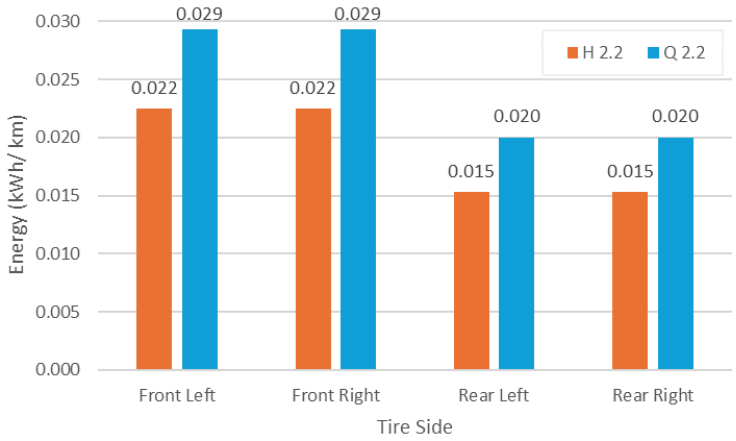


Figure 7.9- Energy losses per kilometre due to the tire rolling resistance for Q and H tire type, with 2.2 bar tire pressure, in the Different Speed test

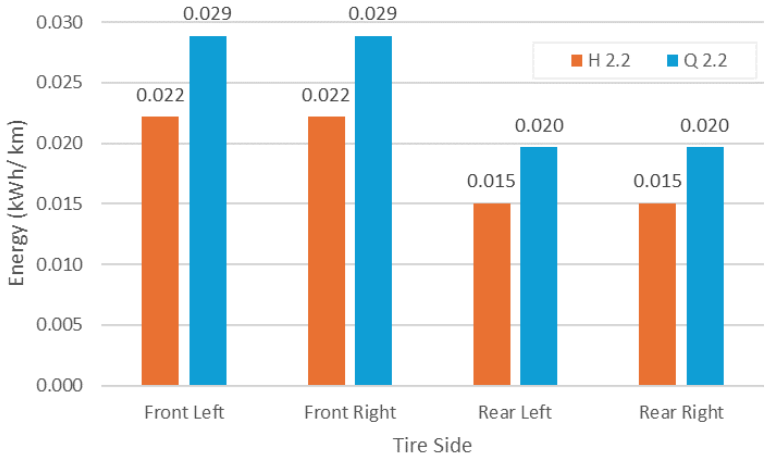


Figure 7.10- Energy losses per kilometre due to the tire rolling resistance for Q and H tire type, with 2.2 bar tire pressure, in the Rectangle Speed test

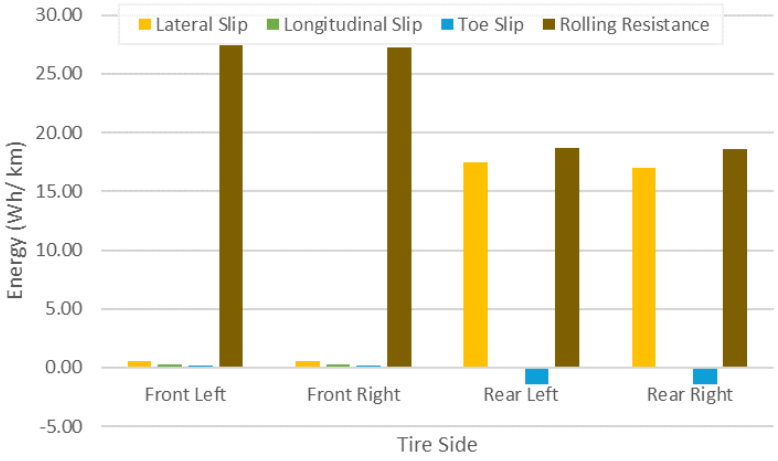


Figure 7.11- Energy losses per kilometre due to the lateral slip, the longitudinal slip, the toe slip, and the rolling resistance for Q tire type, with 2.2 bar tire pressure, in the RDE test

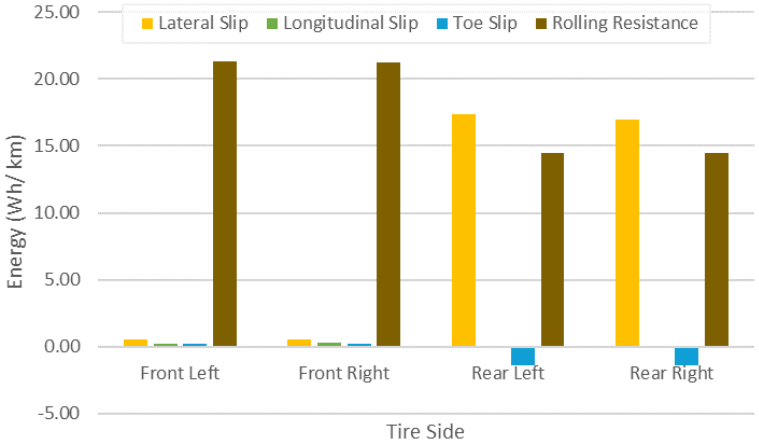


Figure 7.12- Energy losses per kilometre due to the lateral slip, the longitudinal slip, the toe slip, and the rolling resistance for H tire type, with 2.2 bar tire pressure, in the RDE test

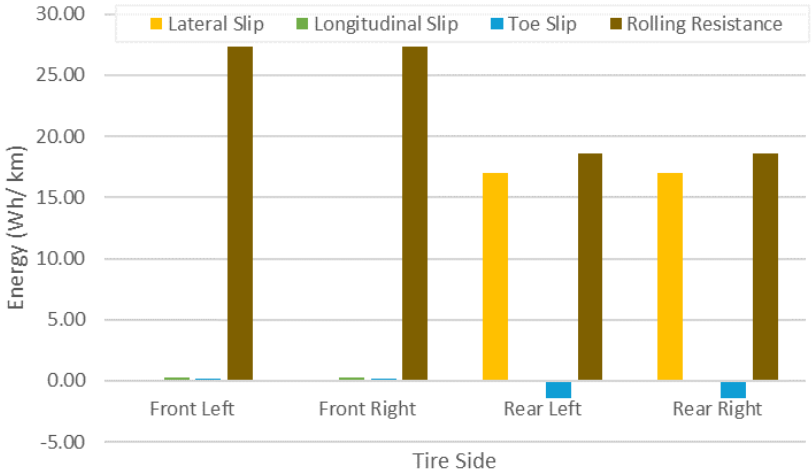


Figure 7.13- Energy losses per kilometre due to the lateral slip, the longitudinal slip, the toe slip and the rolling resistance for Q tire type, with 2.2 bar tire pressure, in the Straight RDE test

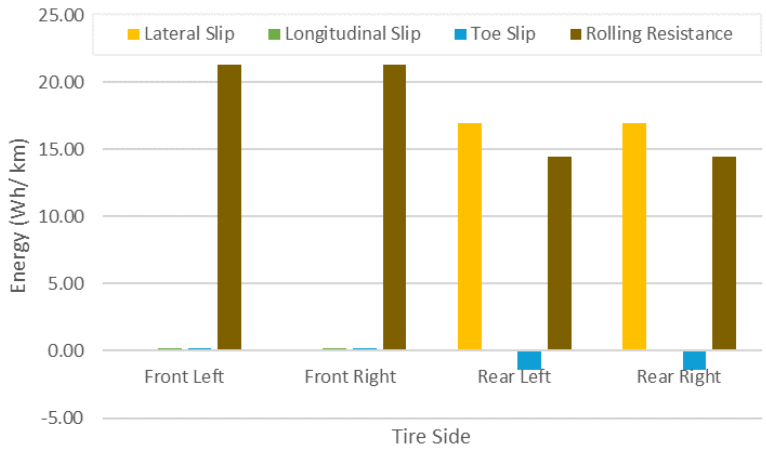


Figure 7.14- Energy losses per kilometre due to the lateral slip, the longitudinal slip, the toe slip and the rolling resistance for H tire type, with 2.2 bar tire pressure, in the Straight RDE test

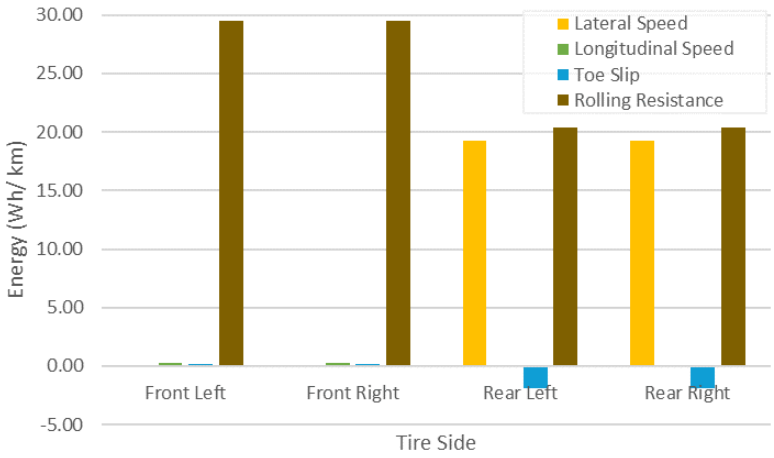


Figure 7.15- Energy losses per kilometre due to the lateral slip, the longitudinal slip, the toe slip and the rolling resistance for Q tire type, with 2.2 bar tire pressure, in the Straight RDE test with the new battery

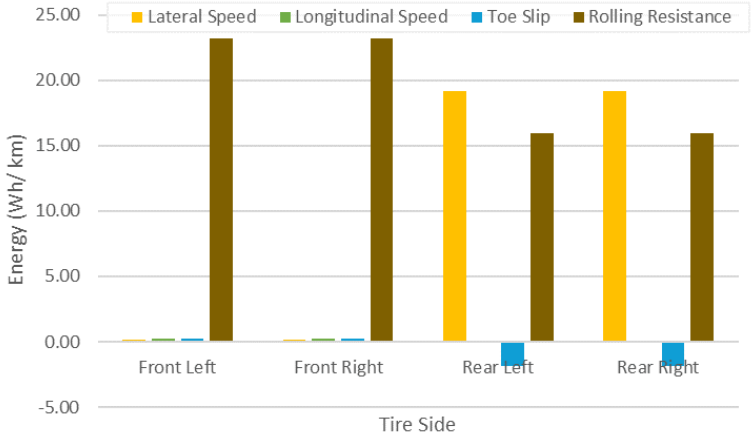


Figure 7.16- Energy losses per kilometre due to the lateral slip, the longitudinal slip, the toe slip and the rolling resistance for H tire type, with 2.2 bar tire pressure, in the Straight RDE test with the new battery

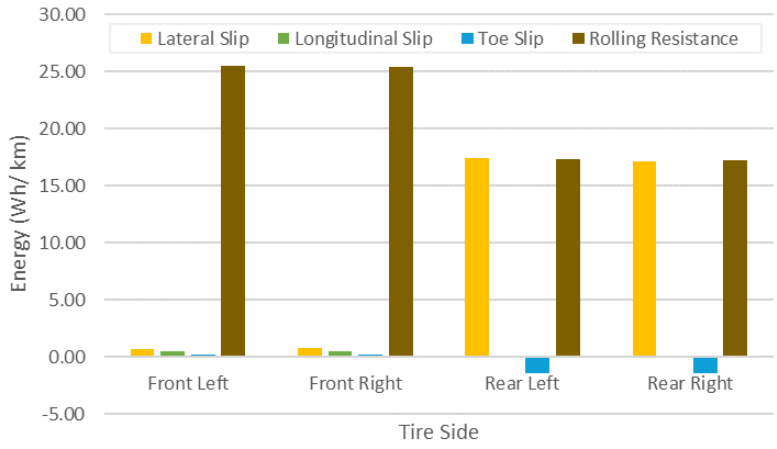


Figure 7.17- Energy losses per kilometre due to the lateral slip, the longitudinal slip, the toe slip and the rolling resistance for Q tire type, with 2.2 bar tire pressure, in the UH test with the new battery

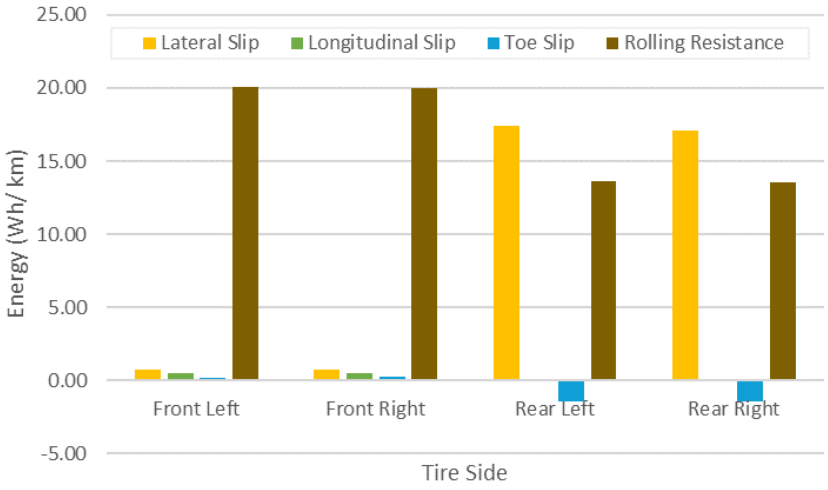


Figure 7.18- Energy losses per kilometre due to the lateral slip, the longitudinal slip, the toe slip and the rolling resistance for H tire type, with 2.2 bar tire pressure, in the UH test with the new battery

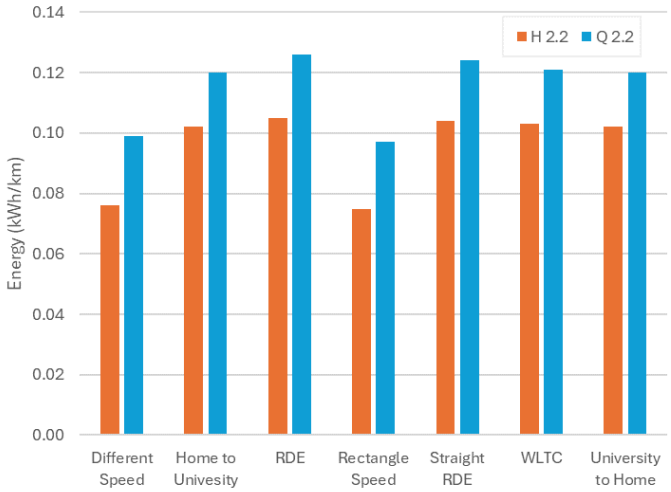


Figure 7.19- Total energy loss per kilometre in the tires for each simulation for the H and Q tire type, with 2.2 bar tire pressure

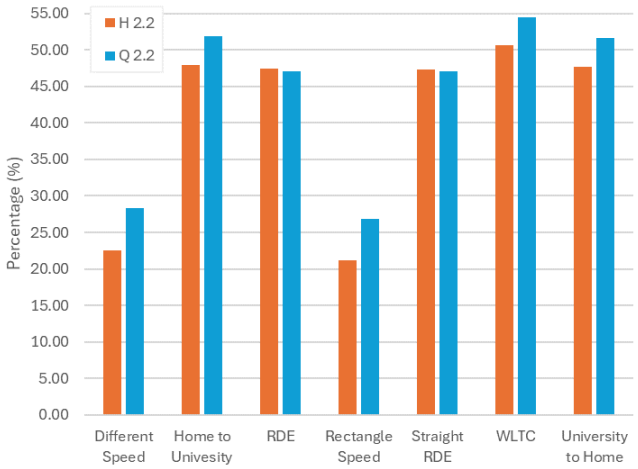


Figure 7.20- Percentage of the total energy lost through the tires that contributed to the total energy consumption of the battery in each simulation, for H and Q tire type, with 2.2 bar tire pressure

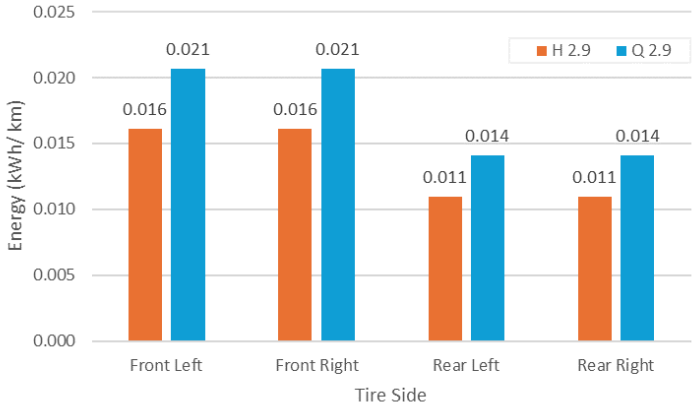


Figure 7.21- Energy losses per kilometre due to the tire rolling resistance for Q and H tire type, with 2.9 bar tire pressure, in the Different Speed test

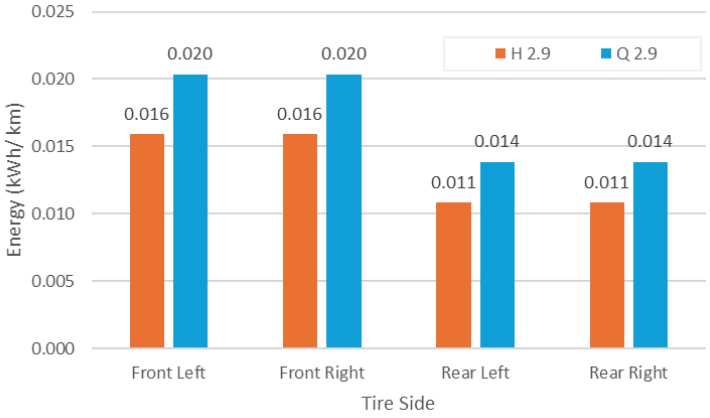


Figure 7.22- Energy losses per kilometre due to the tire rolling resistance for Q and H tire type, with 2.9 bar tire pressure, in the Rectangle Speed test

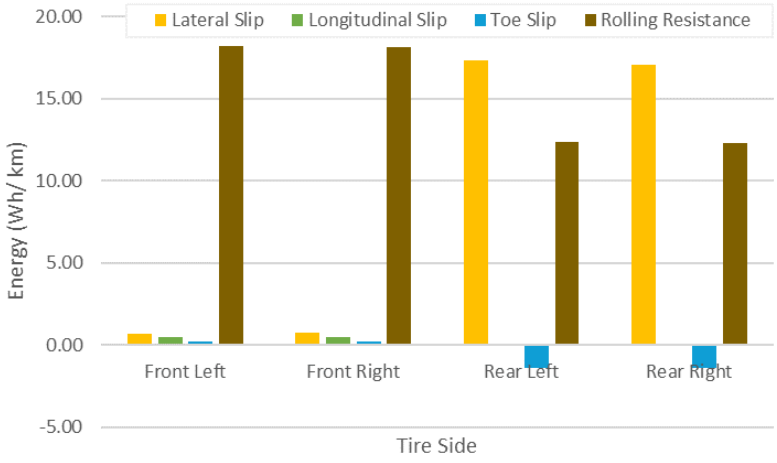


Figure 7.23- Energy losses per kilometre due to the lateral slip, the longitudinal slip, the toe slip and the rolling resistance for Q tire type, with 2.9 bar tire pressure, in the UH test

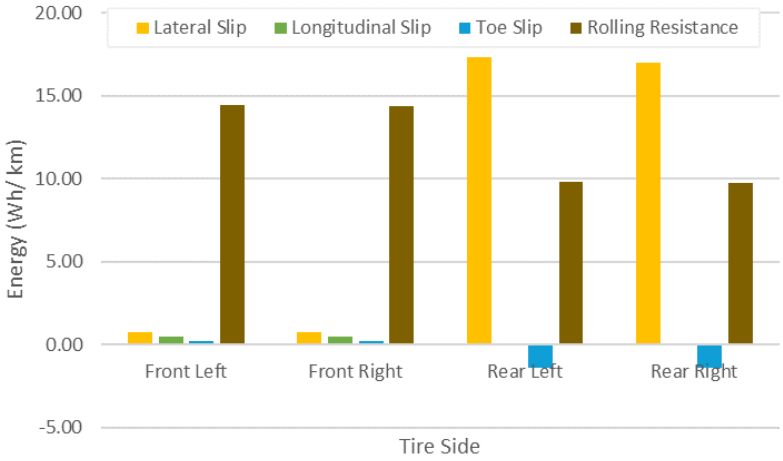


Figure 7.24- Energy losses per kilometre due to the lateral slip, the longitudinal slip, the toe slip and the rolling resistance for H tire type, with 2.9 bar tire pressure, in the UH test

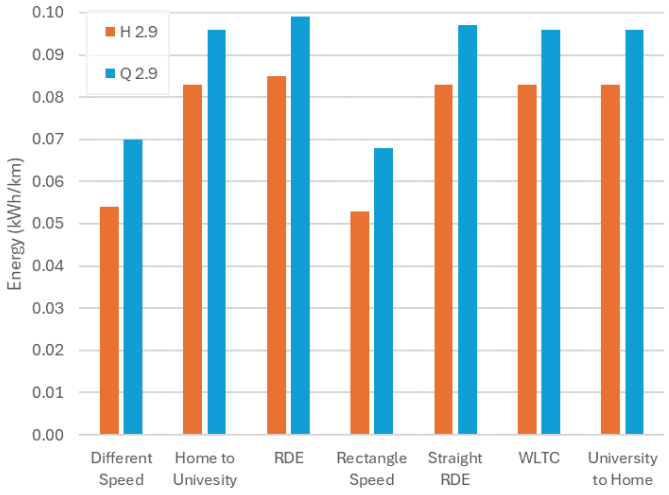

Figure 7.25- Total energy loss per kilometre in the tires for each simulation for the H and Q tire type, with 2.9 bar tire pressure

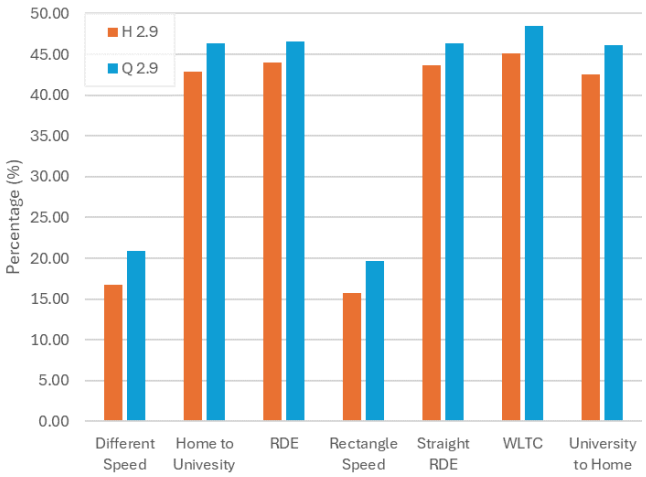


Figure 7.26- Percentage of the total energy lost through the tires that contributed to the total energy consumption of the battery in each simulation, for H and Q tire type, with 2.9 bar tire pressure

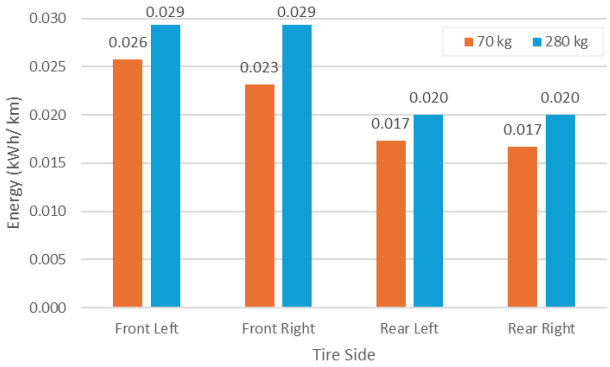


Figure 7.27- Energy losses per kilometre due to the tire rolling resistance for 70 kg and 280 kg extra load in the Different Speed tests

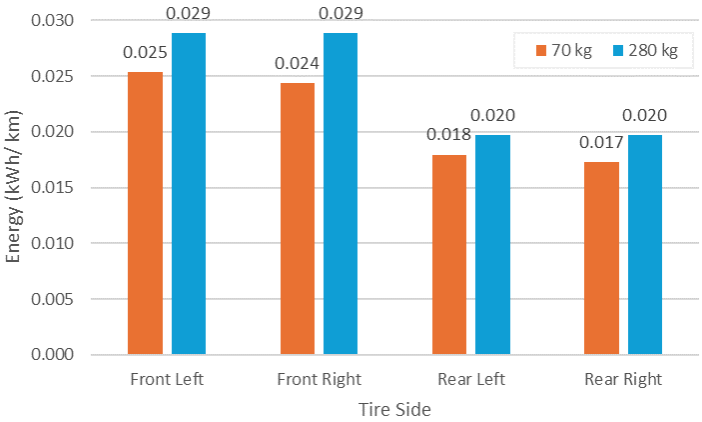


Figure 7.28- Energy losses per kilometre due to the tire rolling resistance for 70 kg and 280 kg extra load in the Rectangle Speed tests

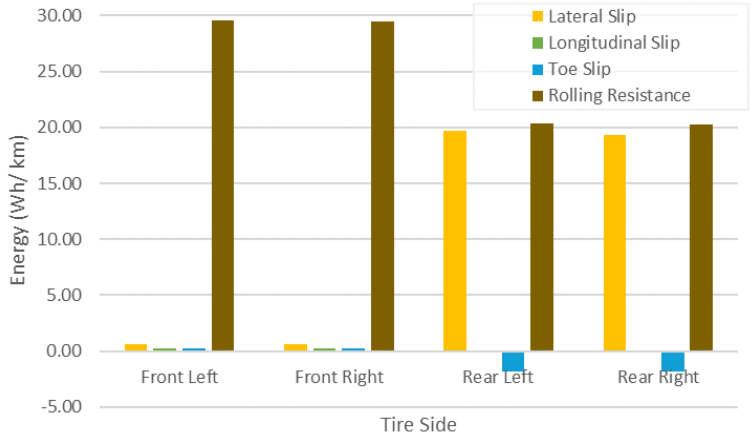


Figure 7.29- Energy losses per kilometre due to the lateral slip, the longitudinal slip, the toe slip, and the rolling resistance for 280 kg extra load in the RDE tests, with the new battery

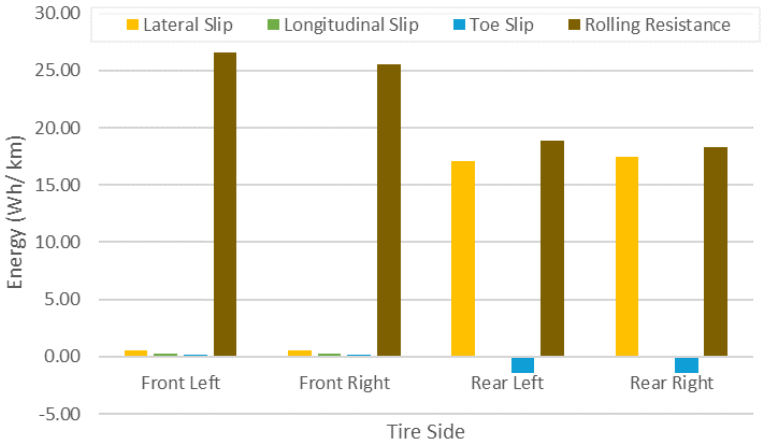


Figure 7.30- Energy losses per kilometre due to the lateral slip, the longitudinal slip, the toe slip, and the rolling resistance for 70 kg extra load in the RDE tests, with the new battery

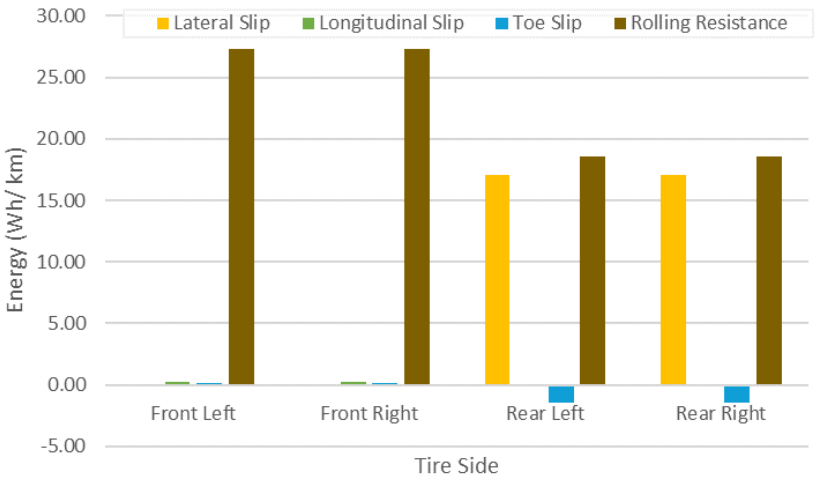

Figure 7.31- Energy losses per kilometre due to the lateral slip, the longitudinal slip, the toe slip, and the rolling resistance for 280 kg extra load in the Straight RDE tests

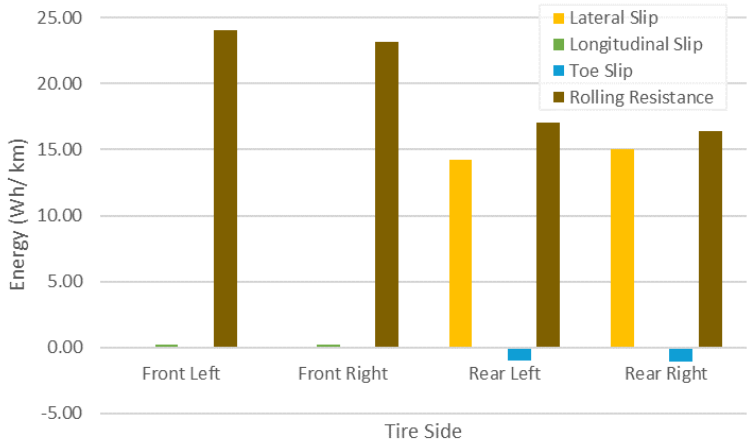


Figure 7.32- Energy losses per kilometre due to the lateral slip, the longitudinal slip, the toe slip, and the rolling resistance for 70 kg extra load in the Straight RDE tests

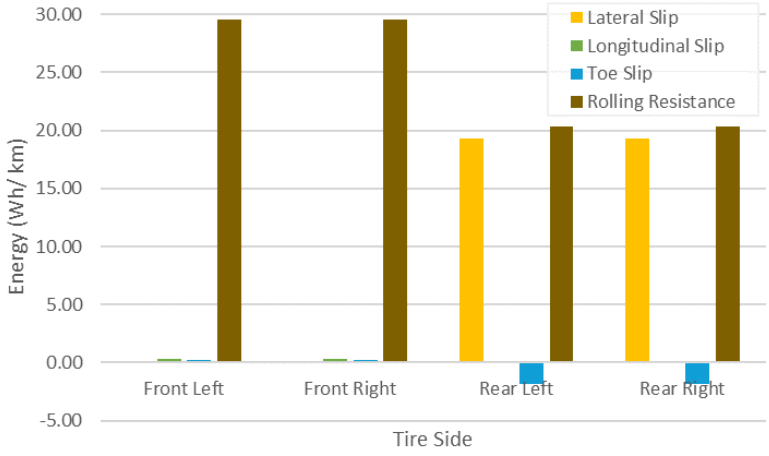


Figure 7.33- Energy losses per kilometre due to the lateral slip, the longitudinal slip, the toe slip, and the rolling resistance for 280 kg extra load in the Straight RDE tests, with the new battery

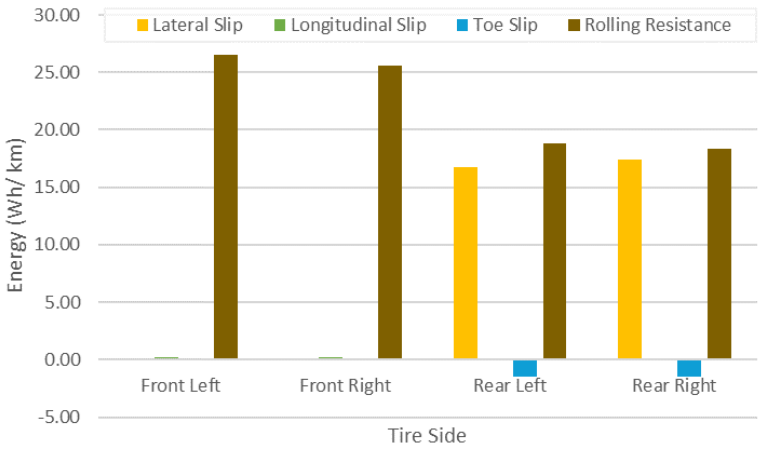


Figure 7.34- Energy losses per kilometre due to the lateral slip, the longitudinal slip, the toe slip, and the rolling resistance for 70 kg extra load in the Straight RDE tests, with the new battery

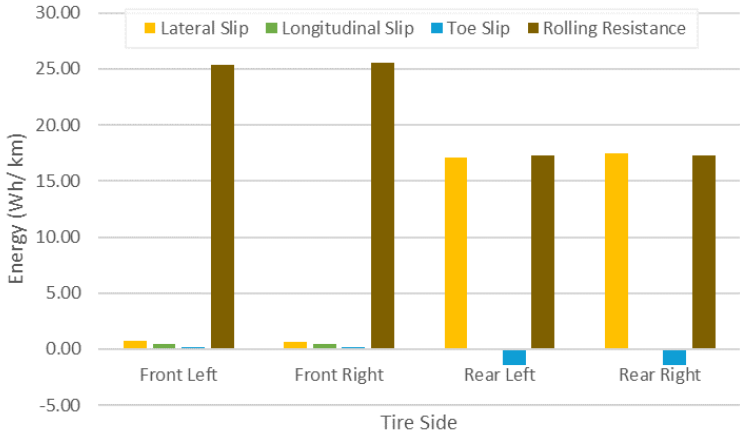


Figure 7.35- Energy losses per kilometre due to the lateral slip, the longitudinal slip, the toe slip, and the rolling resistance for 280 kg extra load in the HU tests

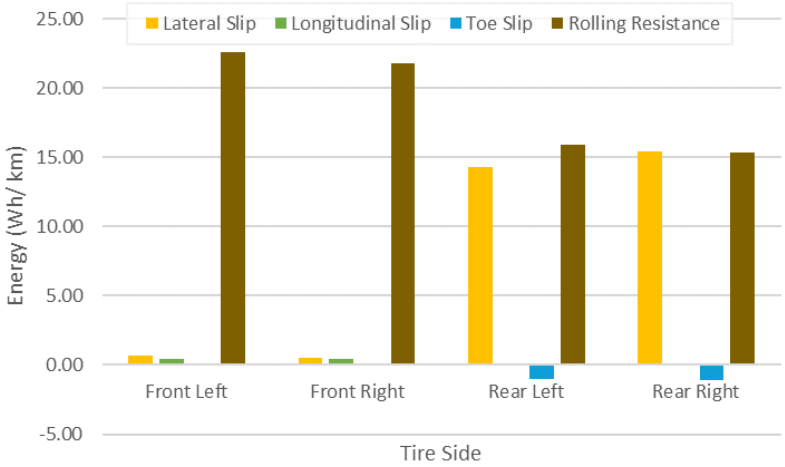


Figure 7.36- Energy losses per kilometre due to the lateral slip, the longitudinal slip, the toe slip, and the rolling resistance for 70 kg extra load in the HU tests

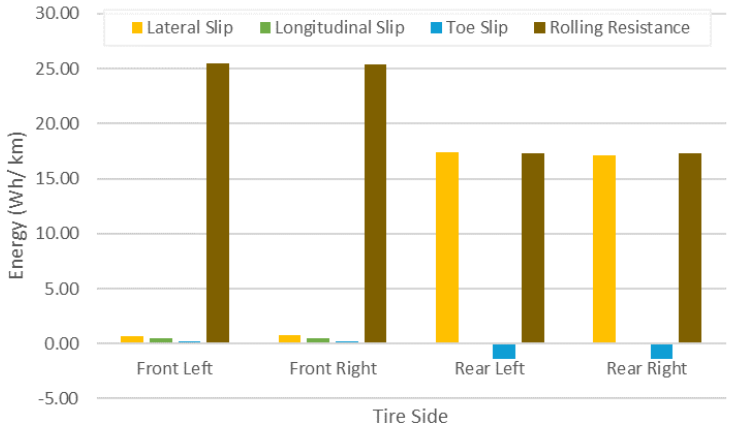


Figure 7.37- Energy losses per kilometre due to the lateral slip, the longitudinal slip, the toe slip, and the rolling resistance for 280 kg extra load in the UH tests

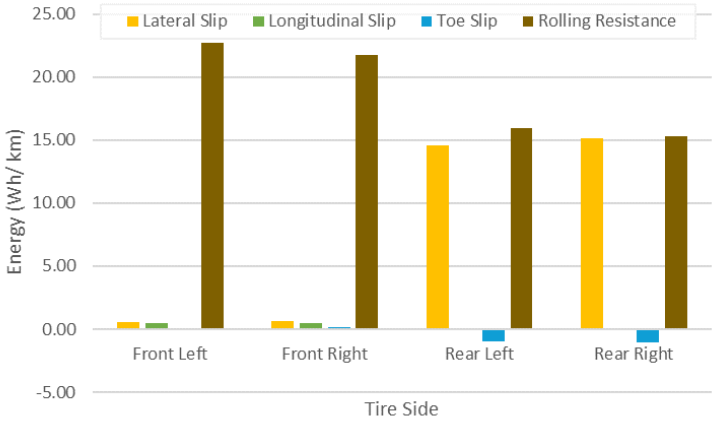


Figure 7.38- Energy losses per kilometre due to the lateral slip, the longitudinal slip, the toe slip, and the rolling resistance for 70 kg extra load in the UH tests

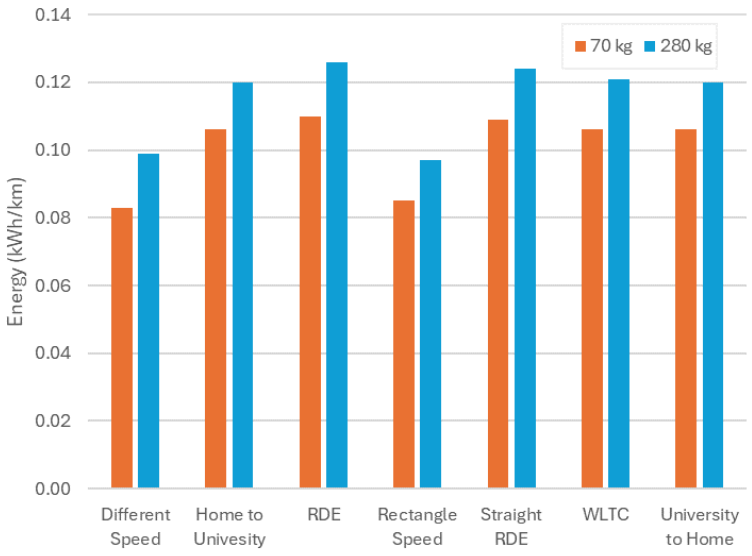


Figure 7.39- Total energy loss per kilometre in the tires for each simulation for 70 kg and 280 kg vehicle load, with the Q tire type and 2.2 bar tire pressure, where the rolling resistance of the vehicle is independent from the tire pressure

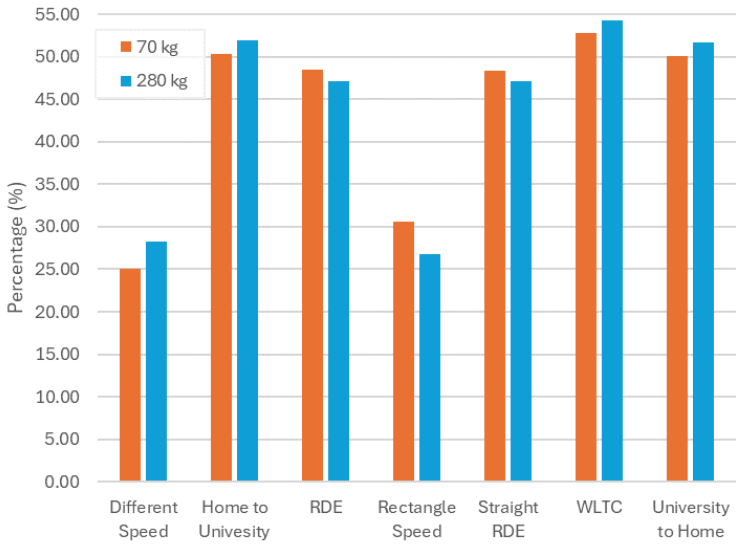


Figure 7.40- Percentage of the total energy lost through the tires that contributed to the total energy consumption of the battery in each simulation for 70 kg and 280 kg vehicle load, with the Q tire type and 2.2 bar tire pressure, where the rolling resistance of the vehicle is independent from the tire pressure